

Stacjonarne Studia Doktoranckie Mikrobiologii,
Biotechnologii i Biologii Eksperymentalnej

Adrian Soboń

**Zmiany w metabolomie i proteomie
Cunninghamella echinulata w trakcie
biodegradacji tributyllocyny**

Alterations in the metabolome and proteome of
Cunninghamella echinulata during tributyltin
biodegradation

Praca doktorska

wykonana w Katedrze Mikrobiologii
Przemysłowej i Biotechnologii,
Instytutu Mikrobiologii, Biotechnologii i
Immunologii

Promotor:

- Prof. dr hab. Jerzy Długoński

Promotor pomocniczy:

- Dr Rafał Szewczyk

Podziękowania

Pragnę serdecznie podziękować Panu dr Rafałowi Szewczykowi za całokształt przekazanej mi wiedzy oraz nieocenioną pomoc w rozwijaniu zainteresowań i podnoszeniu kwalifikacji.

Panu prof. dr hab. Jerzemu Długońskiemu dziękuję za opiekę i cenne wskazówki na każdym z etapów realizacji niniejszej pracy.

Pani dr hab. Sylwii Różalskiej, prof. UŁ oraz Panu dr hab. Przemysławowi Bernatowi, prof. UŁ dziękuję za cenne rady i pomoc w przeprowadzeniu wybranych analiz.

Wszystkim pracownikom Katedry Mikrobiologii Przemysłowej i Biotechnologii UŁ i Zakładu Genetyki Drobnoustrojów UŁ dziękuję za okazaną życzliwość oraz pomoc.

Szczególne podziękowania składam rodzicom, których trud włożony w moje wychowanie i edukację umożliwił mi spełnienie marzeń, oraz żonie i dzieciom za wyrozumiałość, wsparcie i motywację do działania.

Spis treści

I.	Finansowanie.....	4
II.	Wykaz publikacji będących podstawą rozprawy doktorskiej	5
III.	Wykaz pozostałych publikacji składających się na dorobek naukowy.....	6
IV.	Streszczenie w języku polskim	8
V.	Streszczenie w języku angielskim.....	10
VI.	Wprowadzenie.....	12
VII.	Cele pracy.....	15
VIII.	Metodologia badań.....	16
VIII.	1. Techniki wykorzystywane podczas realizacji pracy doktorskiej	16
VIII.	2. Oprogramowanie	17
IX.	Syntetyczne omówienie wyników przedstawionych w cyklu publikacji wchodzących w skład rozprawy doktorskiej.....	19
	P1 <i>Tributyltin (TBT) biodegradation induces oxidative stress of Cunninghamella echinulata</i>	25
	P2 <i>Metabolomics of the recovery of the filamentous fungus Cunninghamella echinulata exposed to tributyltin</i>	38
	P3 <i>A proteomic study of Cunninghamella echinulata recovery during exposure to tributyltin</i>	50
X.	Podsumowanie i stwierdzenia końcowe.....	70
XI.	Literatura uzupełniająca	72
XII.	Oświadczenia współautorów o udziale w publikacjach.....	74

I. Finansowanie

1. Grant zespołowy NCN, Opus 1 „Mikrobiologiczna degradacja ksenoestrogenów i estrogenów w obecności metali ciężkich i NaCl”. Nr projektu: 2011/01/B/NZ9/02898. Lata 2012-2013. Kierownik projektu: Prof. dr hab. Jerzy Długoński.
2. Grant NCN, Preludium 7 „Zmiany w proteomie grzyba strzępkowego *Cunninghamella echinulata* podczas degradacji organicznych związków cyny”. Nr projektu 2014/13/N/NZ9/00878. Lata 2015-2017, **kierownik**, opiekun naukowy: Prof. dr hab. Jerzy Długoński; projekt rozliczony.
3. Dotacja celowa na działalność związaną z prowadzeniem badań naukowych lub prac rozwojowych oraz zadań z nimi związanych, służących rozwojowi młodych naukowców oraz uczestników studiów doktoranckich, przyznany przez Dziekana Wydziału BiOŚ w latach 2014, 2015 i 2016.
4. Realizacja pracy doktorskiej była objęta programem stypendialnym „Doktoranci – Regionalna Inwestycja w młodych naukowców nauk przyrodniczych i technologicznych – Akronim D-RIM BIO” współfinansowanym przez Unię Europejską ze środków Europejskiego Funduszu Społecznego w ramach Programu Operacyjnego Kapitał Ludzki, Poddziałanie 8.2. Lata 2014/2015.

II. Wykaz publikacji będących podstawą rozprawy doktorskiej

Dorobek naukowy obejmujący problematykę wskazaną w tytule rozprawy doktorskiej zawiera się w następujących trzech publikacjach:

P1 – **Soboń A**, Szewczyk R, Długoński J* (2016). *Tributyltin (TBT) biodegradation induces oxidative stress of Cunninghamella echinulata*. International Biodeterioration and Biodegradation, 107, 92-101, doi: 10.1016/j.ibiod.2015.11.013.

IF = 2,962; MNiSW = 30

P2 – **Soboń A**, Szewczyk R, Różalska S, Długoński J* (2018). *Metabolomics of the recovery of the filamentous fungus Cunninghamella echinulata exposed to tributyltin*. International biodeterioration and biodegradation, 127, 130-138, doi: 10.1016/j.ibiod.2017.11.008.

IF = 3,828; MNiSW = 30

P3 – **Soboń A**, Szewczyk R*, Długoński J, Różalska S (2019). *A proteomic study of Cunninghamella echinulata recovery during exposure to tributyltin*. Environmental Science and Pollution Research; doi: 10.1007/s11356-019-06416-z.

IF = 2,914; MNiSW = 70

Sumaryczny IF = 9,704

Łączna liczba punktów MNiSW = 130

Wartość IF oraz punktację MNiSW podano zgodnie z rokiem opublikowania

* Autorzy korespondujący

III. Wykaz pozostałych publikacji składających się na dorobek naukowy

1. Szewczyk R, **Soboń A**, Różalska S, Dzitko K, Waidelich D, Długoński J. (2014). *Intracellular proteome expression during 4-n-nonylphenol biodegradation by the filamentous fungus Metarhizium robertsii*. International Biodeterioration and Biodegradation, 93, 44-53.

IF = 2,131; MNiSW = 30

2. Bernat P, Siewiera P, **Soboń A**, Długoński J. (2014). *Phospholipids and protein adaptation of Pseudomonas sp. to the xenoestrogen tributyltin chloride (TBT)*. World Journal of Microbiology and Biotechnology, 30(9), 2343-2350.

IF = 1,779; MNiSW = 20

3. Szewczyk R, **Soboń A**, Słaba M, Długoński J. (2015). *Mechanism study of alachlor biodegradation by Paecilomyces marquandii with proteomic and metabolomic method*. Journal of hazardous materials, 291, 52-64.

IF = 4,836; MNiSW = 45

4. Różalska S, **Soboń A**, Pawłowska J, Wrzosek M, Długoński J. (2015). *Biodegradation of nonylphenol by a novel entomopathogenic Metarhizium robertsii strain*. Bioresource technology, 191, 166-172.

IF = 4,917; MNiSW = 45

5. Wrońska N, Brzostek A, Szewczyk R, **Soboń A**, Dziadek J, Lisowska K. (2016). *The Role of fadD19 and echA19 in Sterol Side Chain Degradation by Mycobacterium smegmatis*. Molecules, 21(5), 598.

IF = 2,861; MNiSW = 30

6. Kochel K, Tomczyk M D, Simões R F, Fraczek T, **Soboń A**, Oliveira P J, Walczak K Z, Koceva-Chyla A. (2016). *Evaluation of biological properties of 3, 3', 4, 4'-benzophenonetetracarboxylic dianhydride derivatives and their ability to inhibit hexokinase activity*. Bioorganic & Medicinal Chemistry Letters, 27, 427-431.

IF = 2,454; MNiSW = 30

7. Jasińska A, Góralczyk A, **Soboń A**, Długoński J. (2018). *Novel laccase-like multicopper oxidases from the Myrothecium roridum fungus-production enhancement, identification and application in the dye removal process*. Acta Biochimica Polonica. DOI: 10.18388/abp.2017_2546.

IF = 1,626; MNiSW = 15

8. Nowak M, **Soboń A**, Litwin A, Różalska S. (2019). *4-n-nonylphenol degradation by the genus Metarhizium with cytochrome P450 involvement*. Chemosphere, 220, 324-334.

IF = 4,571; MNiSW = 100

9. Jasińska A, Góralczyk-Bińkowska A, **Soboń A**, Długoński J. (2019). *Lignocellulose resources for the Myrothecium roridum laccase production and their integrated application for dyes removal*. International Journal of Environmental Science and Technology, 1-12.

IF = 2,031; MNiSW = 70

10. Jasińska A, **Soboń A**, Góralczyk-Bińkowska A, Długoński J. (2019). *Analysis of decolorization potential of Myrothecium roridum in the light of its secretome and toxicological studies*. Environmental Science and Pollution Research, 26(25), 26313-26323.

IF = 2,914; MNiSW = 70

Sumaryczny IF = 30,12

Łączna liczba punktów MNiSW = 455

Indeks H = 5

Wartość IF oraz punktację MNiSW podano zgodnie z rokiem opublikowania.

IV. Streszczenie w języku polskim

Organiczne związki cyny ze względu na pełnienie funkcji stabilizatorów polichloru poliwynylu (PCW) oraz wysoką skuteczność biobójczą znalazły szerokie zastosowanie w przemyśle i rolnictwie. Wprowadzone do środowiska wywołują wiele niekorzystnych zmian w organizmach. Spośród nich, szczególnie wysoką toksycznością charakteryzuje się tributyllocyna. Proces mikrobiologicznego rozkładu TBT jest dotychczas słabo poznany, chociaż stanowi jedno z głównych źródeł eliminacji tego związku ze środowiska. W prezentowanej pracy oceniono zdolność do degradacji TBT przez grzyb strzępkowy *Cunninghamella echinulata* IM 2611. Określono ponadto wpływ TBT na morfologię i aktywność metaboliczną grzybni, a także zbadano jakie zmiany zachodzą w profilu metabolomicznym i białkowym w wyniku ekspozycji drobnoustroju na badany ksenobiotyk. Badania przeprowadzono z wykorzystaniem szeregu technik analitycznych, opartych przede wszystkim o spektrometrię mas (GC-MS, LC-MS/MS i MALDI-TOF/TOF) i techniki elektromigracyjne (1- i 2-DE). Uzyskane dane analizowano z wykorzystaniem specjalistycznego oprogramowania komputerowego. Przeprowadzone badania wykazały, że grzyb *C. echinulata* IM 2611 był zdolny do eliminacji ponad 90% ksenobiotyku w ciągu 120 godzin hodowli przy stężeniu wyjściowym wynoszącym 5 mg/l. Jednocześnie stwierdzono, że TBT ulega przekształceniu do dibutyllocyny (DBT), monobutyllocyny (MBT) oraz hydroksylowanej pochodnej TBT. Wstępne analizy uwiaryściły zmiany w profilu aminokwasów oraz białek badanego mikroorganizmu i stanowiły punkt wyjścia do rozszerzenia badań nad nimi w dalszych częściach pracy. Wykazano, że obecność ksenobiotyku w hodowli niekorzystnie wpływała na drobnoustrój, co przejawiało się silnym zahamowaniem przyrostu biomasy, połączonym ze spadkiem aktywności metabolicznej grzybni oraz zmniejszonym wykorzystaniem glukozy i wybranych aminokwasów z podłoża hodowlanego. Na podstawie analizy mikroskopowej stwierdzono plazmolizę i wakuolizację cytoplazmy. Wymienionym wyżej zjawiskom towarzyszyły również zmiany w profilu metabolomicznym drobnoustroju. Odnotowano wzrost stężenia metabolitów glikolizy przy jednoczesnym spadku zawartości związków cyklu Krebsa. Pod wpływem TBT, grzyb strzępkowy

zwiększał produkcję związków o właściwościach antyoksydacyjnych (betaina, prolina, kwas γ -aminomasłowy).

Uzyskane wyniki sugerujące zachodzenie istotnych zmian w profilu białkowym grzyba w obecności ksenobiotyku wskazały na konieczność wykonania pogłębionych badań proteomicznych podczas biodegradacji TBT. Przeprowadzona analiza proteomu wykazała indukcję procesów biochemicznych ukierunkowanych na zwiększenie syntezy ATP. Zaobserwowano również nadprodukcję białek i enzymów zaangażowanych w ochronę komórki przed stresem oksydacyjnym, której towarzyszyła zwiększona produkcja reaktywnych form tlenu (RFT) oraz wzrost aktywności dysmutazy ponadtlenkowej (SOD). Odnotowano także wzmożoną biosyntezę prohibityny, białka odgrywającego istotną rolę w prawidłowym funkcjonowaniu mitochondriów. Z kolei nadprodukcja nukleazy C1 może być związana z ochroną DNA przed uszkodzeniami.

Wyniki uzyskane w trakcie realizacji niniejszej pracy doktorskiej przyczyniły się do wyodrębnienia szczepu grzybowego zdolnego do wydajnej biotransformacji TBT. Przeprowadzone badania wykazały niekorzystny wpływ ksenobiotyku na grzybnie *C. echinulata* IM 2611, wskazując jednocześnie mechanizmy odpowiedzialne za oporność drobnoustroju na wysokie stężenie ksenobiotyku przy jednoczesnej wydajnej eliminacji tego związku ze środowiska wzrostu. Zastosowanie zaawansowanych, nowoczesnych technik analitycznych pozwoliło zidentyfikować mechanizmy komórkowe zaangażowane w przeciwdziałanie niekorzystnym zmianom wywołanym obecnością ksenobiotyku w środowisku wzrostu grzyba. Analizy zmian metabolomu i proteomu grzyba poddanego ekspozycji na TBT miały charakter nowatorski i nie były dotychczas przedmiotem badań.

V. Streszczenie w języku angielskim

Due to their role as polyvinyl chloride (PVC) stabilizers and high biocidal effectiveness, organic tin compounds have found wide applications in industry and agriculture. When they are introduced into the environment, they cause many adverse changes in organisms. Among these harmful substances, tributyltin is characterized by particularly high toxicity. The process of microbial degradation of TBT is still poorly understood, although it is one of the main methods of eliminating this compound from the environment. In the presented work, the ability of the filamentous fungus *Cunninghamella echinulata* IM 2611 to degrade TBT was assessed. The effect of TBT on the morphology and metabolic activity of the mycelium was determined. Also, changes in the metabolomic and protein profile as a result of exposure of the microorganism to the xenobiotic were examined. The research was carried out using a number of analytical techniques, primarily based on mass spectrometry (GC-MS, LC-MS/MS and MALDI-TOF/TOF) as well as electromigration techniques (1- and 2-DE). The obtained data were analyzed using specialized computer software. The study showed that the fungus *C. echinulata* IM 2611 was able to eliminate over 90% of the xenobiotic at the initial concentration of 5 m/l during 120 hours of cultivation. At the same time, TBT was found to be converted to dibutyltin (DBT), monobutyltin (MBT) and a hydroxylated TBT derivative. Initial analyses revealed changes in the profile of amino acids and proteins of the studied microorganism and became the starting point for extending the research in further parts of the work. It was shown that the presence of the xenobiotic in the culture adversely affected the microorganism, which was manifested by a strong inhibition of biomass growth, combined with a decrease in the metabolic activity of mycelium and reduced use of glucose and selected amino acids from the culture medium. During the microscopic analysis, plasmolysis and vacuolization of the cytoplasm were observed. These phenomena were accompanied by changes in the metabolomic profile of the microorganism. An increase in the concentration of glycolysis metabolites with a simultaneous decrease in the content of Krebs cycle compounds was noted. Under the influence of TBT, the filamentous fungus increased the production of compounds with antioxidant properties (betaine, proline, γ -aminobutyric acid).

The obtained results, which revealed significant changes in the protein profile of the fungus in the presence of TBT, indicated the need for in-depth proteomic studies during its biodegradation. The performed proteome analysis showed that in response to a decrease in the ATP concentration in fungal cells, resulting from the inhibitory effect of TBT on ATP synthase, the microorganism induced biochemical processes aimed at increasing ATP synthesis. Overproduction of proteins and enzymes involved in cell protection against oxidative stress was also observed, which was correlated with an intensified generation of reactive oxygen species (RFT) and an increase in superoxide dismutase (SOD) activity. Increased biosynthesis of prohibitin, a protein that plays an important role in the proper functioning of mitochondria, was also noted. Overproduction of C1 nuclease might have been associated with DNA protection against damage.

The results obtained during the implementation of this dissertation contributed to the isolation of a fungal strain capable of efficient TBT biotransformation. The metabolomic and proteomic analyses of the microorganism exposed to TBT were innovative and had not been performed before. The conducted experiments showed the adverse effect of the xenobiotic on the mycelium of *C. echinulata* IM 2611, at the same time indicating the mechanisms responsible for the resistance of the microorganism to the high concentration of the xenobiotic with its simultaneous effective elimination from the growth environment. The use of advanced, modern analytical techniques allowed identifying cellular mechanisms involved in counteracting adverse changes caused by the presence of xenobiotics in the fungal growth environment.

VI. Wprowadzenie

Przemysłowa działalność człowieka i intensywny rozwój rolnictwa przyczyniły się do wprowadzenia do środowiska naturalnego wielu nowych związków, które nie są naturalnymi składnikami żywych organizmów. Substancje takie nazywane są ksenobiotykami. Do tej grupy należą między innymi związki metaloorganiczne, w tym organiczne związki cyny. Zawierają one w swych strukturach atomy cyny połączone kowalencyjnie z jednym lub większą liczbą podstawników organicznych, którymi mogą być grupy metylowe, etylowe, butylowe, propylowe lub fenyłowe (Hoch, 2001). Związki cynoorganiczne można scharakteryzować ogólnym wzorem $R(4-n)SnX_n$, gdzie R oznacza grupę organiczną, X – podstawnik nieorganiczny, zaś n przyjmuje wartości od 0 do 3. Obecność określonych podstawników alifatycznych determinuje właściwości fizykochemiczne związku, a także decyduje o jego toksyczności. Najwyższą toksycznością wobec organizmów o różnej przynależności taksonomicznej charakteryzują się trójpodstawione połączenia cynoorganiczne, przy czym ich toksyczność maleje w miarę wydłużania się łańcucha *n*-alkilowego (Falandysz, 2003).

Jednym z głównych przedstawicieli związków cynoorganicznych, uważanym jednocześnie za jeden z najbardziej toksycznych związków wprowadzonych dotychczas do środowiska morskiego jest tributyllocyna (TBT), znajdująca się na liście priorytetowych substancji niebezpiecznych. (Cruz i wsp. 2015). Ze względu na wysoką aktywność biocydobójczą, związek ten jest wykorzystywany w wielu dziedzinach przemysłu, w rolnictwie, konserwacji tekstyliów i ochronie drewna (Sousa i wsp. 2014). Przez szereg lat był wykorzystywany jako składnik farb przeciwporostowych, którymi pokrywano kadłuby statków i konstrukcji podwodnych (Antizar-Ladislao, 2008). W wyniku tego obecność TBT odnotowano w wodach i osadach dennych, szczególnie znajdujących się w pobliżu portów oraz stoczni. W wodzie okres połowicznego rozpadu związku waha się od kilku dni do kilku tygodni, podczas gdy w osadach dennych ksenobiotyk ten utrzymuje się nawet do kilkudziesięciu lat (de Carvalho Oliveira i Santelli, 2010). Uwalnianie TBT do środowiska naturalnego i akumulacja tego związku w tkankach organizmów żywych stanowią poważne zagrożenie dla funkcjonowania ekosystemów ze względu na szerokie spektrum toksycznego oddziaływania. Badania toksykologiczne wykazały,

że TBT charakteryzuje się efektem cyto-, geno-, embrio-, immuno- czy neurotoksycznym wobec organizmów reprezentujących różne poziomy troficzne (Antizar-Ladislao, 2008). Szkodliwy wpływ na organizmy wynika z lipofilnego charakteru cząsteczki TBT, która może oddziaływać na błony biologiczne, w wyniku czego naruszona zostaje ich integralność i przepuszczalność (Bonarska-Kujawa i wsp. 2012). Szczególnie niekorzystnie ksenobiotyk oddziałuje na funkcjonowanie mitochondriów, co skutkuje zmianą ich potencjału błonowego (Tiano i wsp. 2003). Tym samym biocyd zaburza szlak fosforylacji oksydacyjnej sprzężonej z łańcuchem oddechowym, co w połączeniu z udokumentowaną inhibicją syntazy ATP przyczynia się do znacznego zahamowania syntezy ATP - związku kluczowego do prawidłowego funkcjonowania komórki (Nesci i wsp. 2011; Von Ballmoos i wsp. 2004). Wykazano, że TBT indukuje stres oksydacyjny, prowadzący m. in. do peroksydacji lipidów (Bernat i wsp. 2014) czy uszkodzenia DNA (Liu i wsp. 2006). Z kolei stres oksydacyjny i związane z nim uszkodzenia struktur komórkowych, jak również wzrost stężenia wapnia w komórkach prowadzą do apoptozy komórki (Mitra i wsp. 2013; Nakatsu i wsp. 2007). Stwierdzony wpływ ksenobiotyku na metabolizm lipidów, objawiający się zmianami w profilu fosfolipidów może być reakcją obroną organizmu polegającą na zmniejszeniu przepuszczalności błon komórkowych i zwiększenia zawartości jonów potasu w komórce (Bernat i wsp. 2009). Negatywny wpływ TBT na struktury komórkowe przejawia się także dezorganizacją białek cytoszkieletu (Cima i wsp. 1998).

Oprócz silnie toksycznych właściwości, ksenobiotyk ten wykazuje również działanie androgenne, dlatego zaliczany jest do substancji zaburzających gospodarkę hormonalną organizmu (EDCs, ang. *Endocrine Disrupting Compounds*) (Falandysz, 2003). Ekspozycja na TBT powoduje pseudohermafrodytyzm u skorupiaków, czyli wytworzenie dodatkowych męskich narządów płciowych u osobników płci żeńskiej, jak również upośledzeniem wzrostu, rozwoju i cyklu rozrodczego organizmów morskich (Falandysz, 2003; Antizar-Ladislao, 2008).

W eliminacji TBT ze środowiska mogą brać udział mikroorganizmy. Związek ten może być usuwany poprzez biosorpcję lub degradowany w wyniku aktywności metabolicznej drobnoustrojów. Proces mikrobiologicznej biotransformacji TBT polega na stopniowym odłączaniu grup alifatycznych od atomu cyny, prowadzącym

do powstania dibutylocyny (DBT) i monobutylocyny (MBT) oraz ich hydroksylowanych pochodnych (Bernat i wsp. 2013). Uwagę badaczy przykuwają mechanizmy odpowiedzialne za oporność mikroorganizmów oraz zdolność do eliminacji tego ksenobiotyku. Tworzenie hydroksylowanych pochodnych oraz ograniczenie biodegradacji TBT w obecności inhibitorów cytochromu P-450 wskazuje na udział tego układu enzymatycznego w eliminacji ksenobiotyku (Bernat i Długoński, 2002).

W ostatnich latach notuje się znaczący wzrost zainteresowania technikami „omicznymi”, takimi jak proteomika czy metabolomika. Zaliczane są one to nowej dyscypliny naukowej - biologii systemowej, dążącej do holistycznej oceny funkcjonowania układu biologicznego (Silberring i Drabik, 2010). Proteomika jest gałęzią nauki skupiającą się na całościowej analizie i identyfikacji białek organizmu, tkanki, bądź komórki, zaś metabolomika obejmuje ilościowe i jakościowe oznaczanie związków endogennych – metabolitów (Szewczyk i Kowalski, 2016a,b). Są to stosunkowo młode dziedziny wiedzy, niezwykle pomocne w zrozumieniu zjawisk zachodzących w komórce, które wraz z pozostałymi elementami biologii systemowej prowadzą do uzyskania pełnej wiedzy o analizowanym systemie.

Pomimo licznych doniesień uwidaczniających szkodliwe oddziaływanie TBT na organizmy, wiedza na temat wpływu tego związku na metabolizm komórkowy, jak i mechanizmy molekularne odpowiedzialne za oporność bądź zdolność drobnoustrojów do jego degradacji jest ograniczona. Poznanie mechanizmów komórkowych umożliwia wytypowanie kluczowych białek odpowiedzialnych za proces detoksykacji ksenobiotyku, co może być pomocne w projektowaniu metod mikrobiologicznej eliminacji takiego związku ze skażonego środowiska. Dlatego celowe wydaje się badanie wpływu związków cynoorganicznych na metabolizm organizmów i poznanie mechanizmów warunkujących oporność na nie, co stanowi przedmiot prezentowanych w tej pracy badań.

VII. Cele pracy

Główne cele badań przeprowadzonych podczas realizacji pracy doktorskiej obejmowały:

1. Określenie zdolności grzyba strzępkowego *Cunninghamella echinulata* IM 2611 do degradacji TBT.
2. Ocenę wpływu TBT na wzrost, aktywność metaboliczną oraz morfologię drobnoustroju.
3. Analizę metabolomu i proteomu *C. echinulata* w czasie ekspozycji na TBT.

VIII. Metodologia badań

VIII. 1. Techniki wykorzystywane podczas realizacji pracy doktorskiej

Techniki	Zakres badań
Chromatografia gazowa sprzężona ze spektrometrią mas GC-MS	<ul style="list-style-type: none">• Oznaczenia ilościowe TBT i produktów jej degradacji
Chromatografia cieczowa sprzężona ze spektrometrią mas LC-MS/MS	<ul style="list-style-type: none">• Oznaczenia jakościowe produktów biotransformacji TBT• Ilościowa ocena zawartości metabolitów
Spektrofluorymetria	<ul style="list-style-type: none">• Ocena wpływu badanego ksenobiotyku na aktywność metaboliczną mikroorganizmu
Mikroskopia konfokalna	<ul style="list-style-type: none">• Określenie wpływu TBT na morfologię strzępek• Oznaczenia ilościowe reaktywnych form tlenu (RFT)
Elektroforeza 1-D oraz 2-D	<ul style="list-style-type: none">• Analizy zmian profilu białkowego drobnoustroju
Spektrometria mas MALDI-TOF/TOF	<ul style="list-style-type: none">• Oznaczenie peptydów

VIII. 2. Oprogramowanie

W pracy doktorskiej do analizy wyników wykorzystano szereg specjalistycznych programów komputerowych:

- PeakView (Sciex) to oprogramowanie służące do analizy widm masowych, które w prezentowanej pracy zostało zastosowane do identyfikacji hydroksylowanej pochodnej (TBTOH) i określeniu miejsca przyłączenia grupy hydroksylowej do cząsteczki ksenobiotyku.
- LightSight (Sciex) – oprogramowanie dedykowane do systemu LC-MS firmy Sciex wspomagające poszukiwanie metabolitów. Algorytm tej aplikacji na podstawie widma masowego związku wyjściowego generuje możliwe kombinacje par MRM potencjalnych metabolitów, tworząc gotową metodę do zastosowania w systemie LC-MS. Program umożliwia wgląd w uzyskany chromatogram oraz pozwala na jednoczesne porównanie widm masowych związku wyjściowego oraz jego potencjalnego metabolitu. W prezentowanej pracy oprogramowanie zostało wykorzystane do stworzenia szeregu metod analitycznych LC-MS służących poszukiwaniu metabolitów fazy I i II metabolizmu ksenobiotyku.
- MarkerView (Sciex) to aplikacja umożliwiająca wykonanie analiz statystycznych (np. PCA, *ang.* Principal Component Analysis) wyników uzyskanych techniką LC-MS. W pracy doktorskiej przeprowadzono analizy głównych składowych w celu poprawnej interpretacji wyników.
- MultiQuant (Sciex) to oprogramowanie służące do przetwarzania danych uzyskanych podczas analiz z wykorzystaniem spektrometrów masowych. W pracy doktorskiej MultiQuant został wykorzystany do ilościowej oceny zawartości metabolitów.
- Image Lab (Bio-Rad) – aplikacja wykorzystywana do analizy densytometrycznej białek rozdzielonych techniką 1-DE. W pracy **P1** przy jego pomocy określono zmiany profilu białkowego *C. echinulata*.
- Image Master 2D Platinum (GE Healthcare) to program do wizualizacji i analizy danych żeli 2-D. W pracy doktorskiej został wykorzystany do oznaczania i porównania spotów białek uzyskanych podczas elektroforezy dwukierunkowej.

- ProteinPilot (Sciex) to oprogramowanie umożliwiające identyfikację białek, które wykorzystuje algorytmy przeszukiwania bazy danych MASCOT oraz PARAGON będący autorskim algorytmem firmy Sciex. Sekwencjom białek zdeponowanych w bazach danych pochodzących z National Center for Biotechnology Information (NCBI) algorytm przypisuje widma fragmentacyjne peptydów uzyskanych w wyniku uprzedniej proteolizy białka z użyciem dedykowanego enzymu, którym w przypadku niniejszej pracy była tripsyna. W pracy wykorzystano to oprogramowanie do identyfikacji białek badanego drobnoustroju na podstawie widm masowych uzyskanych podczas analiz z zastosowaniem spektrometrów mas QTRAP oraz MALDI-TOF/TOF.

IX. Syntetyczne omówienie wyników przedstawionych w cyklu publikacji wchodzących w skład rozprawy doktorskiej

Eliminacja TBT przez grzyby jest stosunkowo słabo poznana. W literaturze przedmiotu został opisany tylko jeden szczep grzybowy (*C. elegans* IM 1785/21Gp) zdolny do efektywnej degradacji TBT z wytworzeniem mniej toksycznych pochodnych – DBT oraz MBT. Podczas badań skriningowych prowadzonych w Katedrze Mikrobiologii Przemysłowej i Biotechnologii UŁ z moim udziałem, stwierdzono, że wyodrębniony wcześniej z gleby szczep grzybowy IM 2611, oznaczony jako *C. echinulata*, jest zdolny do wzrostu w obecności TBT i prawie całkowitej eliminacji ksenobiotyku przy stężeniu wyjściowym toksycznego substratu 5 mg/l, co stało się podstawą do wybrania go jako obiektu badań w prezentowanej pracy doktorskiej.

W pierwszej pracy składającej się na niniejszą rozprawę doktorską (P1 – Soboń A, Szewczyk R, Długoński J (2016), *Tributyltin (TBT) biodegradation induces oxidative stress of Cunninghamella echinulata*; International Biodeterioration and Biodegradation 107, 92-101) zawarto wyniki opisujące dynamikę eliminacji ksenobiotyku wraz z ilościową i jakościową oceną powstających pochodnych oraz analizę zmian w poziomie aminokwasów i białek wewnątrzkomórkowych. Szczep *C. echinulata* IM 2611 wydajnie degraduje TBT w stężeniu wyjściowym 5 mg/l, eliminując 91% początkowej zawartości ksenobiotyku w czasie 120 godzin hodowli. Procesowi temu towarzyszył wzrost zawartości produktów degradacji biocydu, głównie DBT, obserwowany od 48 godziny hodowli. Przeprowadzono szereg analiz z wykorzystaniem chromatografu cieczowego sprzężonego z tandemowym spektrometrem mas (LC-MS/MS) oraz oprogramowaniem LightSight™ (Sciex), ukierunkowanych na poszukiwanie potencjalnych produktów metabolizmu ksenobiotyku. Na podstawie otrzymanych wyników stwierdzono obecność hydroksylowanej pochodnej TBT, zaś przeprowadzone z wykorzystaniem spektrometru mas oznaczenia widm masowych badanego związku cynoorganicznego uwzględniające charakterystyczny profil izotopowy pierwiastka cyny wykazały, iż grupa hydroksylowa jest przyłączona bezpośrednio do atomu cyny. Jednocześnie, zaobserwowano silne zahamowanie

wzrostu drobnoustroju w podłożu hodowlanym w obecności ksenobiotyku, szczególnie podczas pierwszych 48 godzin inkubacji. Należy również zaznaczyć, że dynamika procesu degradacji TBT była skorelowana ze wzrostem drobnoustroju. Zaobserwowane początkowe silne zahamowanie wzrostu mikroorganizmu, a następnie intensywny przyrost biomasy, wskazują na zmiany biochemiczne zachodzące w komórce. Obserwacja ta posłużyła jako punkt wyjścia do dalszych badań. W związku z tym, eksperymenty rozszerzono o nieukierunkowaną analizę wewnątrzkomórkowego profilu aminokwasowego. Zaobserwowano istotne statystycznie różnice w zawartości 19 spośród 26 aminokwasów oznaczonych w hodowlach zawierających TBT w porównaniu do kontroli. Stwierdzono, że TBT w zróżnicowany sposób wpływa na profil aminokwasowy u badanego drobnoustroju. Zaobserwowano zwiększenie stężenia betainy i proliny, które mogą być związane z odpowiedzią drobnoustroju na stres oksydacyjny..

Na tym etapie pracy, dokonano również wstępnej oceny wpływu ksenobiotyku na zmiany profilu białkowego badanego grzyba strzępkowego Wewnątrzkomórkowe białka *C. echinulata* rozdzielono elektroforetycznie techniką jednokierunkowej elektroforezy (1-DE, ang. 1-Dimensional Electrophoresis), a następnie 22 prążki białkowe poddano analizie porównawczej i identyfikacji z wykorzystaniem techniki LC-MS/MS. Obecność biocydu w środowisku indukowała wzrost biosyntezy białek związanych z cyklem Krebsa (dehydrogenaza jabłczanowa), glikolizą (enolazą), syntezą ATP (syntaza ATP), syntezą aminokwasów (metylotransferaza tetrahydropteroglutaminowa homocysteiny). W obecności TBT stwierdzono także wzrost syntezy peroksyredoksyny, co wraz z akumulacją betainy i proliny wskazuje na istotną rolę komórkowych mechanizmów antyoksydacyjnych w odpowiedzi na pojawienie się tego ksenobiotyku. Z kolei nukleaza C1, której nadprodukcję również stwierdzono w obecności TBT, może być związana z ochroną komórki przed uszkodzeniami DNA. Zaobserwowane zmiany biochemiczne w komórkach badanego mikroorganizmu stanowiły punkt wyjścia do przeprowadzenia rozszerzonych badań metabolomicznych (**P2**) oraz proteomicznych (**P3**) w dalszych częściach pracy.

Metabolomika to stosunkowo młoda i intensywnie rozwijająca się dziedzina biologii systemowej, mająca na celu całościową analizę metabolitów (metabolomu)

obecnych w danym czasie i warunkach w komórce. Uzyskane dzięki niej wyniki umożliwiają badanie dynamiki zmian biochemicznych zachodzących w badanym układzie pod wpływem różnych czynników zewnętrznych, takich jak np. ekspozycja na ksenobiotyki. **Kolejna praca wchodząca w skład rozprawy doktorskiej (P2 – Soboń A, Szewczyk R, Różalska S, Długoński J (2018), *Metabolomics of the recovery of the filamentous fungus Cunninghamella echinulata exposed to tributyltin*; International Biodeterioration and Biodegradation 127, 130-138)** obejmowała ukierunkowaną analizę metabolomiczną 92 metabolitów komórkowych znajdujących się w komórkach *C. echinulata* oraz w podłożu wzrostowym. Badania te zostały rozszerzone o pomiary dynamiki wykorzystania glukozy z podłoża hodowlanego przez mikroorganizm, pozwalające na ocenę aktywności metabolicznej drobnoustroju. W strzępkach grzyba pochodzących z 24-godzinnych hodowli inkubowanych z dodatkiem TBT stwierdzono zwiększone stężenie związków powstających w procesie glikolizy (glukozo-6-fosforan, fruktozo-6-fosforan, fosfoenolopirogronian) oraz zmniejszoną zawartość wszystkich metabolitów występujących w cyklu Krebsa (za wyjątkiem szczawiooctanu). W komórkach poddanych ekspozycji na ksenobiotyk wykazano wzrost stężenia związków wykazujących antyoksydacyjne właściwości w komórkach - betainy, proliny i kwasu γ -aminomasłowego (GABA), a także odnotowano nagromadzenie kwasu glutaminowego, będącego prekursorem do syntezy tych związków. Dodatkowo, zmniejszona zawartość lizyny i zwiększony poziom kwasu 2-aminoadipowego przy jednoczesnym niewielkim wykorzystaniu lizyny zawartej w podłożu hodowlanym sugeruje aktywację szlaku biosyntezy lizyny u badanego grzyba w trakcie ekspozycji na ksenobiotyk.

Interesujące wyniki uzyskano podczas oceny zawartości metabolitów w podłożu wyjściowym oraz pohodowlanym. Analiza składu podłoż po 24-godzinnej inkubacji z dodatkiem biocydu wykazała podobny profil metabolitów do wyjściowego podłoża hodowlanego (bez dodatku mikroorganizmu). Z kolei w układzie kontrolnym (niezawierającym TBT) grzyb strzępkowy po 24 godzinach hodowli wykorzystał większość oznaczanych związków wchodzących w skład podłoża. W kolejnych godzinach hodowli w układach niezawierających ksenobiotyku zaobserwowano zwiększoną sekrecję kwasów organicznych do

podłoża, co powoduje szybsze zakwaszanie środowiska i tym samym stymuluje zwiększenie przyswajania substancji odżywczych z podłoża. Zjawiska tego nie stwierdzono w hodowlach z TBT. Wykazano, że obecność TBT w podłożu skutkuje znacznie wolniejszym spadkiem wartości pH, w porównaniu do hodowli kontrolnych. Po 24 godzinach inkubacji, wartość pH w układzie z TBT była zbliżona do wyjściowej wartości pH podłoża. Zaobserwowano również zahamowanie wykorzystania glukozy w hodowlach suplementowanym ksenobiotykiem w początkowym okresie inkubacji. Spowolnienie wzrostu grzyba w czasie ekspozycji na TBT, połączone ze zmniejszoną asymilacją glukozy oraz związków organicznych z podłoża, skłoniły do zbadania żywotności grzybni za pomocą zmodyfikowanej metody z wykorzystaniem diocjanu fluoresceiny (FDA) oraz oceny wpływu badanego związku na morfologię strzępek. Przeprowadzona analiza wykazała statystycznie istotną inhibicję aktywności metabolicznej drobnoustroju w kontakcie z TBT. Po 24 godzinach, w próbach z dodatkiem ksenobiotyku stwierdzono 3,9% aktywności metabolicznej w stosunku do układu kontrolnego. W kolejnych dobach hodowli zaobserwowano stopniowy wzrost tego parametru, aż do osiągnięcia wartości 50,85% po 120 godzinach inkubacji. Równolegle przeprowadzone obserwacje mikroskopowe z wykorzystaniem mikroskopii konfokalnej uwiarygodniły wysoce niekorzystne działanie ksenobiotyku na strzępki, objawiające się silną wakuolizacją oraz plazmolizą komórek. Najwięcej zmian wykazano po 24 godzinach inkubacji i zanikały one wraz z czasem trwania hodowli.

Reasumując tę część badań można stwierdzić, że pomimo toksycznego wpływu związku na strzępki grzyba, drobnoustrój aktywnie przeciwdziałal niekorzystnym zmianom w komórce indukowanym przez ksenobiotyk poprzez akumulację związków pełniących ochronną rolę w warunkach stresu oksydacyjnego i zaburzonej osmoregulacji komórki.

Białka pełnią kluczową rolę we wszystkich procesach biologicznych. Są odpowiedzialne za zmiany zawartości metabolitów, które omówiono we wcześniejszych pracach (**P1 i P2**). Przeprowadzona analiza 1-DE białek wewnątrzkomórkowych badanego szczepu zaprezentowana w pracy **P1** wykazała występowanie różnic w profilu białkowym *C. echinulata*, indukowanych obecnością ksenobiotyku w podłożu hodowlanym. Dlatego też, **trzecia praca składająca się na**

niniejszą rozprawę doktorską obejmowała analizę zmian w proteomie badanego grzyba wywołanych ekspozycją na TBT, jak również ocenę zawartości wolnych rodników w strzępkach mikroorganizmu (**P3** – Soboń A, Szewczyk R, Długoński J, Różalska S. (2019), *A proteomic study of Cunninghamella echinulata recovery during exposure to tributyltin*; Environmental Science and Pollution Research, 1-14). Analizie porównawczej poddano białka rozdzielone techniką dwukierunkowej elektroforezy (2-DE, *ang.* 2-Dimensional Electrophoresis), pochodzące z 24, 48, 72 i 96 godziny hodowli z układów zawierających oraz niezawierających TBT (układ kontrolny). Przeprowadzona ocena obrazów 2-DE z wykorzystaniem dedykowanego oprogramowania Image Master 2-D Platinum (GE Healthcare) umożliwiła detekcję średnio 116 plam proteinowych na żel, spośród których zidentyfikowano i dopasowano aż 92 białka, dla których wyznaczono względny poziom ekspresji. Stwierdzono różnice w profilu białkowym grzyba rosnącego w obecności toksycznego związku. Najistotniejsze zmiany zaobserwowano po 24 godzinach inkubacji. Przeprowadzone badania uwidoczniły zwiększoną biosyntezę białek związanych z produkcją energii na drodze oddychania komórkowego, co wskazuje na jej deficyt w komórce, skutkujący zahamowaniem przyrostu biomasy czy zmniejszoną aktywnością metaboliczną. Stwierdzono zwiększony poziom biosyntezy enzymów zaangażowanych w szlak glikolizy oraz nadprodukcję dehydrogenazy NADH (kompleks I łańcucha oddechowego) i dehydrogenazy jabłczanowej. Odnotowano zwiększony poziom oksydazy cytochromu c, jak również katalitycznie aktywnych podjednostek syntazy ATP oraz pirofosfatazy nieorganicznej, czyli elementów bezpośrednio zaangażowanych w wytwarzanie ATP. Uzyskane dane wskazują na indukcję szlaków odpowiedzialnych za wytworzenie NADH, jego utlenienie przez dehydrogenzę NADH z jednoczesnym wytworzeniem gradientu elektrochemicznego, redukcji tlenu i zwiększenia gradientu protonowego poprzez ostatni element łańcucha transportu elektronów - oksydazę cytochromu c. Wytworzony gradient elektrochemiczny wykorzystywany jest do produkcji ATP przez syntazę ATP. Szlak oksydacji fosforylacyjnej jest głównym miejscem powstawania RFT, a funkcjonujący nieprawidłowo może prowadzić do zwiększonego generowania tych form tlenu w komórkach. W 24-godzinnej hodowli w obecności TBT stwierdzono w strzępkach dużą ilość RFT, która malała wraz z czasem trwania hodowli, podczas gdy w układzie kontrolnym zaobserwowano ich

niewielką ilość przez cały okres trwania hodowli. Grzybnia poddana ekspozycji na TBT charakteryzowała się zwiększonym poziomem białek Hsp70 i Hsp71 uważanych za markery stresu oksydacyjnego. W komórkach grzybowych hodowanych na podłożu zawierającym TBT wykazano wzrost aktywności dysmutazy ponadtlenkowej (SOD), podczas gdy aktywność katalazy (CAT) utrzymywała się na niskim, zbliżonym poziomie, w obu analizowanych układach. Jednocześnie, zaobserwowano w nich zwiększoną biosyntezę enzymów o właściwościach antyoksydacyjnych, takich jak dysmutaza nadtlenkowa cynkowo-miedzianowa (Cu-Zn) i manganowa (Mn), tioredoksyny czy redoksyna. Nadprodukcja tych enzymów była skorelowana ze zwiększonym wytwarzaniem RFT w strzępkach badanego grzyba. Co istotne, do prawidłowego funkcjonowania tioredoksyny czy dysmutaz nadtlenkowych kluczowa jest obecność NADPH, produkowanego głównie w szlaku pentozofosforanowym. W hodowlach inkubowanych z ksenobiotykiem stwierdzono zwiększoną biosyntezę enzymów tego szlaku - transaldolazy i dehydrogenazy 6-fosfoglukonianowej, zwiększających pulę równoważników redukujących niezbędnych do przeprowadzania szeregu reakcji redukcji w komórce. Natomiast wzrost produkcji białek cytoszkieletu (aktyna, tubulina) może być związany z przeciwdziałaniem niekorzystnym zmianom morfologicznym, które zaobserwowano w strzępkach grzyba podczas ekspozycji na TBT.

Odnotowano również zwiększoną zawartość prohibityny. Jest to wielofunkcyjne białko, niezbędne do prawidłowego funkcjonowania mitochondriów, uczestniczące również w ochronie komórki przed stresem oksydacyjnym. Z uwagi na fakt, że TBT niekorzystnie oddziałuje są procesy zachodzące w tym organelum, zwiększona biosynteza prohibityny u badanego grzyba może być odpowiedzialna za jego zdolność do wzrostu w obecności TBT, jak i biodegradację tego związku.

Wyniki przedstawione w pracy P3 wskazują na złożoną odpowiedź komórek badanego grzyba strzępkowego w obecności TBT. Procesy biochemiczne w grzybni poddanej ekspozycji na TBT ukierunkowane są głównie na zwiększenie produkcji ATP i równoważników redukujących przy jednoczesnym przeciwdziałaniu skutkom stresu oksydacyjnego i toksycznego oddziaływania samej cząsteczki TBT.

P1

***Tributyltin (TBT) biodegradation induces oxidative stress
of Cunninghamella echinulata***

SOBOŃ A, SZEWCZYK R, DŁUGOŃSKI J

International Biodeterioration and Biodegradation

doi: 10.1016/j.biod.2015.11.013



Contents lists available at ScienceDirect

International Biodeterioration & Biodegradation

journal homepage: www.elsevier.com/locate/ibiod

Tributyltin (TBT) biodegradation induces oxidative stress of *Cunninghamella echinulata*



Adrian Soboń, Rafał Szewczyk, Jerzy Długoński*

Department of Industrial Microbiology and Biotechnology, Institute of Microbiology, Biotechnology and Immunology, Faculty of Biology and Environmental Protection, University of Łódź, Banacha 12/16, 90-237 Łódź, Poland

ARTICLE INFO

Article history:

Received 3 October 2015

Received in revised form

11 November 2015

Accepted 11 November 2015

Available online xxx

Keywords:

Fungi

Tributyltin

Biodegradation

LC-MS/MS

Proteomics

Oxidative stress

ABSTRACT

Tributyltin (TBT) is one of the most deleterious compounds introduced into natural environment by humans. The ability of *Cunninghamella echinulata* to degrade tributyltin (TBT) (5 mg l^{-1}) as well as the effect of the xenobiotic on fungal amino acids composition and proteins profile were examined. *C. echinulata* removed 91% of the initial biocide concentration and formed less hazardous compounds dibutyltin (DBT) and monobutyltin (MBT). Moreover, the fungus produced a hydroxylated metabolite (TBT-OH), in which the hydroxyl group was bound directly to the tin atom. Proteomics analysis showed that in the presence of TBT, the abundances of 22 protein bands were changed and the unique over-expressions of peroxiredoxin and nuclease enzymes were observed. Determination of free amino acids showed significant changes in the amounts of 19 from 23 detected metabolites. A parallel increase in the level of selected amino acids such as betaine, alanine, aminoisobutyrate or proline and peroxiredoxin enzyme in TBT-containing cultures revealed that TBT induced oxidative stress in the examined fungus.

© 2015 Elsevier Ltd. All rights reserved.

1. Introduction

Endocrine-disrupting compounds (EDCs) are a large group of exogenous chemicals that cause adverse health effects in numerous organisms. The receptor affinity mentioned here is mainly due to hormonal mimicry (Tabb and Blumberg, 2006). A highly hazardous representative of this group is tributyltin (TBT), used for many years as a biocide in the textile industry and as an antifoulant agent in marine paints (Antizar-Ladislao, 2008; Cruz et al., 2007). TBT demonstrates several cytotoxic properties on bacteria and higher living organisms (Liu et al., 2006; Gupta et al., 2011; Cruz et al., 2015). The presence of the toxic compounds in the environment induces changes in the cell structure and metabolism. A special role is played by the overproduction of reactive oxygen species (ROS), which cause extensive oxidation damage to numerous biomolecules including DNA, proteins and lipids. The ROS-originated damage may lead to cellular dysfunctions or even cell death (Ishihara et al., 2012), but the cells may fight with the high level of ROS with the use of enzymatic or non-enzymatic mechanisms. The first components of self-defence are antioxidant enzymes like superoxide dismutase (SOD), catalase (CAT) or guaiacol peroxidase (GPX). The other antioxidants involved in the cellular elements protection include: ascorbic acid, reduced glutathione,

α -tocopherol, carotenoids, flavonoids and selected amino acids such as betaine or proline (Das and Roychoudhury, 2014). However, the nature of molecular response against stress factors induced by organotin compounds remains poorly characterized. Studies conducted on *Cunninghamella elegans* as a eukaryotic model revealed a number of negative effects of TBT on the organism, such as changes in the lipid profile, increased potassium retention and disturbances in the hyphae morphology (Bernat et al., 2009; Bernat and Długoński, 2012; Bernat et al., 2014a).

Proteomics and metabolomics are useful tools for the research on the processes occurring in the cell leading to a deeper and more complex understanding of the cell behaviour under various stress or physiological conditions (Baxter et al., 2007; Bundy et al., 2009; Kroll et al., 2014). The current work was focused on the examination of the influence of TBT biodegradation on the amino acids composition and proteome expression of *Cunninghamella echinulata*, and revealed a significant upregulation of oxidative stress biomarkers.

2. Materials and methods

2.1. Chemicals

Tributyltin (TBT), dibutyltin (DBT), monobutyltin (MBT), tetrabutyltin (TTBT) and tropolone were purchased from Sigma-Aldrich

* Corresponding author.

E-mail address: jdlugo@bio.uni.lodz.pl (J. Długoński).

(Germany). All other chemicals and ingredients used in the GC–MS and LC–MS/MS analysis and protein sample preparation were of high purity grade and were obtained from Sigma–Aldrich (Germany), Serva (Germany), Bio–Rad (USA), Avantor (Poland), or Promega (USA).

2.2. Strain and growth conditions

C. echinulata IM 2611 from the fungal collection of the Department of Industrial Microbiology and Biotechnology, University of Łódź, Poland, was the subject of the work. Spores originating from 10-day-old cultures on ZT slants (Bernat et al., 2013) were used to inoculate 20 ml of Sabouraud dextrose broth medium (Difco) supplemented with 2% glucose. The incubation was conducted in a 100-ml Erlenmeyer flask with a wide neck at 28 °C on a rotary shaker (160 rpm). After 24 h, the precultures were transferred to fresh Sabouraud dextrose broth medium (in the ratio 1:4) and incubated for another 24 h in the same conditions as above. Two millilitres of the homogenous preculture was introduced into 18 ml of fresh Sabouraud dextrose broth medium (in a 100-ml Erlenmeyer flask with a wide neck) supplemented with TBT at 5 mg l⁻¹ (TBT stock solution 5 mg ml⁻¹ in ethanol) or without the xenobiotic as a biotic control. Additionally, an abiotic control of TBT (without the microorganism) was prepared. The cultures and controls were incubated for 5 days in the same conditions as described above. All samples were prepared in triplicate.

2.3. Butyltin determination

The organotins analysis was conducted according to the modified procedure described by Bernat and Długoński (2009). The sample was acidified (pH 2) and homogenized using a mixer mill (Retsch MM400) with glass beads Ø1 mm for 5 min at 30 Hz. Next, the sample was extracted twice using a 20 ml mixture of 0.05% tropolone in hexane, dried over anhydrous Na₂SO₄ and evaporated. The extract was dissolved in 2 ml of hexane and derivatized by adding 0.5 ml of a Grignard reagent. The reaction was carried out in darkness at room temperature for 20 min. Next, the process was quenched by slow addition of cooled, 20% NH₄Cl (2 ml). The sample was next centrifuged at 3000 g for 10 min and the supernatant was analyzed. The butyltin determination was conducted using an Agilent 7890 gas chromatograph coupled with an Agilent 5975C mass detector. The separation was performed using an Agilent HP-5MS capillary column (30 m × 0.25 mm id. × 0.25 µm film thickness). The injection volume was set to 1.6 µl. The inlet was set to a split mode with a split ratio 10:1 and the temperature maintained at 280 °C. Helium was used as a carrier gas. The column temperature parameters were as follows: 60 °C maintained for 4 min, then increased at 20 °C min⁻¹ ratio to 280 °C and maintained for 3 min. Ions 165 *m/z* (for MBT), 151 *m/z* (DBT) and 193 *m/z* (TBT) were chosen for targeted quantitative analysis.

2.4. Sample preparation for LC–MS/MS analysis of TBT intermediates

The cultures were homogenized using a mixer mill (Retsch MM 400) with glass beads Ø1 mm for 5 min at 30 Hz. The analytes were extracted according to the modified QuEChERS protocol (available online at <http://quechers.cvuua-stuttgart.de>). A 10-ml sample of the homogenate was mixed with 10 ml of ACN in a 50-ml centrifuge tube and was vortexed for 1 min. Next, 4 g of magnesium sulphate anhydrous, 1 g of sodium chloride, 1 g of trisodium citrate dihydrate and 0.5 g of disodium hydrogencitrate sesquihydrate were added, and the sample was vortexed for another 1 min. The samples were centrifuged for 3 min at 5000 g, and the supernatant was analysed

by LC–MS/MS. All samples were prepared in triplicate.

2.5. Sample preparation for amino acids analysis

The sample preparation was performed according to the procedure described by Szewczyk et al. (2015). Mycelium (100 mg) was placed into 2-ml Eppendorf tubes containing 1 ml of cold water and homogenized with a cold glass matrix Ø1 mm on FastPrep-24 (MP Biomedicals, USA) three times for 30 s at a velocity 4 m s⁻¹ using a 2 min break between each homogenization in order to cool the sample; the sample was then centrifuged at 4000 g at 4 °C for 10 min. Supernatant (100 µl) was vortexed with 900 µl 0.1% formic acid in ethanol for 3 min and incubated for 2 h at –20 °C. Next, the sample was centrifuged at 14,000 g for 20 min at 4 °C and the supernatant was collected into a separate 1.5-ml Eppendorf tube and evaporated at 30 °C under a vacuum. Dry extracts were stored at –70 °C for further analysis. The content of a frozen sample was resuspended in 1 ml of 2% ACN in water, sonicated and vortexed for 2 min, and incubated for 1 h at 4 °C. Finally, the samples were diluted 20-times prior to LC–MS/MS analysis.

2.6. LC–MS/MS analysis of TBT metabolites

LightSight™ software was used to predict the multiple reaction monitoring (MRM) transitions for various phase I and II metabolites. Moreover, neutral loss and precursor ion scans for glucuronide and glutathione conjugates were performed. Qualitative analyses were performed using an Eksigent expert™ microLC200 chromatograph coupled with an AB Sciex QTRAP 4500 mass spectrometer. Chromatographic separation was conducted on a reverse-phase Eksigent C18-AQ (0.5 mm × 150 mm × 3 µm, 120 Å) column: temperature 40 °C, injection volume: 5 µl. The applied eluents consisting of 2 mM of ammonium formate and 0.1% of formic acid in both water (A) and acetonitrile (B) were used. The gradient with a constant flow of 10 µl min⁻¹ and 0.5 min preflush conditioning was as follows: started from 98% of eluent A for 0.2 min; 100% of eluent B after 15 min and maintained until 7 min; reversed to the initial conditions from 22.1 to 23 min. The optimized ESI ion source parameters were as follows: CUR: 25; IS: 5000 V; TEMP: 400 °C; GS1: 20; GS2: 40; ihe: ON for the positive ionization mode and IS: –4500 V for the negative ionization mode, respectively. Several methods with different CE settings were tested (30 ± 15 V; 50 ± 15 V; 60 ± 15 V), especially for phase II metabolites.

2.7. Amino acids analysis

The LC–MS/MS screening method in the MRM mode applied for investigation of the amino acids composition was based on a multi-method developed by Wei et al. (2010). An Eksigent expert™ microLC chromatograph coupled with an AB Sciex QTRAP 4500 mass spectrometer was employed for the analysis. Chromatographic separation was performed on a reverse-phase Eksigent ChromXP C8EP (0.5 × 150 mm × 3 µm, 120 Å) column. The temperature was set to 35 °C and the injection volume was set to 5 µl. The applied eluents were water with 0.1% of formic acid (A) and acetonitrile with 0.1% of formic acid. (B). The gradient with a constant flow of 50 µl min⁻¹ and 0.5 min preflush conditioning was as follows: start from 98% of eluent A for 0.2 min; 90% of eluent B after 2.2 min and maintained to 3.4 min; reversed to the initial conditions from 4 min. The positive ionization ESI ion source parameters were as follows: CUR: 25; IS: 5000 V; TEMP: 300 °C; GS1 and GS2: 30; ihe: ON. The compound-dependent MRM parameters were presented in Tables S–1.

2.8. Protein extraction

Protein extraction was performed as described previously (Szewczyk et al., 2014). Mycelia (3.5 ± 0.2 g) from the 5-day-old control and TBT-containing samples were separated from the culture media, transferred to a lysis buffer and mechanically homogenized using glass beads on a FastPrep-24 (MP Biomedicals, USA). Proteins were precipitated with 20% trichloroacetic acid and resuspended in an SSSB buffer (8 M urea, 4% w/v CHAPS, 1% w/v DTT). The total protein content was measured using the Bradford method with BSA (Sigma-Aldrich, Germany) as the protein standard. The samples were stored at -70°C for further use.

2.9. 1-D electrophoresis

The protein samples (10 μg) were separated on 12% mini gels (mini-Protein tetra cell, Bio-Rad) as described previously (Bernat et al., 2014b). The gels were stained with Coomassie blue, imaged using the ChemiDoc System (Bio-Rad) and analysed using the Image Lab v.4.1 (Bio-Rad).

2.10. Protein digestion

Protein digestion with trypsin was conducted according to the procedure described by Shevchenko et al. (2006). The selected protein bands were excised and placed into 0.5-ml LoBind tubes (Eppendorf). The gels were cut into approximately 1×1 mm fragments. Then, the reduction and acylation of proteins were performed. Next, the gels were saturated with trypsin (Sequencing Grade Modified Trypsin, Promega) and incubated overnight at 37°C . After digestion, peptides were extracted with 50 μl of 0.1% trifluoroacetic acid (TFA) solution in 2% ACN and analysed.

2.11. LC-MS/MS analysis of peptides

The LC-MS/MS analysis of digested proteins was performed using the Eksigent expertTM microLC 200 system coupled with a QTRAP 4500 (AB Sciex) (Bernat et al., 2014b). The 10 μl of peptides was injected onto a reversed-phase Eksigent C8CL-120 column (0.5×100 mm, 3 μm) and separated for 53 min at 40°C . MS/MS analysis was operated in a data-dependent mode with optimized ESI parameters as follows: ion spray (IS) voltage of 5000 V, declustering potential of 100 V, and temperature of 300°C . The precursor ions range was chosen from m/z 500 to m/z 1500, and the product ions range was chosen from m/z 50 to m/z 2000. The ion source GS1, GS2 and CUR parameters were set at 20, 20, and 25, respectively.

2.12. Database search

The Protein Pilot v4.0 software (AB Sciex), coupled with the MASCOT search engine v2.3, was used for the database searches. The data were searched against the NCBI and Swiss-Prot + TrEMBL databases with taxonomy filtering set to fungi (ver. 04.2015, total number of fungi sequences 5566597 and 3479123, respectively). Mascot MS/MS ion searches were performed with trypsin chosen as a protein digesting enzyme, up to two missed cleavages were tolerated and the following variable modifications were applied: Acetyl (N-term), Carbamidomethyl (C), Deamidated (NQ), Formyl (N-term), Gln- > pyro-Glu (N-term Q), Glu- > pyro-Glu (N-term E), and Oxidation (M). Searches were conducted with a peptide mass tolerance of 1 Da and a fragment ion mass tolerance of 0.5 Da.

2.13. Statistical analysis

All experiments were prepared in triplicate. T-test was used to determine the significance of the differences between the samples. The data were considered as significant if $P < 0.05$. Principal component analysis (PCA) of the MRM data (chromatography peak areas and retention times) obtained from the microLC-MS/MS analysis was conducted with the MarkerViewTM software (AB Sciex, USA). Pareto algorithm was applied for the PCA calculation. Statistical analysis and hit map presentation of the data obtained from PCA loadings were performed with the use of Excel 2007 (Microsoft Corporation, USA).

3. Results

3.1. TBT quantitative analysis

C. echinulata IM 2611 was capable of efficient TBT (5 mg l^{-1}) degradation to less toxic metabolites—DBT and MBT during 5 days of the culture (Fig. 1). After 5 days of incubation, fungus eliminated 91% of the initial xenobiotic concentration (0.42 mg l^{-1}) and transformed the substrate to DBT (1.77 mg l^{-1}) and MBT (0.08 mg l^{-1}). Moreover, TBT strongly inhibited the growth of the tested strain during the first 48 h of incubation (Fig. 2). Additionally, an increase in the concentration of degradation by-products was correlated with the fungus growth.

3.2. TBT qualitative analysis

The TBT fragmentation pattern had been described previously (Banoub et al., 2004; Békri et al., 2006). On the basis of the optimized product ions of TBT, the predicted MRM LC-MS/MS methods were developed using LightSightTM software and applied for the screening of possible metabolites. These methods included phase I, phase II and distinct GSH conjugates screening. Samples for qualitative analysis, including corresponding biotic and abiotic controls acting as a reference for TBT intermediates searching, were collected every 24 h during 5 days of the experiment. A novel TBT intermediate, tributyltin hydroxide (TBTOH) (Fig. 3C), was detected. The mass spectrum analysis of the 309 m/z , 307 m/z and 305 m/z tin isotopes (RT 10.6 min) showed that the hydroxyl group was attached directly to the tin atom. The characteristic 251 m/z ion was formed by the loss of one butyl group from TBTOH $[\text{M}-\text{C}_4\text{H}_9]^+$; the 233 m/z species were attributed to the loss of the butyl and the hydroxyl group $[\text{M}-\text{C}_4\text{H}_9\text{OH}]^+$, which gave the DBT ion; 195 m/z corresponded to

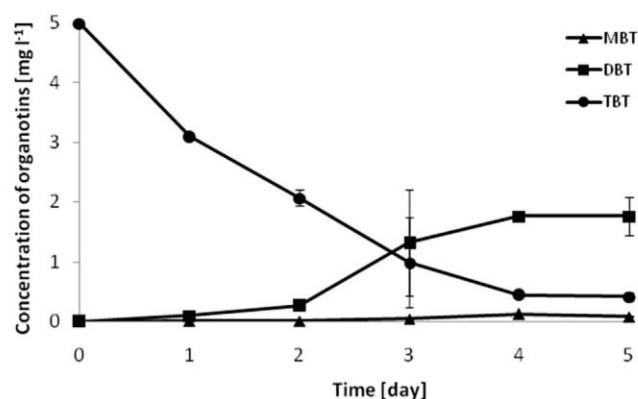


Fig. 1. TBT degradation by *C. echinulata* IM 2611 ($n = 3$).

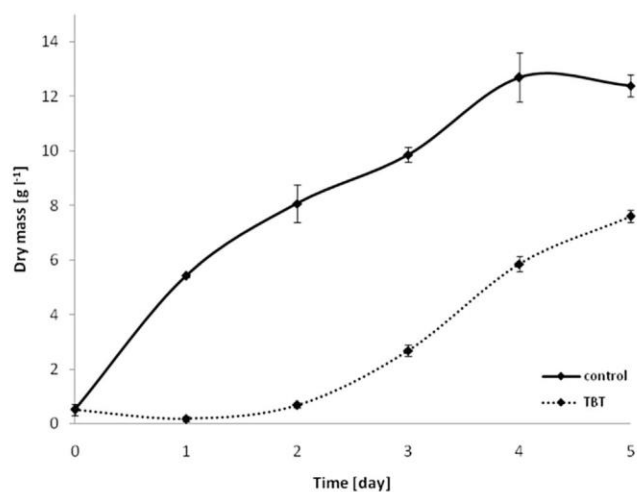


Fig. 2. Time course of growth of *C. echinulata* IM 2611 in the presence of TBT in concentration 5 mg l^{-1} (dotted lines) compared to the control samples (continuous lines). ($n = 3$).

3.3. Amino acids analysis

The influence of TBT on 26 amino acids composition was examined with the use of LC-MS/MS technique and 23 of them were detected, whereas isoleucine and leucine could not be separated under the tested conditions. Cysteine, glycine and homocysteine were not detected. The LC-MS/MS data from control (c) and TBT-treated (TBT) samples were subjected to principal component analysis (PCA) with MarkerView™ software. PCA analysis showed the impact of TBT on the selected *C. echinulata* amino acids content. The main differences occurred during the first 48 h of the culture, as presented in Fig. 4, where the samples '0h', 'TBT24' and 'TBT48' are located on the chart at the longest mutual distances to each other and other samples. The analytes determining differences between the samples are located on the Pc1 loadings chart (Fig. 4). To examine all the data, the PCA loadings (peak areas) for each analyte were averaged and recalculated as relative percentage values (100% is the highest loading for each analyte). To facilitate data evaluation, a hit map and simple chart scoring were applied (Table 1). The most important differences were observed for the results

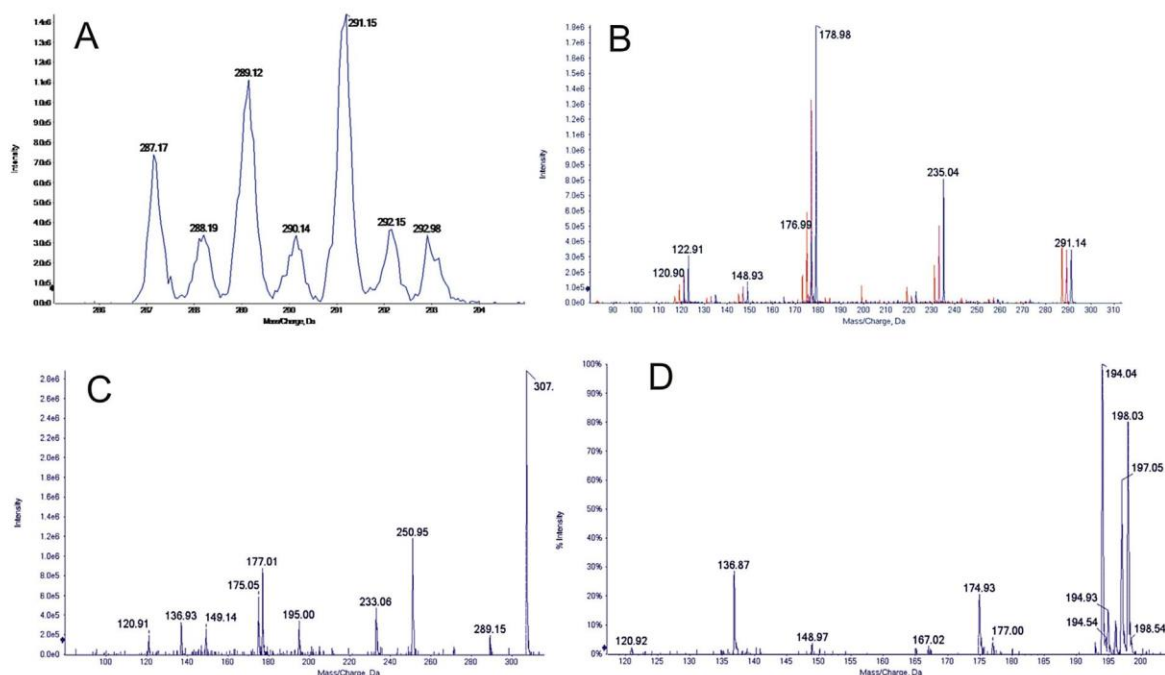


Fig. 3. Mass spectra and fragmentation patterns of TBT and novel, hydroxylated TBT intermediate (TBT-OH). (A) ER scan of TBT; (B), fragmentation pattern of TBT (287, 289 and 291 m/z) containing characteristic tin isotopes: ^{116}Sn (orange), ^{118}Sn (purple) and ^{120}Sn (blue), respectively; (C) mass spectra of TBT-OH (307 m/z) containing ^{118}Sn ; (D) MS^3 experiment for 195 m/z originating from TBT-OH (307 m/z). (For interpretation of the references to colour in this figure legend, the reader is referred to the web version of this article.)

an MBT ion coupled with the hydroxylated group; the 175–177 m/z ion was produced by the loss of another butyl and hydroxyl group $[\text{M}-\text{C}_4\text{H}_9-\text{C}_4\text{H}_8\text{OH}]^+$; the 137 m/z was attributed to the loss of the third butyl group from TBT-OH $[\text{M}-\text{C}_{12}\text{H}_{26}]^+$; finally, the 16 Da mass shift between 137 and 121 m/z showed that the oxygen atom was bonded to the tin (Fig. 3C). Additionally, selected MS^3 experiments aimed at the characterization of a unique 195 m/z ion (and its tin isotopes) fragmentation pathway were performed to confirm the point of oxygen attachment (Fig. 3D). The LC-MS/MS analysis did not show any other TBT intermediates of phases I and II.

obtained after 24 h and 48 h of incubation, where the fungus growth was strongly inhibited by TBT (Fig. 2).

Under stress conditions caused by TBT, the contents of 19 from 23 detected amino acids were affected in at least two consecutive time points, demonstrating that the xenobiotic caused a considerable impact on the fungus primary metabolism. During 24–48 h of the experiment aminoisobutyrate, alanine, asparagine, betaine, proline, serine and threonine were significantly upregulated in the TBT containing cultures (Table 1). Alanine and betaine showed a maximum relative concentration after 24 h of incubation in the presence of TBT. Interestingly, accumulation of betaine was

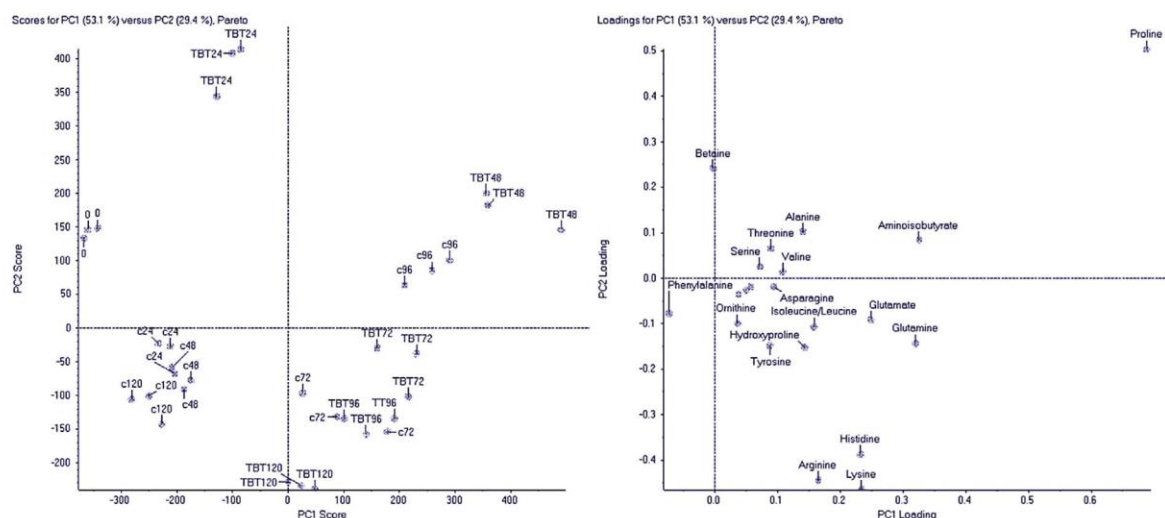


Fig. 4. PCA analysis of the mycelial amino acids metabolism on TBT-containing (5 mg l^{-1}) and control cultures on Sabouraud medium. On the left – PC1 against PC2 loading charts; on the right – PC1 against PC2 scoring chart.

Table 1

Relative concentration of the monitored amino acids during TBT (5 mg l^{-1}) biodegradation by *C. echinulata* IM 2611 on Sabouraud medium.

Amino acid	Control culture						TBT containing culture					
	0	24c	48c	72c	96c	120c	24TBT	48TBT	72TBT	96TBT	120TBT	
Aminoisobutyrate ^{24,48}	13	29	33	63	69	35	72	100	80	74	57	
Alanine ^{24,48,120}	26	31	40	79	64	27	99	100	72	75	49	
Arginine ^{24,48,120}	11	36	49	81	70	57	4	31	71	90	100	
Asparagine ^{48,72,96,120}	19	27	26	42	34	27	22	100	76	71	49	
Aspartate ^{24,48,96,120}	26	31	30	67	100	26	20	51	42	42	53	
Betaine ^{24,120}	12	9	14	13	16	6	100	24	12	13	10	
Dimethyl glycine ²⁴	35	73	70	80	92	53	32	100	72	76	68	
Glutamate ^{48,96,120}	6	14	17	81	100	10	26	51	47	55	72	
Lysine ^{24,96}	23	67	84	93	74	79	4	89	100	100	99	
Glutamine ^{24,48,72,120}	7	37	28	50	90	26	8	97	100	94	68	
Histidine ^{24,96,120}	17	45	54	99	52	62	9	81	84	91	100	
Hydroxyproline ^{48,72,120}	19	10	16	87	72	29	11	53	66	91	100	
Isoleucine/Leucine ²⁴	17	100	70	83	85	52	36	96	85	70	61	
Methionine ^{24,48,72,120}	27	61	54	61	46	28	18	93	100	62	55	
Ornithine ^{24,48,96,120}	12	66	100	63	51	45	21	65	59	63	64	
Phenylalanine ²⁴	100	84	93	65	59	65	20	64	66	51	52	
Proline ^{24,48,96,120}	20	14	17	41	78	5	55	100	58	44	25	
Serine ^{48,96,120}	22	62	54	57	44	45	72	100	69	60	61	
Threonine ¹²⁰	36	44	45	85	96	68	86	100	90	74	29	
Tryptophan ^{72,96,120}	75	33	26	43	36	30	24	62	92	100	66	
Tyrosine ^{24,72,96,120}	28	38	36	66	49	38	10	55	88	100	95	
Valine ^{24,96}	22	78	73	62	57	30	33	100	60	37	30	

Superscript numbers indicates time points where significant difference to equivalent control point was observed (t-test, $P < 0.05$)

observed only after 24 h; afterwards, the relative concentration of betaine was maintained at a constant low level (Table 1). Significant downregulation after 24 h of incubation in the TBT presence was observed for arginine, dimethyl glycine, lysine, glutamine, histidine, isoleucine/leucine, methionine, ornithine, phenylalanine, tyrosine and valine (Table 1). However, after 48 h or later the amount of these amino acids in TBT-containing cultures increased and demonstrated even higher relative concentrations at the end of the experiment compared to the control samples (e.g. arginine,

histidine or tyrosine). Except for 24 h cultures, only in the case of dimethyl glycine, isoleucine/leucine and phenylalanine, there were no significant differences between TBT-containing and control samples.

3.4. Protein analysis

A preliminary study of the TBT impact on the intracellular protein profile of the filamentous fungus was conducted for the

first time. Based on the 1D SDS-PAGE analysis (Fig. 5), 22 protein bands from the TBT-containing sample and two intensive protein bands from the control culture (3 and 8) were taken for tryptic digestion followed by LC-MS/MS analysis. The homology (MASCOT searches) and functional alignments (BLAST searches with the use of delta-blast algorithm) of the 24 tested protein bands allowed for the identification and/or functional alignment of 15 protein bands, resulting in the final number of 20 identified proteins (Table 2). The tested organism was not sequenced; however, on the basis of sequence homology, it was revealed that the majority of the identified proteins belonged to the fungi from the *Mucorales* order, the same as the tested strain. In 1D electrophoresis one band often contains more than one protein; therefore, the conclusion concerning the role of identified proteins in the examined process was difficult. Only two protein bands (3 K and 8 K) were overexpressed in the control sample; the other protein bands had a higher intensity in the TBT-containing sample.

Identified proteins could be classified as involved in the ROS defence system (peroxiredoxin, nuclease C1), cell wall architecture (chitin deacetylase, UDP-glucose dehydrogenase), TCA cycle (malate dehydrogenase), sugar and energy-related systems

(enolase and ATP synthase) and amino acids synthesis (5-methyltetrahydropteroyltriglutamate-homocysteine methyltransferase). The most conspicuous observation was strong overexpression of peroxiredoxin during TBT exposure. As showed in Fig. 5, peroxiredoxin had the most intensive band (no. 19) when compared to the other proteins. This difference is particularly evident in relation to control sample. An interesting result was obtained for the overexpression of nuclease C1 (bands 15 and 16) and malate dehydrogenase in TBT-treated sample.

4. Discussion

The major role in the elimination of xenobiotics from the environment is played by microorganisms (Gadd, 2000; Desai et al., 2010). Only one described fungal strain—*C. elegans* (Bernat and Długoński, 2002), was capable of effectively eliminating high concentrations of TBT with DBT and MBT by-products formation. *C. echinulata* conducted TBT degradation on Sabouraud medium in a manner similar to *C. elegans*. In contrast to *C. elegans* which eliminated over 60% of TBT (5 mg l⁻¹) after 7 days of incubation (Bernat and Długoński, 2002), *C. echinulata* degraded 91% of the xenobiotic after 5 days of culturing. In addition, the TBT biodegradation curve in *C. echinulata* (TBT concentration 5 mg l⁻¹) was similar to that in *C. elegans* (TBT concentration 10 mg l⁻¹ of TBT) (Bernat and Długoński, 2002, 2007). The first significant amount of DBT and MBT observed on 3rd day of the culture as well as the general biodegradation process in the tested *Cunninghamella* species were closely related to the microorganisms growth.

The ability of *Cunninghamella* sp. to biotransform a wide range of xenobiotics and drugs using both phase I and phase II mechanisms is well-known due to the similarity to the mammalian metabolism (Asha and Vidyavathi, 2009; Murphy, 2015). Therefore, a search for other TBT by-products was performed. LightSight™ is a useful tool in the development of methods applied for the metabolites of phase I or II screening. The software analyses the data by comparing the test sample against the control sample, followed by the generation of a list of probable metabolite hits (Ramírez-Molina and Burton, 2009; Song et al., 2014). Except DBT and MBT, only hydroxylated TBT (TBTOH) was detected. Interestingly, the hydroxyl group was bound directly to a tin atom. This type of TBT hydroxylation has not been postulated in a biological system although hydroxylated intermediates formed during TBT degradation had been reported previously (Matsuda et al., 1993; Bernat et al., 2013). The process of TBT elimination was accompanied by cytochrome P450 activity (Bernat and Długoński, 2002; Ohhira et al., 2006). The comparison of the obtained mass spectra with the one presented by Békri et al. (2006) and Bernat et al. (2013) confirmed that the detected compound was a novel tin-hydroxylated TBT. Taking into account the results obtained for *C. elegans* and *C. echinulata*, the formation of DBT, MBT and hydroxylated intermediates seems to be an integral part of TBT removal by fungi belonging to the *Cunninghamella* genus.

ROS cause several negative effects on both, the structure and the cellular metabolism (Circu and Aw, 2010), therefore organisms developed a number of enzymatic and non-enzymatic antioxidant mechanisms. The majority of the mechanisms of ROS defence systems involve various kinds of reactive oxygen scavenging redox reactions. These reactions may be catalysed by stress response enzymes or be a result of the chemical and biochemical pathways incorporating various compounds, which leads to the modulation of the intracellular redox environment. Biodegradation of TBT by *C. echinulata* presented in this work occurs effectively on the rich Sabouraud medium as an oxygen-related metabolic pathway. The time courses of the TBT elimination and formation of biodegradation intermediates—DBT, MBT

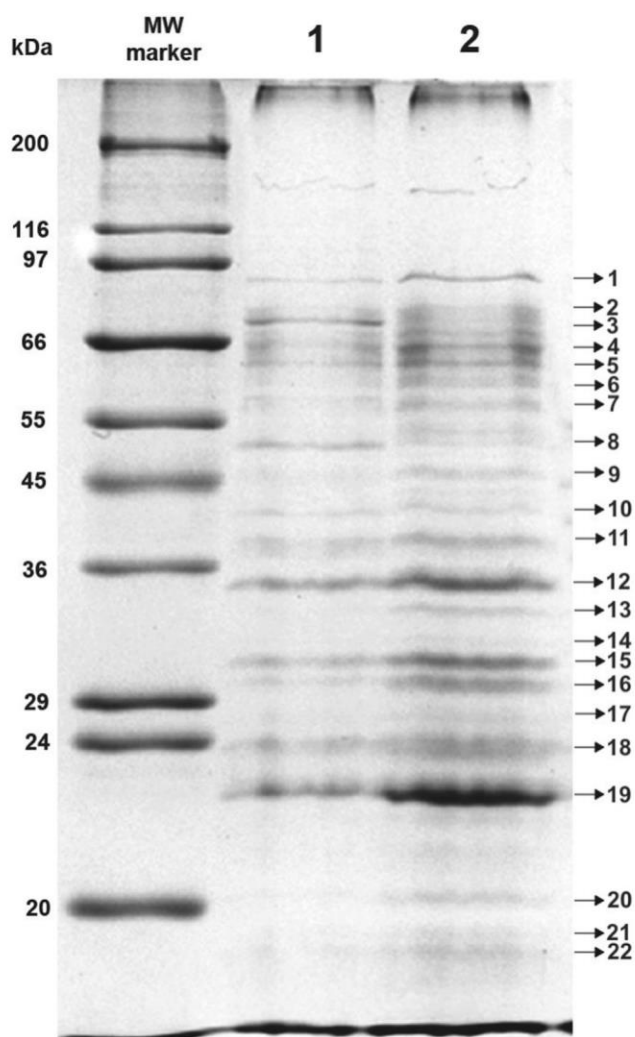


Fig. 5. 1-D SDS-PAGE analysis of the *C. echinulata* proteome in the absence (line 1) or presence of TBT (line 2).

Table 2
Proteins identified by LC-MS/MS.

Band no ^a	Protein name ^b	Species homology	Accession no ^c	Score	Matched sequence/Unique peptides	Sequence coverage	Delta-BLAST results	Fold change ^{d,e}
1	5-methyltetrahydropteroyltri-glutamate-homocysteine methyltransferase	<i>Lichtheimia corymbifera</i> JMRC:FSU:9682	A0A068SGC6_9FUNG	117	1/1	2%	[cd03312] CIMS - Cobalamine-independent methionine synthase, or MetE, N-terminal domain_like	2,2
2	Hypothetical protein S7711_11496	<i>Stachybotrys chartarum</i> IBT 7711	A0A084AHD0_STACH	81	2/2	2%	[COG2051] Ribosomal protein S27E [Translation, ribosomal structure and biogenesis]	1,9
	TAT-binding protein-like protein 7	<i>Cryptococcus gattii</i> WM276	gi 317460266	74	2/2	3%	[pfam03941] Inner centromere protein, ARK binding region	
	Uncharacterized protein	<i>Mucor circinelloides</i> f. <i>circinelloides</i> (strain 1006PhL)	S2JG8_MUCC1	77	2/2	3%	[cd00086] Homeodomain; DNA binding domains involved in the transcriptional regulation of key eukaryotic developmental processes	
3 K	Uncharacterized protein	<i>Absidiaida hoensis</i> var. <i>thermophila</i>	A0A077WJ15_9FUNG	102	1/1	4%	[cd10952] Catalytic NodB homology domain of <i>Mucor rouxii</i> chitin deacetylase and similar proteins	1,3
	Chitin deacetylase	<i>Mucor circinelloides</i> f. <i>circinelloides</i> (strain 1006PhL)	S2JG56_MUCC1	83	1/1	4%		
3	Chitin deacetylase	<i>Amylomyces rouxii</i>	CDA_AMYRO	72	2/2	7%		
	Chitin deacetylase	<i>Mucor circinelloides</i> f. <i>circinelloides</i> (strain 1006PhL)	S2JG56_MUCC1	72	2/2	7%		
4	NOT IDENTIFIED							1,6
5	UDP-glucose dehydrogenase	<i>Lichtheimia corymbifera</i> JMRC:FSU:9682	A0A068SBD3_9FUNG	154	3/1	7%	[pfam03721] UDP-glucose/GDP-mannose dehydrogenase family, NAD binding domain	4,2
		<i>Absidiaida hoensis</i> var. <i>thermophila</i>	A0A077WFT0_9FUNG	154	3/1	7%	[cd00882] Rat sarcoma (Ras)-like superfamily of small guanosine triphosphatases (GTPases). [pfam03721] UDP-glucose/GDP-mannose dehydrogenase family, NAD binding domain	
		<i>Rhizopus deleamar</i> (strain RA 99-880/ATCC MYA-4621/FGSC 9543/NRRL 43880)	I1BJF8_RHIO9	154	3/1	9%	[pfam00984] UDP-glucose/GDP-mannose dehydrogenase family, central domain	
6	NOT IDENTIFIED							7,3
7	V-type ATPase	<i>Lichtheimia corymbifera</i> JMRC:FSU:9682	gi 661185643	80	1/1	2%	[cd01135] V/A-type ATP synthase (non-catalytic) subunit B	1,8
	Putative ZYRO0C16984p	<i>Absidiaida hoensis</i> var. <i>thermophila</i>	gi 671690638	80	1/1	2%		
8 K	Enolase	<i>Cunninghamella elegans</i>	ENO_CUNEL	512	8/5	28%	[cd03313] Enolase	1,9
	ATP synthase subunit beta	<i>Mucor circinelloides</i> f. <i>circinelloides</i> (strain 1006PhL)	S2IV94_MUCC1	248	6/3	17%	[cd01133] F1 ATP synthase beta subunit, nucleotide-binding domain	
	Putative ATP synthase subunit beta	<i>Rhizopus microsporus</i>	gi 729711200	245	6/4	17%		
8	ATP synthase subunit beta	<i>Mucor circinelloides</i> f. <i>circinelloides</i> (strain 1006PhL)	S2IV94_MUCC1	112	3/2	8%	[cd01133] F1 ATP synthase beta subunit, nucleotide-binding domain	
	Enolase	<i>Cunninghamella elegans</i>	ENO_CUNEL	92	2/2	8%	[cd03313] Enolase	
	Putative ATP synthase beta chain, mitochondrial	<i>Rhizopus microsporus</i>	gi 727144303	88	2/1	6%	[cd01133] F1 ATP synthase beta subunit, nucleotide-binding domain	
9	NOT IDENTIFIED							5,5
10	NOT IDENTIFIED							1,4
11	Putative Malate dehydrogenase	<i>Rhizopus microsporus</i>	gi 729714123	311	5/0	23%	[cd01337] Glyoxysomal and mitochondrial malate dehydrogenases	1,6
	malate dehydrogenase	<i>Rhizopus deleamar</i> (strain RA 99-880/ATCC MYA-4621/FGSC 9543/NRRL 43880)	I1BQQ7_RHIO9	296	4/0	16%		
	malate dehydrogenase	<i>Mucor circinelloides</i> f. <i>circinelloides</i> (strain 1006PhL)	S2J7L6_MUCC1	291	5/0	23%		
12	malate dehydrogenase	<i>Paracoccidioides lutzii</i> (strain ATCC MYA-826/Pb01)	C1GNF8_PARBA	98	3/2	11%	[cd01337] Glyoxysomal and mitochondrial malate dehydrogenases	2,6
	malate dehydrogenase	<i>Paracoccidioides brasiliensis</i>	Q7ZA65_PARBR	98	3/2	11%		
	Transaldolase	<i>Rhizopus deleamar</i> (strain RA 99-880/ATCC MYA-4621/FGSC 9543/NRRL 43880)	I1CEK5_RHIO9	93	2/2	7%	[cd00957] Transaldolases including both TalA and TalB	

Table 2 (continued)

Band no ^a	Protein name ^b	Species homology	Accession no ^c	Score	Matched sequence/Unique peptides	Sequence coverage	Delta-BLAST results	Fold change ^{d,e}
13	NOT IDENTIFIED	4621/FGSC 9543/NRRL 43880)						7,2
14	NOT IDENTIFIED							TBT
15	Nuclease C1	<i>Cunninghamella echinulata</i> var. <i>echinulata</i>	NUC1_CUNEE	206	4/4	19%	[cd00091] DNA/RNA non-specific endonuclease	3,0
	Minor nuclease C1B isoform	<i>Cunninghamella echinulata</i> var. <i>echinulata</i>	Q9UUS3_CUNEE	206	4/4	18%		
	Voltage-dependent ion-selective channel	<i>Lichtheimia corymbifera</i> JMRC:FSU:9682	A0A068RIS3_9FUNG	88	2/2	7%	[cd07306] Voltage-dependent anion channel of the outer mitochondrial membrane	
16	Minor nuclease C1B isoform	<i>Cunninghamella echinulata</i> var. <i>echinulata</i>	Q9UUS3_CUNEE	515	11/11	44%	[cd00091] DNA/RNA non-specific endonuclease	4,4
	Nuclease C1	<i>Cunninghamella echinulata</i> var. <i>echinulata</i>	gi 3914183	409	8/8	36%		
	Elongation factor 1-beta	<i>Cladophialophora yegresii</i> CBS 114405	W9VTJ9_9EURO	61	1/1	5%	[cd00292] Elongation factor 1 beta (EF1B) guanine nucleotide exchange domain	
17	Hypothetical protein RMATCC62417_06621	<i>Rhizopus microsporus</i>	gi 727147104	104	2/2	6%	[pfam00450] Serine carboxypeptidase	TBT
	Putative Rho-gdp dissociation inhibitor	<i>Rhizopus microsporus</i>	gi 727153664	71	2/2	21%	[pfam02115] RHO protein GDP dissociation inhibitor	
18	NOT IDENTIFIED							2,1
19	Peroxiredoxin 1	<i>Lichtheimia corymbifera</i> JMRC:FSU:9682	gi 661185649	87	2/1	13%	[cd03015] Peroxiredoxin (PRX) family	3,1
	Putative Peroxiredoxin	<i>Absidia hoensis</i> var. <i>thermophila</i>	gi 671690634	87	2/1	13%		
	Peroxiredoxin	<i>Mucor circinelloides</i> f. <i>circinelloides</i> (strain 1006PhL)	S2K2B6_MUCC1	84	2/1	12%		
20	Pc22g23680 protein	<i>Penicillium chrysogenum</i> (strain ATCC 28089/DSM 1075/Wisconsin 54-1255)	B6HW37_PENCW	63	1/1	8%	[pfam12680] Snoal-like domain; This family contains a large number of proteins that share the Snoal fold	5,6
21	NOT IDENTIFIED							3,4
22	NOT IDENTIFIED							2,8

^a Bands 3 K and 8 K were from the control sample.

^b Maximum of three best proteins with the highest score were presented.

^c If a protein was identified using both databases, the accession for the protein with the highest score was described.

^d Fold change was calculated as a ratio of the intensity of the protein bands between the control sample and the TBT-containing sample.

^e TBT means that protein band was present only in the sample from the TBT-incubated culture.

and TBTOH reflects the changes in the mycelium growth as well as in the examined proteins and selected amino acids. In TBT-containing cultures a significant upregulation of peroxiredoxin (band 19) and nuclease C1 (band 15 and 16) (Fig. 5, Table 2) and an increased contents of aminoisobutyrate, alanine, betaine and proline (Table 1) supports the fact that ROS were generated during the xenobiotic biodegradation.

Peroxiredoxins are important antioxidant enzymes found in organisms from all kingdoms. This group of enzymes are mainly involved in cellular response against oxidative damage by reducing hydrogen peroxide (Rhee et al., 2001). Previous studies had focused on the study of the activity of the other antioxidant enzymes, such as SOD or CAT rather than peroxiredoxin participation in the regulation of oxidative stress in organisms exposed to TBT. Jia et al. (2009) examined the level of the activity of selected enzymatic antioxidants in TBT-treated abalone *Haliotis diversicolor supertexta*. Exposure to TBT (0.35 µg Sn l⁻¹) caused changes in the acidic (ACP) and alkaline (AKP) phosphatase activity in abalone hepatopancreas and hemolymph. Thus, SOD and CAT do not seem to be involved in the TBT detoxification process in *H. diversicolor supertexta* hepatopancreas. On the other hand, the study conducted by Zhou et al. (2010) on the same research model showed a decreased SOD

activity and increased peroxidase activity in abalone hemolymph. Thus, the obtained results suggest that peroxiredoxin should be taken into account as an important ROS scavenger in TBT exposed organisms. The increased expression of peroxiredoxin may also be caused by a high concentration of DBT after 5 days of incubation (Fig. 1) due to the fact, that DBT also induces oxidative stress (Chantong et al., 2014). An interesting result was obtained for nuclease C1 – highly upregulated in a TBT-containing sample. Nuclease C1 in *C. echinulata* was described by Ho et al. (1998) and showed a significant similarity to the sequence of the mitochondrial nucleases of *Saccharomyces cerevisiae* (44% identity) and *Schistosaccharomyces pombe* (42% identity). However, its role in the fungal cells remains ambiguous as the enzyme has a complex nature. Additionally, *Cunninghamella* sp. were not sequenced, and the reported nuclease was described only once. The DELTA-BLAST search conducted on band 15 digest confirmed that the protein is a member of the NUC superfamily. The nuclease from *C. echinulata* showed a similarity to the endonuclease G from *Rhizopus micrococcus* (57% identity) and mitochondrial endonuclease G from *Mucor circinelloides* f. *circinelloides* 1006PhL (57% identity), in contrast to Nuc1p from *S. cerevisiae* (45% identity) (Marchler-Bauer et al., 2015). Endonuclease G is a mitochondrial nuclease employed

in life and death processes in the cell (Büttner et al., 2007). Moreover, it was involved in the nucleosomal DNA fragmentation under oxidative stress in rat primary hepatocytes (Ishihara and Shimamoto, 2006). Considering the fact that TBT induced DNA damage (Liu et al., 2006; Morales et al., 2013), the overexpression of this enzyme points it as a possible DNA protector in the examined process.

Mitochondria are key structures involved in several cellular mechanisms. TBT is known to disrupt the mitochondrial functions, especially related with the respiratory chain (Nesci et al., 2011). The downregulation of ATP synthase in the presence of TBT confirmed the negative effect of the compound on mitochondria. Moreover, TCA cycle components located in this organelle are correlated with many metabolic pathways occurring in the cell. Enolase and malate dehydrogenase are involved in sugar and energy-related metabolism and they down- and upregulation, respectively, suggest a varied disrupting action on the cell metabolism. The disorders in metabolism caused by TBT were showed in bacteria and abalone (Cruz et al. 2012; Zhou et al., 2010). Methionine synthases are enzymes that catalyse the formation of methionine from homocysteine. Thus, the upregulated 5-methyltetrahydropteroyltriglutamate-homocysteine methyltransferase (band 1) and an increased level of methionine seem to be responsible for the accumulation of methionine in fungal cells (Table 1). It was proved, that methionine accumulation exhibits cytoprotective and antioxidant properties in living cells (Bender et al., 2008). Because the highest level for methionine was observed in 48 and 72 h of the culture, it can be assumed that the level of expression of the methionine synthase was higher at earlier stages implying a high concentration of methionine in this stage of the culture. Chitin deacetylase and UDP-glucose dehydrogenase are involved in cell wall biosynthesis. The observed changes in the hyphae structure and membrane lipid composition in *C. elegans* during the exposure to TBT (Bernat and Długosiński, 2012; Bernat et al., 2009; 2014a) can indicate a role of these enzymes in the TBT induced modification of cell membranes.

The second antioxidant strategy examined in this work involved free amino acids analysis. TBT-related stress induced changes in the relative concentration of selected amino acids, whose accumulation is a known marker of the defence mechanism towards ROS. However, the impact of stress conditions on fungal amino acids composition is still poorly understood. In a *C. echinulata* TBT-treated culture, significant changes in the amount of 19 from 23 detected free amino acids were observed in a time-dependent way. Some of them showed maximum amount after 24 h, 48 h or at the later time points. Proline and betaine are many the most important organic compounds accumulated in a variety of organisms in response to oxidative stress (Ashraf and Foolad, 2007; Liu et al., 2011). Particularly proline is the object of an intense study, showing its broad influence on the physiology of the cells under stress, which is not limited only to osmoregulation but also enables the removal of reactive oxygen species or stabilization of the cell membranes (Takagi, 2008). In the examined fungal cultures the relative concentration of proline and betaine were significantly increased during the exposure to the xenobiotic. The study conducted by Zhou et al. (2010) revealed disturbances in the metabolism of abalone (*Haliotis diversicolor supertexta*) during the exposure to TBT. Incubation with the xenobiotic showed increased levels of alanine and glutamine as well as the other kinds of compounds such as: lactate, acetate, and succinate. A decreased level in concentrations of TCA cycle compounds pyruvate and glucose was also observed. Another example of an amino acid linked with oxidative stress is aminoisobutyric acid (Mimura et al., 1994). Similar trends for alanine and aminoisobutyrate and glutamine

were observed in *C. echinulata* in TBT-treated samples.

5. Conclusions

C. echinulata was capable of effective TBT biodegradation during 5 days of culture. The TBT hydroxylation directly on a tin atom has been described for the first time, and TBT-OH appears to be a key intermediate that may be involved in the TBT debuthylation leading to DBT and MBT formation. However, the exposure to the biocide was a stress factor for the fungus manifested by a strong inhibition of growth at the initial stages of the culture. In the presented study the microorganism strategy against TBT-induced stress was examined on the protein and amino acids level. Proteomics analysis showed changes in the protein profile, especially related with the antioxidant defence mechanism (peroxiredoxin and nuclease). Significant changes in most of the analysed free amino acids were also observed, especially the accumulation of oxidative stress markers such as aminoisobutyrate, betaine and proline. The obtained data proved that during TBT biodegradation oxidative stress occurred. A deeper explanation of TBT impact on the fungus metabolism requires further investigation incorporating comparative proteomics as well as broader targeted metabolomics.

Acknowledgements

The authors are grateful to Dr P. Bernat, University of Łódź, for help with the sample preparation for the organotin analysis and discussion of the obtained results. The study was supported by the National Science Centre, Poland (Project No. UMO-2014/13/N/NZ9/00878).

Appendix A. Supplementary data

Supplementary data related to this article can be found at <http://dx.doi.org/10.1016/j.ibiod.2015.11.013>.

References

- Antizar-Ladislao, B., 2008. Environmental levels, toxicity and human exposure to tributyltin (TBT)-contaminated marine environment. A review. *Environ. Int.* 34, 292–308.
- Asha, S., Vidyavathi, M., 2009. *Cunninghamella*. A microbial model for drug metabolism studies—a review. *Biotechnol. Adv.* 27, 16–29.
- Ashraf, M., Foolad, M., 2007. Roles of glycine betaine and proline in improving plant abiotic stress resistance. *Environ. Exp. Bot.* 59, 206–216.
- Banoub, J.H., Miller-Banoub, J., Sheppard, G.V., Hodder, H.J., 2004. Electrospray tandem mass spectrometric measurements of organotin compounds. *J. Spectro.* 18, 95–112.
- Baxter, C.J., Redest, H., Schauer, N., Repsilber, D., Patil, K.R., Nielsen, J., Selbig, J., Liu, J., Fernie, A.R., Sweetlove, L.J., 2007. The metabolic response of heterotrophic *Arabidopsis* cells to oxidative stress. *Plant Physiol.* 143, 312–325.
- Békri, K., Saint-Louis, R., Pelletier, E., 2006. Determination of tributyltin and 4-hydroxybutyldibutyltin chlorides in seawater by liquid chromatography with atmospheric pressure chemical ionization-mass spectrometry. *Anal. Chim. Acta* 578, 203–212.
- Bender, A., Hajieva, P., Moosmann, B., 2008. Adaptive antioxidant methionine accumulation in respiratory chain complexes explains the use of a deviant genetic code in mitochondria. *Proc. Natl. Acad. Sci. U.S.A.* 105, 16496–16501.
- Bernat, P., Długosiński, J., 2002. Degradation of tributyltin by the filamentous fungus *Cunninghamella elegans*, with involvement of cytochrome P-450. *Biotechnol. Lett.* 24, 1971–1974.
- Bernat, P., Długosiński, J., 2007. Tributyltin chloride interactions with fatty acids composition and degradation ability of the filamentous fungus *Cunninghamella elegans*. *Int. Biodeterior. Biodegr.* 60, 133–136.
- Bernat, P., Długosiński, J., 2009. Isolation of *Streptomyces* sp. strain capable of butyltin compounds degradation with high efficiency. *J. Hazard. Mater.* 171, 660–664.
- Bernat, P., Długosiński, J., 2012. Comparative study of fatty acids composition during cortexolone hydroxylation and tributyltin chloride (TBT) degradation in the filamentous fungus *Cunninghamella elegans*. *Int. Biodeterior. Biodegr.* 74, 1–6.
- Bernat, P., Staba, M., Długosiński, J., 2009. Action of tributyltin (TBT) on the lipid content and potassium retention in the organotin degrading fungus *Cunninghamella elegans*. *Curr. Microbiol.* 59, 315–320.
- Bernat, P., Szewczyk, R., Krupiński, M., Długosiński, J., 2013. Butyltins degradation by

- Cunninghamella elegans and Cochliobolus lunatus co-culture. J. Hazard. Mater. 246, 277–282.
- Bernat, P., Gajewska, E., Szewczyk, R., Staba, M., Długoński, J., 2014a. Tributyltin (TBT) induces oxidative stress and modifies lipid profile in the filamentous fungus *Cunninghamella elegans*. Environ. Sci. Pollut. R. 21, 4228–4235.
- Bernat, P., Siewiera, P., Soboń, A., Długoński, J., 2014b. Phospholipids and protein adaptation of *Pseudomonas* sp. to the xenoestrogen tributyltin chloride (TBT). World J. Microbiol. Biotechnol. 30, 2343–2350.
- Bundy, J.G., Davey, M.P., Viant, M.R., 2009. Environmental metabolomics: a critical review and future perspectives. Metabolomics 5, 3–21.
- Büttner, S., Eisenberg, T., Carmona-Gutierrez, D., Ruli, D., Knauer, H., Ruckenstein, C., Sigrist, C., Wissing, S., Kollroser, M., Frohlich, K., Sigrist, S., Madeo, F., 2007. Endonuclease G regulates budding yeast life and death. Mol. Cell. 25, 233–246.
- Chantong, B., Kratschmar, D.V., Lister, A., Odermatt, A., 2014. Dibutyltin promotes oxidative stress and increases inflammatory mediators in BV-2 microglia cells. Toxicol. Lett. 230, 177–187.
- Circu, M.L., Aw, T.Y., 2010. Reactive oxygen species, cellular redox systems, and apoptosis. Free Radic. Biol. Med. 48, 749–762.
- Cruz, A., Caetano, T., Suzuki, S., Mendo, S., 2007. *Aeromonas veronii*, a tributyltin (TBT)-degrading bacterium isolated from an estuarine environment, Ria de Aveiro in Portugal. Mar. Environ. Res. 64, 639–650.
- Cruz, A., Oliveira, V., Baptista, I., Almeida, A., Cunha, A., Suzuki, S., Mendo, S., 2012. Effect of tributyltin (TBT) in the metabolic activity of TBT-resistant and sensitive estuarine bacteria. Environ. Toxicol. 27, 11–17.
- Cruz, A., Anselmo, A.M., Suzuki, S., Mendo, S., 2015. Tributyltin (TBT): a review on microbial resistance and degradation. Crit. Rev. Env. Sci. Technol. 45, 970–1006.
- Das, K., Roychoudhury, A., 2014. Reactive oxygen species (ROS) and response of antioxidants as ROS-scavengers during environmental stress in plants. Front. Environ. Sci. 2, 53.
- Desai, C., Pathak, H., Madamwar, D., 2010. Advances in molecular and “-omics” technologies to gauge microbial communities and bioremediation at xenobiotic/anthropogen contaminated sites. Bioresour. Technol. 101, 1558–1569.
- Gadd, G.M., 2000. Microbial interactions with tributyltin compounds: detoxification, accumulation, and environmental fate. Sci. Total Environ. 258, 119–127.
- Gupta, M., Dwivedi, U.N., Khandelwal, S., 2011. C-Phycocyanin: an effective protective agent against thymic atrophy by tributyltin. Toxicol. Lett. 204, 2–11.
- Ho, H.C., Shiau, P.F., Liu, F.C., Chung, J.G., Chen, L.Y., 1998. Purification, characterization and complete amino acid sequence of nuclease CI from *Cunninghamella echinulata* var. *echinulata*. Eur. J. Biochem. 256, 112–118.
- Ishihara, Y., Shimamoto, N., 2006. Involvement of endonuclease G in nucleosomal DNA fragmentation under sustained endogenous oxidative stress. J. Biol. Chem. 281, 6726–6733.
- Ishihara, Y., Kawami, T., Ishida, A., Yamazaki, T., 2012. Tributyltin induces oxidative stress and neuronal injury by inhibiting glutathione S-transferase in rat organotypic hippocampal slice cultures. Neurochem. Int. 60, 782–790.
- Jia, X., Zhang, Z., Wang, S., Lin, P., Zou, Z., Huang, B., Wang, Y., 2009. Effects of tributyltin (TBT) on enzyme activity and oxidative stress in hepatopancreas and hemolymph of small abalone, *Haliotis diversicolor supertexta*. Chin. J. Oceanol. Limnol. 27, 816–824.
- Kroll, K., Pähz, V., Kniemeyer, O., 2014. Elucidating the fungal stress response by proteomics. J. Proteomics 97, 151–163.
- Liu, H.G., Wang, Y., Lian, L., Xu, L.H., 2006. Tributyltin induces DNA damage as well as oxidative damage in rats. Environ. Toxicol. 21, 166–171.
- Liu, J., Wisniewski, M., Droby, S., Vero, S., Tian, S., Hershkovitz, V., 2011. Glycine betaine improves oxidative stress tolerance and biocontrol efficacy of the antagonistic yeast *Cystofilobasidium infirmominium*. Int. J. Food Microbiol. 146, 76–83.
- Marchler-Bauer, A., Derbyshire, M.K., Gonzales, N.R., Lu, S., Chitsaz, F., Geer, L.Y., Geer, R.C., He, J., Gwadz, M., Hurwitz, D.I., Lanczycki, C.J., Lu, F., Marchler, G.H., Song, J.S., Thanki, N., Wang, Z., Yamashita, R.A., Zhang, D., Zheng, C., Bryant, S.H., 2015. CDD: NCBI's conserved domain database. Nucleic Acids Res. 43, 222–226.
- Matsuda, R., Suzuki, T., Saito, Y., 1993. Metabolism of tri-n-butyltin chloride in male rats. J. Agric. Food. Chem. 41, 489–495.
- Mimura, H., Nagata, S., Matsumoto, T., 1994. Concentrations and compositions of internal free amino acids in a halotolerant *Brevibacterium* sp. in response to salt stress. Biosci. Biotechnol. Biochem. 58, 1873–1874.
- Morales, M., Martínez-Paz, P., Ozáez, I., Martínez-Guitarte, J.L., Morcillo, G., 2013. DNA damage and transcriptional changes induced by tributyltin (TBT) after short in vivo exposures of *Chironomus riparius* (Diptera) larvae. Comp. Biochem. Physiol. C-Toxicol. Pharmacol. 158, 57–63.
- Murphy, C.D., 2015. Drug metabolism in microorganisms. Biotechnol. Lett. 37, 19–28.
- Nesci, S., Ventrella, V., Trombetti, F., Pirini, M., Borgatti, A.R., Pagliarini, A., 2011. Tributyltin (TBT) and dibutyltin (DBT) differently inhibit the mitochondrial Mg-ATPase activity in mussel digestive gland. Toxicol. Vitro 25, 117–124.
- Ohhira, S., Enomoto, M., Matsui, H., 2006. Sex difference in the principal cytochrome P-450 for tributyltin metabolism in rats. Toxicol. Appl. Pharmacol. 210, 32–38.
- QuEChERS-A Mini-Multiresidue Method for the Analysis of Pesticide Residues in Low-Fat Products, protocol available online at <http://quechers.cvu-stuttgart.de>.
- Ramírez-Molina, C., Burton, L., 2009. Screening strategy for the rapid detection of *in vitro* generated glutathione conjugates using high-performance liquid chromatography and low-resolution mass spectrometry in combination with LightSight® software for data processing. Rapid Commun. Mass Spectrom. 23, 3501–3512.
- Rhee, S.G., Kang, S.W., Chang, T.S., Jeong, W., Kim, K., 2001. Peroxiredoxin, a novel family of peroxidases. IUBMB Life 52, 35–42.
- Shevchenko, A., Tomas, H., Havli, J., Olsen, J.V., Mann, M., 2006. In-gel digestion for mass spectrometric characterization of proteins and proteomes. Nat. Protoc. 1, 2856–2860.
- Song, Y.L., Jing, W.H., Yan, R., Wang, Y.T., 2014. Metabolic characterization of (±)-praeuraptin A *in vitro* and *in vivo* by high performance liquid chromatography coupled with hybrid triple quadrupole-linear ion trap mass spectrometry and time-of-flight mass spectrometry. J. Pharm. Biomed. Anal. 90, 98–110.
- Szewczyk, R., Soboń, A., Różalska, S., Dzitko, K., Waidelich, D., Długoński, J., 2014. Intracellular proteome expression during 4-n-nonylphenol biodegradation by the filamentous fungus *Metarhizium robertsii*. Int. Biodeterior. Biodegr. 93, 44–53.
- Szewczyk, R., Soboń, A., Staba, M., Długoński, J., 2015. Mechanism study of alachlor biodegradation by *Paecilomyces marquandii* with proteomic and metabolomic methods. J. Hazard. Mater. 291, 52–64.
- Tabb, M.M., Blumberg, B., 2006. New modes of action for endocrine-disrupting chemicals. Mol. Endocrinol. 20, 475–482.
- Takagi, H., 2008. Proline as a stress protectant in yeast: physiological functions, metabolic regulations, and biotechnological applications. Appl. Microbiol. Biotechnol. 81, 211–223.
- Wei, R., Li, G., Seymour, A.B., 2010. High-throughput and multiplexed LC/MS/MS method for targeted metabolomics. Anal. Chem. 82, 5527–5533.
- Zhou, J., Zhu, X.S., Cai, Z.H., 2010. Tributyltin toxicity in abalone (*Haliotis diversicolor supertexta*) assessed by antioxidant enzyme activity, metabolic response, and histopathology. J. Hazard. Mater. 183, 428–433.

SUPPORTING MATERIAL

Table S-1. Multiple reaction monitoring (MRM) MS/MS scan mode – compound dependant parameters applied in the screening method.

Q1 mass (Da)	Q3 Mass (Da)	Dwell time (ms)	Amino acid	DP (V)	EP (V)	CE (V)	CXP (V)
90	44	5	Alanine	25	10	17	10
104.1	87	5	Aminoisobutyrate	30	10	17	10
175.1	70	5	Arginine	25	10	32	10
133.1	74	5	Asparagine	30	10	23	10
134.	74	5	Aspartate	25	10	21	10
118.1	58	5	Betaine	40	10	41	10
122	76	5	Cysteine	25	10	20	10
104.1	58	5	Dimethyl glycine	30	10	20	10
148.1	84	5	Glutamate	25	10	23	10
147.1	84	5	Glutamine/Lysine	25	10	25	10
76	30.2	5	Glycine	20	10	21	10
156.1	110	5	Histidine	25	10	21	10
136	90	5	Homocysteine	50	10	20	10
132.1	86.2	5	Hydroxyproline/Isoleucine/Leucine	50	10	18	10
150.1	61	5	Methionine	40	10	31	10
133.1	70	5	Ornithine	40	10	30	10
166.1	120.2	5	Phenylalanine	50	10	19	10
116.1	70	5	Proline	50	10	20	10
106.0	60	5	Serine	25	10	18	10
120.1	102	5	Threonine	30	10	10	10

205.1	188.3	5	Tryptophan	25	10	16	10
182.1	136.3	5	Tyrosine	25	10	19	10
118.1	72	5	Valine	25	10	18	10

P2

*Metabolomics of the recovery of the filamentous fungus *Cunninghamella echinulata* exposed to tributyltin*

SOBOŃ A, SZEWCZYK R, RÓŻALSKA S, DŁUGOŃSKI J

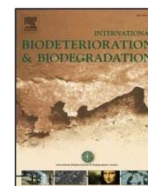
International Biodeterioration and Biodegradation

doi: 10.1016/j.biod.2017.11.008



Contents lists available at ScienceDirect

International Biodeterioration & Biodegradation

journal homepage: www.elsevier.com/locate/ibiodMetabolomics of the recovery of the filamentous fungus *Cunninghamella echinulata* exposed to tributyltin

Adrian Soboń, Rafał Szewczyk, Sylwia Różalska, Jerzy Długoński*

Department of Industrial Microbiology and Biotechnology, Institute of Microbiology, Biotechnology and Immunology, Faculty of Biology and Environmental Protection, University of Lodz, Łódź, Poland

ARTICLE INFO

Keywords:

Cunninghamella echinulata
Tributyltin
Metabolomics
LC-MS/MS
Oxidative stress
Metabolic activity

ABSTRACT

The exposure of microorganisms to toxic compounds induces a range of responses at different levels of the cell morphology, biochemistry and physiology. Tributyltin (TBT) is a highly toxic compound used for many years in industry as a marine anti-fouling agent or as a biocide in preservatives of wood. We previously described a microscopic filamentous fungus *Cunninghamella echinulata* IM 2611 capable of efficient degradation of TBT at a high concentration. Additionally, we demonstrated that TBT showed a negative effect on fungal growth, as well as protein and amino acid profiles. This study used microscopic, metabolic and targeted metabolomic analyses for a better understanding of the processes occurring in the fungal hyphae of *C. echinulata* during exposure to highly toxic TBT. The exposure to TBT strongly inhibited the metabolic activity of *C. echinulata*, leading to changes in the hyphal structure. In addition, the study showed disturbances in the functioning of the major biochemical pathways in the cells through changes in the profile of metabolites belonging to glycolysis, tri-carboxylic acid (TCA) cycle, amino acids and nucleotides pathways. Despite many adverse changes, the fungus was able to recover in the toxic environment.

1. Introduction

Metabolomics is a dynamically growing field in systems biology. It is focused on the metabolites and small molecules present in biological samples (Szewczyk and Kowalski, 2016). Next to genomics, transcriptomics and proteomics, metabolomics is classified as an omic approach and an important tool used for a better understanding of the biology of organisms and their response to environmental conditions (Roessner and Bowne, 2009).

Tributyltin is a well-known endocrine disruptor which shows several negative and toxic effects on living organisms: from bacteria to higher organisms (Antizar-Ladislao, 2008; Cruz et al., 2015; Długoński, 2016). Mitochondria are particularly susceptible to the effects of TBT (Yamada et al., 2015). Tributyltin shows high affinity to cell membranes and interferes with their integrity (Bernat and Długoński, 2012). In mitochondria two important biochemical pathways (glycolysis and TCA) occur, which are necessary for the proper function of the cell. This xenobiotic not only negatively affects the above-mentioned mitochondrial pathways but also generates oxidative stress which causes damage to different cell components and macromolecules, e.g. DNA (Ishihara et al., 2012), proteins (Gupta et al., 2011) or lipid composition (Bernat et al., 2014). This damage could lead to cell apoptosis (Jurkiewicz et al.,

2004). Organisms use enzymatic and non-enzymatic defense strategies against unfavorable changes. However, changes at the metabolome level are still poorly understood, particularly in the context of microorganisms capable of degrading compounds harmful to the environment.

Only a few microorganisms capable of TBT elimination have been described (Cruz et al., 2015). Fungi from the genus *Cunninghamella*, capable of TBT elimination in high concentrations (up to 40 mg l⁻¹ by *C. elegans*) are very interesting (Bernat and Długoński, 2002). In our earlier study, *C. echinulata* was characterized as resistant to a high concentration of TBT (5 mg l⁻¹) and able to effectively transform the xenobiotic to less toxic metabolites – dibutyltin (DBT) and monobutyltin (MBT). TBT led to a strong inhibition of the fungus growth and significant changes in protein profiles (Soboń et al., 2016). In the present study, we used the metabolic activity assay, morphological analyses and targeted metabolomics for a detailed research on the TBT influence on the primary metabolism of the filamentous fungus *C. echinulata*.

* Corresponding author.

E-mail address: jerzy.dlugonski@biol.uni.lodz.pl (J. Długoński).

2. Materials and methods

2.1. Chemicals and reagents

Chemicals and reagents of the highest commercially available grade were used. TBT chloride (96% purity) was purchased from Sigma-Aldrich (Germany). Methanol, acetonitrile, formic acid and water were of LC-MS grade and came from Avantor (Poland) and Sigma-Aldrich (Germany). Metabolites were purchased from Sigma-Aldrich (Germany), Fluka (Germany), Supelco (Germany) or Calbiochem (Germany), and had a minimum purity of 95%.

2.2. Culture conditions

The strain *C. echinulata* IM 2611 from the microorganisms collection of the Department of Industrial Microbiology and Biotechnology, University of Łódź, Poland, was used in the investigation. Ten-day-old cultures on ZT slants (g l⁻¹: glucose, 4; Difco yeast extract, 4; agar, 25; malt extract 6 BLG up to 11; pH 7.0) were used to inoculate 20 ml of Sabouraud dextrose liquid medium (Difco) supplemented with 2% glucose as described previously (Soboń et al., 2016). The initial preculture was prepared to contain spores density of 1×10^7 ml⁻¹. Incubation was conducted in a 100-ml Erlenmeyer flask with a wide neck on a rotary shaker (160 rpm) at 28 °C. After 24 h, the precultures were transferred to fresh medium (in the ratio 1:4) and incubated for another 24 h. Two milliliters of the homogenous preculture were introduced into 18 ml of fresh Sabouraud medium (in a 100-ml Erlenmeyer flask with a wide neck) either supplemented with TBT at 5 mg l⁻¹ (TBT stock solution 5 mg ml⁻¹ in ethanol) or without the xenobiotic as a biotic control. Additionally, an abiotic control of TBT (without the microorganism) was prepared. The cultures and controls were incubated for 5 days in the same conditions.

2.3. Metabolic activity and morphological analyses

Metabolic activity measurements were performed according to the procedure described by Różalska et al. (2014), using a modified FDA (fluorescein diacetate) method in a FLUOstar Omega fluorescence microplate reader (BMG Labtech), where the fluorescence was read at an excitation of 485 nm and emission of 530 nm. The data obtained from the microplate reader (mean fluorescent units) were divided by the amount of dry mass obtained for each sample. The results were presented as Fluorescence intensity (AU) in time. Microscopic images were taken using an LSM 5 (Zeiss) confocal laser scanning microscope equipped with a Nomarski DIC and Plan-Neofluar 63 × (1.25 oil) objective lenses.

2.4. Glucose analysis

Sample preparation for glucose quantitation was performed according to a previously described procedure (Różalska et al., 2010). The samples (200 µl) were withdrawn aseptically and placed in Eppendorf tubes followed by centrifugation $2600 \times g$ for 10 min. Next, supernatants were transferred to new Eppendorf tubes and diluted prior to LC-MS/MS.

2.5. Intracellular metabolite extraction

Samples were collected every 24 h. Whole mycelium was separated from the medium during the filtration using polycarbonate membrane filters (0.4 µm of pore size) and washed using 100 ml of deionized water. Next, 100 mg of wet biomass was placed in a 1.5-ml Eppendorf tube for immediate storage in a freezer (−70 °C). L-phenyl-d₅-alanine and succinic acid-2,2,3,3-d₄ were used as internal standards for the analysis of amino and organic acids, respectively. Homogenization and the extraction were performed at the same time. For this purpose,

approximately 0.5 ml of glass beads, 320 µl of 80% acetonitrile/20% water solution and 40 µl (1.25 mg ml⁻¹) of internal standards were added to an Eppendorf tube containing 100 mg of frozen filtered mycelium, and homogenized for 30 s at a velocity of 4 m s⁻¹ using FastPrep-24, and then incubated for 10 min on ice. At the end of the 10-min incubation, the sample was spun in a microcentrifuge at $12,000 \times g$ for 2 min at 4 °C. The extraction process was carried out thrice and the resulting extracts were combined.

2.6. Extracellular metabolite analysis

For the analysis of extracellular metabolites, the culture medium was centrifuged and the supernatant was stored at −70 °C for further examination. Before the analysis, the supernatant was thawed, diluted and analyzed by LC-MS/MS.

2.7. LC conditions

Qualitative analyses were performed using an Eksigent expert™ microLC 200 chromatograph with Eksigent columns and an Agilent 1200 chromatograph with a Phenomenex AQ column coupled with an AB Sciex QTRAP 4500 mass spectrometer.

LC separations were carried out on three different columns in the reverse phase mode. An Eksigent 3C8-EP-120 (0.5 × 150 mm, 3 µm) column (Eksigent, USA) was used to separate the majority of the amino acids, vitamins and nucleic bases in positive ionization mode. The mobile phases used were 0.1% formic acid in water (A) and 0.1% formic acid in acetonitrile (B). The 4-min separation time started from 2% B for 0.2 min, followed by a linear increase to 95% B for 2 min; held at 95% B for 1.2 min, and then decreased to 2% B and held for 0.6 min. The flow rate was set to 50 µl min⁻¹ at 40 °C and the injection volume was set to 2 µl.

An Eksigent 3C18-AQ-120 (0.5 × 150 mm, 3 µm) column (Eksigent, USA) was used to separate selected organic acids, both forms of glutathione, and pantothenate in negative ionization mode. The mobile phase consisted of 0.1% formic acid in water (A) and 0.1% formic acid in acetonitrile (B). The 4-min separation time started from 2% B for 0.1 min, followed by a linear increase to 30% B for 0.4 min and a linear increase to 98% B for 2 min; held at 98% for 1 min, and then decreased to 2% B and held for 0.5 min. The flow rate was set to 50 µl min⁻¹ at 40 °C and the injection volume was set to 2 µl.

A Synergi Hydro-RP column (2 × 150 mm, 4 µm) (Phenomenex, Germany) was used to separate other organic acids, nucleotides and metabolites containing a phosphate group in the molecule. The mobile phase consisted of 4 mM ammonium acetate in 95/5 water/acetonitrile (A) and 4 mM ammonium acetate in 5/95 water/acetonitrile (B). The 15-min separation time started from 0% B for 0.2 min followed by a linear increase to 95% B for 4.8 min; held for 2 min, and then decreased to 0% B and held for 8 min. The flow rate was set to 500 µl min⁻¹ at 40 °C and the injection volume was set to 10 µl.

2.8. Mass spectrometry

Ionization polarity, optimal declustering potential (DP), product ion and collision energy (CE) for all metabolites were manually tuned using standard solutions as presented in Table S-1. For microLC analysis, MS parameters were as follows: nebulizer gas (GS1) and drying gas (GS2) were set to 28 and 40, respectively; curtain gas (CUR) was set to 25; source temperature (TEM) was set to 400 °C and Ion Spray voltage (IS) was set to 5000 V and −4500 V for the positive and negative mode, respectively. For HPLC analysis, the MS parameters were as follows (in negative ionization mode): IS: −4500 V, Cur: 30, GS1: 50, GS2: 40, TEM: 500 °C.

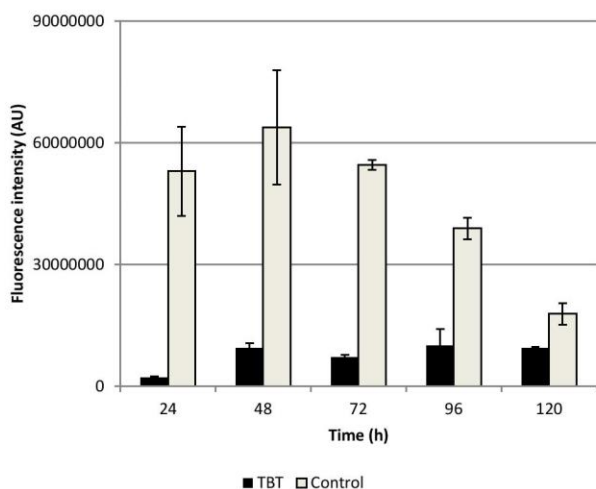


Fig. 1. *Cunninghamella echinulata* IM 2611 viability during the incubation with TBT (5 mg l^{-1}). The measurement was performed using a modified FDA (fluorescein diacetate) method in a fluorescence microplate reader (485 nm and 530 nm of excitation and emission, respectively). The data are presented as a fluorescence intensity (AU) according the time.

2.9. Statistical analysis

The experiments were carried out in triplicate. The T-test using Excel 2013 (Microsoft Corporation, USA) was used to determine the significance of the differences between the samples. An average standard deviation (\pm SD) was calculated for each data. Values were considered significant if $P < 0.05$. Principal component analysis (PCA) of the statistically processed quantitative data obtained from the LC-MS/MS analysis was conducted with MarkerView™ software (AB Sciex, USA). The Pareto scaling was applied for the PCA calculation. Normalization using the Z-score algorithm and the heatmap were performed using Perseus Software (Tyanova et al., 2016).

3. Results

3.1. Metabolic activity in the presence of TBT

In order to show the influence of TBT, the metabolic activity of *C. echinulata* was assessed using the FDA staining method coupled with morphological analyses. The results presented in Fig. 1 show that it was significantly lower during the exposure to TBT. The most significant TBT impact on *C. echinulata* was observed at the initial stage of incubation, especially after 24 h of culturing. In the cultures containing TBT, the calculated metabolic activity value was only 3.9% in comparison to untreated cells (Fig. 1). The metabolic activity of *C. echinulata* in the presence of TBT gradually increased during incubation to a value of 50.85% after 120 h. This proves that the applied concentration of TBT (5 mg l^{-1}) was highly toxic to the microorganism, which finally resulted in severe growth inhibition after the first 24 h of culturing. These findings are also in agreement with microscopic observations, where the most severe damage (shrinking of the protoplasts) to *C. echinulata* cells was observed on the first day of incubation (Fig. 2b). After 48–72 h of incubation with TBT, where an increase in fungal metabolic activity was observed, the morphological damage to the cells was different from that noted after 24 h of culturing. Only few cells with gaps between the cell wall and the membrane were observed, while in the majority of the cells multiple, circular vesicles were detected (Fig. 2c and d). At the end of the experiment (120 h), the metabolic activity in the TBT supplemented cultures increased in comparison to the control and microscopic data revealed the presence of

hyphae comparable to the control samples (Fig. 2a and f).

3.2. TBT disrupts the functioning of cellular biochemical pathways

Using a targeted LC-MS-MS analysis, a total of 92 metabolites from *C. echinulata* were measured at various time-points (0, 24, 72, 96, and 120 h incubation) across three biological replicates. For the LC-MS/MS data acquired for control (c) and TBT-treated samples (TBT), Principal Component Analysis (PCA) (Ringnér, 2008) was performed using MarkerView™ software (AB Sciex, USA). Analyses of intracellular and extracellular metabolites allowed the monitoring of changes occurring in the cell. The major differences appeared during the first 48 h of culture. Fig. 4A and B show that for both intracellular and extracellular metabolite profiles, the samples “0 h” (or “Sabouraud” in extracellular analysis), “TBT24” and “TBT48” are located farthest from the other samples on the PCA chart. The data from intra- and extracellular metabolite concentrations were plotted as a heatmap chart presented in Fig. 5. Those metabolites were responsible for the observed changes and together covered various metabolic pathways, such as purine, pyrimidine, amino acid, TCA and the sugar metabolism.

3.2.1. TBT interferes with glycolysis

The negative effect of TBT on glucose utilization was noted. A reduced uptake of glucose from the medium was observed during the exposure to TBT (Fig. 3). Especially after 24 h of incubation, a slight amount of glucose from the medium was used in xenobiotic-treated samples. At the end of the experiment, microorganisms used 62% and 78.3% of the initial glucose amount in both control samples and those containing TBT, respectively. Further insights into carbon source usage in the presence of the xenobiotic were gained by sugar metabolism analysis. All tested glycolysis intermediates – glucose-6-phosphate (G6P), fructose-1,6-bisphosphate (F16bP) and phosphoenolpyruvate (PEP), were accumulated in TBT-treated samples - this accumulation was especially noticeable after 24 h of incubation (Figs. 5 and 6).

3.2.2. TBT disrupts proper functioning of the TCA cycle

A decreased accumulation of the total TCA cycle metabolites (except for oxaloacetate) was observed in cultures containing TBT after 24 h of incubation. Oxaloacetate (the first intermediate of the TCA cycle) was the only TCA-related compound present in higher concentrations in TBT-treated cells. Limited organic acid production was observed during the analysis of Sabouraud medium composition. Media acidification by *C. echinulata* was significantly reduced after the treatment with the xenobiotic (Fig. 3). In contrast to untreated cells, which were able to reduce the external pH from 5.69 to less than 5.00 after 24 h of incubation, the treated cells reduced the pH slowly during cultivation and reached a value below 5 after 4 days. In control conditions, the fungus extensively secreted organic acids (mainly malic and succinic acid) to the medium (Fig. 5). However, in samples containing TBT (especially after the first two days of incubation) the fungus did not secrete organic acids in large amounts. The exceptions were cis-aconitate and adipate, which were the only organic acids excreted to the medium in the amounts higher than in the control sample.

3.2.3. TBT induces changes in the amino acid composition

Both glycolysis and TCA cycles are key processes involved in amino acid biosynthesis. For the analysis of intracellular amino acids, one of the observed trends was a delay in the uptake and synthesis of amino acids under the influence of TBT. A reduced concentration was observed for the majority of amino acids in treated cells after 24 h of incubation. After 48 h of incubation with the xenobiotic, the fungus contained the amount of amino acids comparable to that in the control samples after 24 h. A similar trend was observed for extracellular metabolite profiles, where most significant changes occurred after the first two days of culturing (Figs. 4B and 5). An interesting result was obtained for L-aminoadipate, which is a precursor for lysine synthesis. In

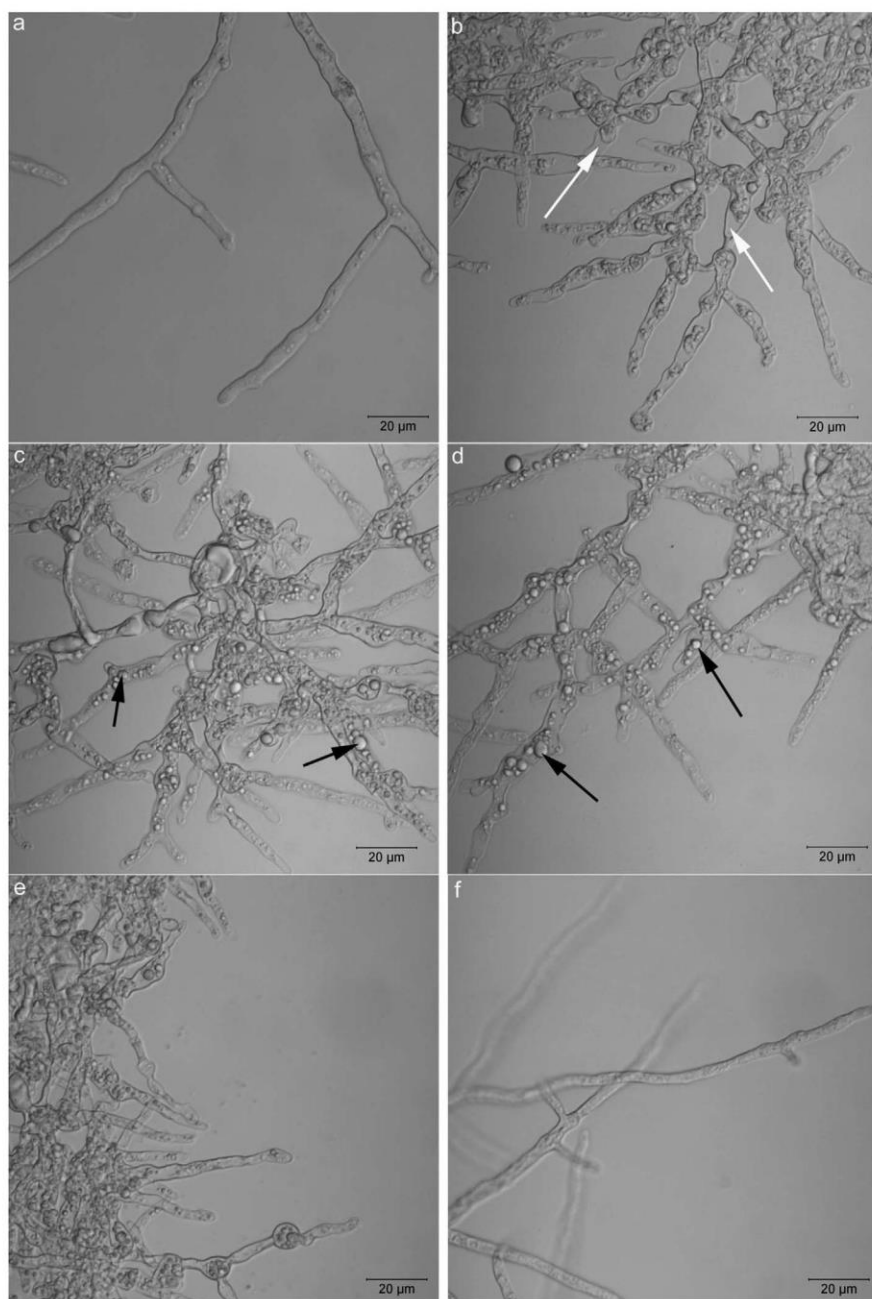


Fig. 2. Influence of TBT on the morphology of *C. echinulata*. (a) Control-without TBT, samples supplemented with TBT at (b) 24 h, (c) 48 h, (d) 72 h, (e) 96 h, (f) 120 h. Cell protoplast damage (shrinking of the protoplasts) is marked with white arrows, while the presence of round vesicles is marked with black arrows.

the control system, the fungus exhausted all the lysine from the medium during 24 h of culturing, and the maximum intracellular concentration of lysine was observed after 24 h and, at subsequent measuring points, its contents fluctuated around a similar level. A completely opposite situation was observed for TBT-treated samples. After 24 h the microorganism did not use lysine from the medium – a low measurable concentration of intracellular lysine was observed until 72 h of culture. Another significant observation concerned the accumulation of stress-related metabolites. Betaine was strongly accumulated in the fungal cells and showed a maximum concentration after 24 h of incubation. This was one of the few examples of metabolites where maximum concentrations were found after 24 h of the exposure to TBT. Proline showed an over three-fold increased concentration compared to the control sample, and was the amino acid produced in the largest quantities by the fungus, reaching a value of 733.2 µg per 100 mg of

biomass. A higher concentration of proline in samples containing TBT did not increase the content of hydroxyproline, which continued to occur at a similar level to that in the control system. However, after 96 h the concentration of hydroxyproline increased and the proline level decreased. A significant increase in the γ -aminobutyrate (GABA) concentration was observed after 48 h in TBT-samples.

The extracellular amino acid composition showed that the utilization of compounds was limited under the exposure to TBT. As presented on the PC scores chart (Fig. 4B), the samples “Sabouraud”, “TBT24” and “TBT48” are located at close distances to each other, and farthest from the other samples. The main analytes determining differences between the samples located on the PC loadings chart included amino acids (Fig. 4B). After 24 h the microorganism did not use arginine, lysine and phenylalanine, or it used only part of the amino acids soluble in medium (serine). Despite the strong intracellular accumulation, proline

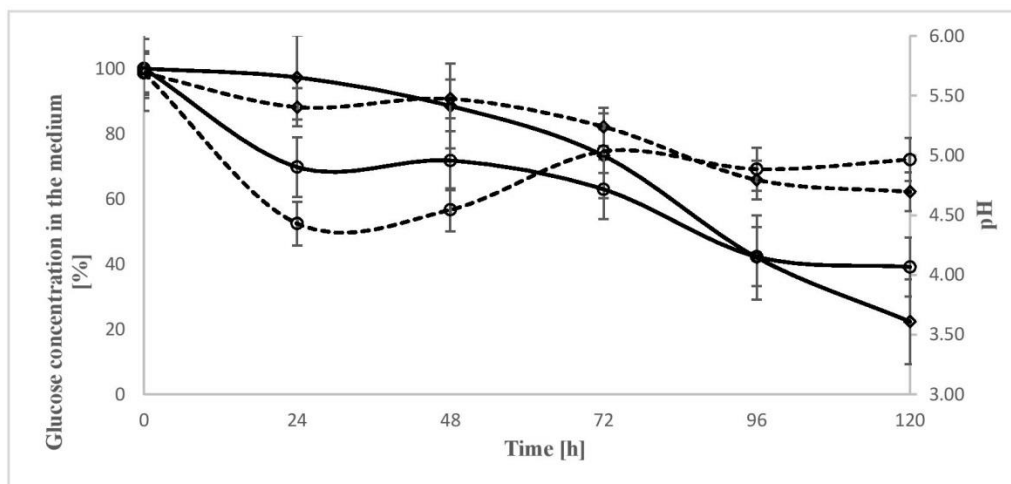


Fig. 3. Glucose utilization (solid line) and medium acidification (dotted line) by *C. echinulata* in the presence of TBT (5 mg l^{-1}) (white diamond) compared to the control without toxic substrate (white circle).

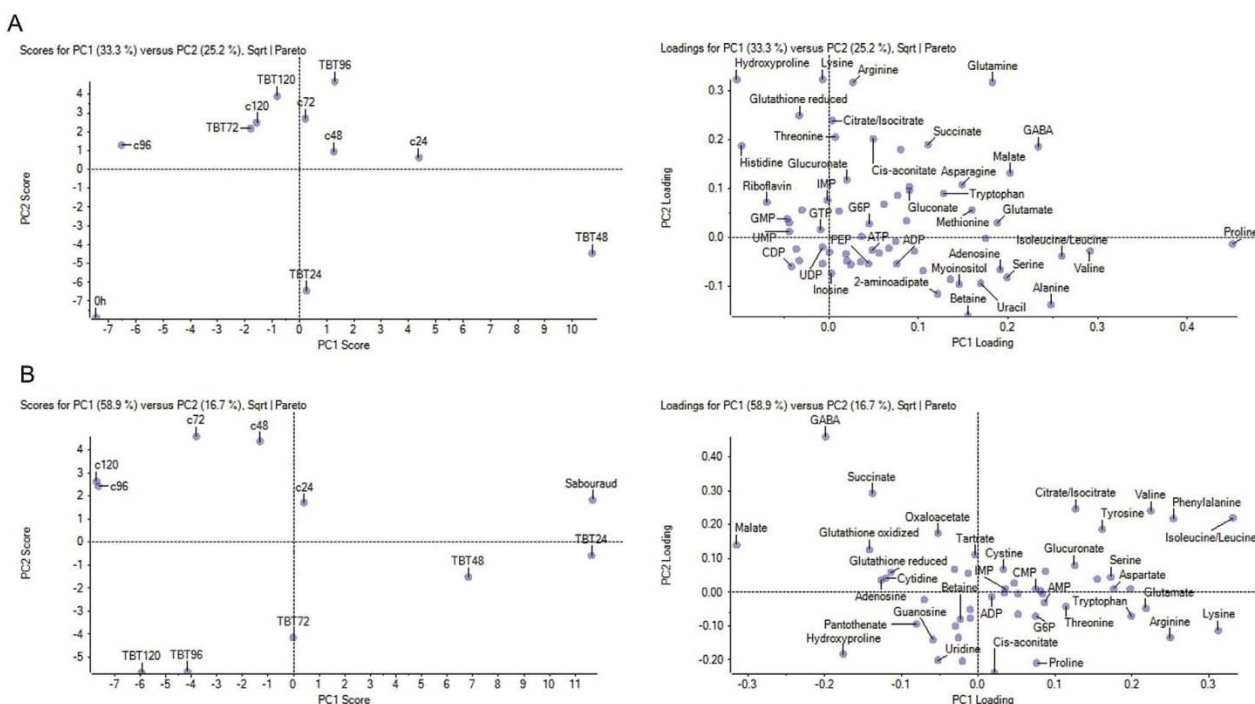


Fig. 4. PCA analysis of intracellular (A) and extracellular (B) metabolite compositions in control (c) and TBT-containing cultures (TBT) of *C. echinulata* on Sabouraud medium. The numbers on the PC Score section represent the time of culturing, and metabolites responsible for the data clustering were presented in the PC loading section.

was secreted in large quantities into the culture medium. In contrast, under control conditions the microorganism intensively utilized amino acids and therefore after 24 h either a minimal concentration was observed or no signal was detected.

3.2.4. Effect of TBT on purine and pyrimidine biosynthesis

Disturbance in the nucleotide biosynthesis is another common cell response against stress. In the tested fungal cultures, a significant effect of biocide was observed on nucleotide synthesis in the early stages of the exposure to TBT. As a result, uridine monophosphate (UMP) content decreased in the cell, compared to both the corresponding control sample and the preculture sample. The same correlation was observed for cytidine monophosphate (CMP). After 24 h exposure to the xenobiotic, UMP and CMP were still present in the medium. A completely

reverse correlation was observed for purine nucleotides such as adenosine monophosphate (AMP), adenosine diphosphate (ADP), adenosine triphosphate (ATP), guanosine monophosphate (GMP), guanosine diphosphate (GDP) and inosine monophosphate (IMP). These metabolites were present in higher concentrations in fungal cells cultivated in the presence of the xenobiotic.

4. Discussion

Metabolism is the foundation of life processes, and consists of a number of biochemical processes in cells, determining their growth and functioning. Metabolic disorders may lead to cellular dysfunctions or even cell death. Many factors, such as xenobiotics, can adversely affect metabolism. Metabolomics is a helpful tool, which is currently being



Fig. 5. Heatmaps of intracellular (left) and extracellular (right) metabolite compositions in untreated (c) and TBT-treated samples (TBT) of *C. echinulata*. The numbers represent the time of culturing. The metabolites which were not detected during the whole time of the experiments are presented in grey.

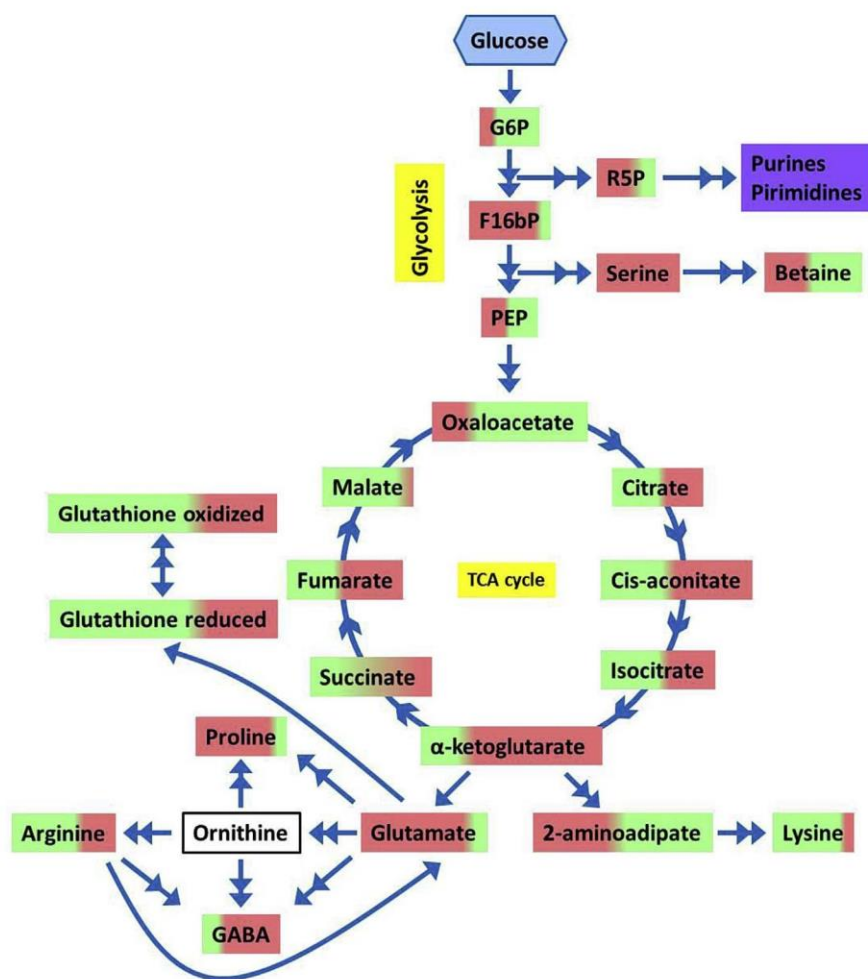


Fig. 6. Analysis of TBT impact on the regulation of selected metabolic pathways in *C. echinulata*. Single and double arrows indicate one and two (or more) reaction steps, respectively. Colors are used to schematically represent changes in compounds concentrations (red for up-regulation and green for down-regulation) during 120 h of incubation in TBT-treated samples. (For interpretation of the references to colour in this figure legend, the reader is referred to the web version of this article.)

extensively used for a better understanding of the processes occurring in the cell. This may be particularly important in the monitoring of the effects of toxic compounds. The smooth operation of biochemical pathways is essential for the proper functioning of the cell – its growth, differentiation and division.

During the exposure to TBT, an interesting observation was the recovery of the fungus. The previous study showed that TBT strongly inhibited *C. echinulata* growth and generated oxidative stress (Soboń et al., 2016). Moreover, disturbance in microorganisms growth, as well as morphological changes caused by the exposure to TBT were previously reported (Cruz et al., 2012; Bernat et al., 2009). After an initial lag in the fungal growth during the first 48 h of culturing, the increment of the culture biomass was noticed. Interestingly, despite exerting negative effects on cells, *C. echinulata* was able to effectively degrade over 91% of TBT (5 mg l^{-1}) after 5 days of incubation. It seems that it is a unique feature of the genus *Cunninghamella*, as it was described also for *C. elegans* (Bernat and Długoński, 2002), however, the mechanism of the fungal adaptation is still not clear.

In the present study TBT strongly reduced the metabolic activity of the tested microorganism. After 24 h the fungus showed only 3.9% of the metabolic activity, which then gradually increased along with the incubation time. Cruz et al. (2012) showed that the metabolic activity of *Aeromonas molluscorum*, as determined by ATP and NADH levels, was reduced in the presence of TBT. The literature indicates a number of mechanisms correlated with several cell networks that may be involved in the organism survival and TBT degradation. The xenobiotic is known to modify fatty acid compositions of the *C. elegans* cell membrane and

the saturation of fatty acids is an important factor of the microorganism's resistance (Bernat et al., 2009). The overexpression of ROS-scavenging enzymes, like peroxiredoxin (Soboń et al., 2016), can also be responsible for the fungus recovery.

The analysis of extracellular metabolites composition, pH and glucose concentration also confirmed decreased levels of metabolic activity. After 24 h in the samples containing TBT, the levels of compounds soluble in the medium were similar to the initial metabolite concentrations in the Sabouraud medium. After 24 and 48 h of the exposure to TBT, the pH values were similar to the initial medium values. In the case of glucose, a significant inhibition of its uptake from the medium was observed in the cultures supplemented with the xenobiotic. The acidification of culture media is a characteristic feature of *Mucorales* (Rosling et al., 2007). Rousk et al. (2009) proposed two reasons for fungal acidification of their habitat: (i) low pHs favor fungal growth and prevent undesired growth of other microorganisms; and (ii) the acidic environment increases the availability of carbon, nutrient and metal. Acidification of the growth environment by fungi improves the availability of nutrients, for example phosphorus (Rosling et al., 2004), as a result of microbial secretion of organic acids, proton efflux over the plasma membrane, and the formation of carbonic acid in the media from respiratory CO_2 production (Burford et al., 2003). The stable pH in samples containing xenobiotics could be responsible for the decreased bioavailability of nutrients, such as amino acids or compounds containing phosphorus. In the samples containing TBT (especially after the first two days of incubation) the fungus did not secrete large amounts of organic acids to the medium, which resulted in lower

acidification of the medium during exposure to TBT. This further led to lower utilization of amino acids, such as isoleucine/leucine, lysine, valine and phenylalanine found in the medium in high concentrations.

The intracellular accumulation of energy-related metabolites is a determinant of disturbances in the metabolism of energy. PEP and FBP are key contributors to the assessment of the nutrient starvation response in glucose assimilation (Brauer et al., 2006). In particular, PEP is a strong marker of carbon starvation. Other helpful contributors are α -ketoglutarate (nitrogen assimilation), glutamine (ammonia utilization) and IMP or carbamoyl-aspartate (purine or pyrimidine biosynthesis). The exposure to TBT revealed that only glycolysis intermediates were accumulated, while glutamine levels were not significantly affected. As stated by Thomsson et al. (2005), the major response of the organism to general stress is energy conservation. Increased levels of PEP or F16bP have been also observed in *Saccharomyces cerevisiae* as a result of carbon starvation (Brauer et al., 2006). Moreover, there is evidence that PEP could inhibit the activity of glycolytic enzymes (Ogawa et al., 2007). Disturbances in the glycolysis pathway and glucose uptake were observed in human embryonic carcinoma cells during exposure to TBT (Yamada et al., 2013). Intracellular accumulation of sugar-related metabolites was observed during biodegradation of alachlor by the filamentous fungus *Paecilomyces marquandii* (Szewczyk et al., 2015). Energy saving seems to be a characteristic microorganism's response to stress conditions. A clear explanation of the observed accumulation of glycolysis compounds in fungal cells is still difficult. Blockage of glucose utilization caused by xenobiotic-induced oxidative stress, as well as inhibition of glycolytic-related enzymes leads to carbon starvation and an increased content of metabolites associated with the central carbon metabolism. The higher levels of glycolysis intermediates may also reinforce blockage of the sugar metabolism, and thus, a reduce the uptake of glucose resulting in arrested growth, as presented in our previous work (Soboń et al., 2016). The obtained results have confirmed that TBT disrupt glycolytic pathway in the tested microorganism.

TBT exerts an undesirable effect on the TCA cycle and amino acid pathways of *C. echinulata*. Changes in the metabolite profiles of human embryonic carcinoma cells exposed to TBT were described by Yamada et al. (2014). Yamada and co-workers observed a decreased content of α -ketoglutarate, succinate and malate during exposure to TBT, whereas the levels of acetyl coenzyme A and isocitrate remained unchanged. Another study using the metabolomics approach to TBT toxicology was conducted by Zhou et al. (2010). *Haliotis diversicolor supertexta* exposed to TBT revealed increased levels of succinate, acetate, lactate, alanine and glutamine, as well as decreased concentrations of pyruvate and glucose in abalone hemolymphs.

IMP, a precursor for AMP and GMP synthesis, is another important contributor to the starvation response in purine and pyrimidine biosynthesis (Brauer et al., 2006). The content of ribose-5-phosphate (R5P), which is a precursor for nucleotide synthesis (Jozefczuk et al., 2010), also increased in TBT-containing samples. The negative effect of TBT on energy production by ATP synthase and related enzymes inhibition is well-known (Pagliarini et al., 2013). Similarly to our results, the increased content of AMP and ADP in the abalone hepatopancreas during exposure to organotin (TBT and triphenyltin) was observed by Lu et al. (2017).

Despite the negative effect of xenobiotics on the proper functioning of many elementary cellular processes, *C. echinulata* actively counteracts adverse changes caused by TBT by accumulating metabolites, which play a protective role against oxidative and osmotic stress. Betaine, proline and GABA are amino acids which are well-known for their beneficial role in various stress conditions and cellular osmoregulation (Ashraf and Foolad, 2007; Liang et al., 2013; Shelp et al., 1999). The experiments demonstrated the effect of TBT on the metabolism of glutamic acid (Fig. 6). The major activated pathway starts at glutamate and leads to a formation of high amounts of proline, GABA and both forms of glutathione. The disturbance of glutamate uptake

from the medium and increased concentration of α -ketoglutarate after 48 h of incubation indicate the importance of the glutamate network for the fungus recovery. Moreover, the absence of ornithine suggests that either it was rapidly utilized or the fungus switched its metabolism by omitting or silencing the ornithine pathway. Oxidative stress was also confirmed during biodegradation of ametryn by *Metarhizium brunneum* (Szewczyk et al., 2018), where betaine, proline and GABA were accumulated intracellularly. GABA, together with betaine and proline, seems to play a key role in cell protection in the presence of toxic xenobiotics, including TBT. Moreover, microscopic observation showed a large number of vesicles in *C. echinulata*, and potassium retention in *C. elegans* (Bernat et al., 2009). Due to their involvement in the osmoregulation, intracellular accumulation may be responsible for the maintenance of homeostasis.

5. Conclusions

Changes in the metabolome and metabolic activity of *C. echinulata* during the exposure to TBT were studied. TBT had a significant wide-range negative impact on fungal metabolism. The exposure to TBT caused damage to the protoplasts resulting in significant changes in the hyphal morphology, as well as significant inhibition of metabolic activity, resulting in reduced utilization of carbon and energy media sources. On the intracellular level, TBT disrupted sugar metabolism by blockage of the glycolytic pathway leading to accumulation of glycolysis intermediates and TCA cycle malfunctions, when compared to control cultures. TBT also exerts an undesirable effect on the purine and pyrimidine metabolism of *C. echinulata*, as evidenced by nucleotides profiling. Disturbances in glycolysis and TCA cycle were also reflected in changes in the amino acids composition. Profiling of these compounds revealed the oxidative stress condition caused by TBT. In response to a number of adverse changes, the fungus switched its metabolic network to counteract the harmful effects of TBT by accumulating amino acids with antioxidant properties such as betaine, proline or GABA. Despite the strong growth inhibition and metabolic disorders, the fungus was able to recover. Further research on the effects of TBT biodegradation on *C. echinulata* is needed to reveal its impact on the other levels of cellular organisation including large biomolecules expression and profiling in lipidomics, proteomics and genetics study.

Acknowledgements

These studies were supported by the National Science Center, Poland (Project No. UMO-2014/13/N/NZ9/00878) and by a subsidy targeted at young scientists and doctoral students (5811/E-345/M/2015).

Appendix A. Supplementary data

Supplementary data related to this article can be found at <http://dx.doi.org/10.1016/j.ibiod.2017.11.008>.

References

- Antizar-Ladislao, B., 2008. Environmental levels, toxicity and human exposure to tributyltin (TBT)-contaminated marine environment. A review. *Environ. Int.* 34, 292–308.
- Ashraf, M., Foolad, M., 2007. Roles of glycine betaine and proline in improving plant abiotic stress resistance. *Environ. Exp. Bot.* 59, 206–216.
- Bernat, P., Długoński, J., 2002. Degradation of tributyltin by the filamentous fungus *Cunninghamella elegans*, with involvement of cytochrome P-450. *Biotechnol. Lett.* 24, 1971–1974.
- Bernat, P., Ślaba, M., Długoński, J., 2009. Action of tributyltin (TBT) on the lipid content and potassium retention in the organotins degrading fungus *Cunninghamella elegans*. *Curr. Microbiol.* 59, 315–320.
- Bernat, P., Długoński, J., 2012. Comparative study of fatty acids composition during cortaxolone hydroxylation and tributyltin chloride (TBT) degradation in the filamentous fungus *Cunninghamella elegans*. *Int. Biodeterior. Biodegrad.* 74, 1–6.
- Bernat, P., Gajewska, E., Szewczyk, R., Ślaba, M., Długoński, J., 2014. Tributyltin (TBT) induces oxidative stress and modifies lipid profile in the filamentous fungus

- Cunninghamella elegans*. Environ. Sci. Pollut. Res. 21, 4228–4235.
- Brauer, M.J., Yuan, J., Bennett, B.D., Lu, W., Kimball, E., Botstein, D., Rabinowitz, J.D., 2006. Conservation of the metabolomic response to starvation across two divergent microbes. Proc. Natl. Acad. Sci. 103, 19302–19307.
- Burford, E.P., Fomina, M., Gadd, G.M., 2003. Fungal involvement in bioweathering and biotransformation of rocks and minerals. Mineral. Mag. 67, 1127–1155.
- Cruz, A., Oliveira, V., Baptista, I., Almeida, A., Cunha, A., Suzuki, S., Mendo, S., 2012. Effect of tributyltin (TBT) in the metabolic activity of TBT-resistant and sensitive estuarine bacteria. Environ. Toxicol. 27, 11–17.
- Cruz, A., Anselmo, A.M., Suzuki, S., Mendo, S., 2015. Tributyltin (TBT): a review on microbial resistance and degradation. Crit. Rev. Environ. Sci. Technol. 45, 970–1006.
- Długoński, J., 2016. Microbial elimination of endocrine disrupting compounds. In: Długoński, J. (Ed.), Microbial Biodegradation: from Omics to Function and Application. Caister Academic Press, Norfolk, UK, pp. 99–117.
- Gupta, M., Dwivedi, U.N., Khandelwal, S., 2011. C-Phycocyanin: an effective protective agent against thymic atrophy by tributyltin. Toxicol. Lett. 204, 2–11.
- Ishihara, Y., Kawami, T., Ishida, A., Yamazaki, T., 2012. Tributyltin induces oxidative stress and neuronal injury by inhibiting glutathione S-transferase in rat organotypic hippocampal slice cultures. Neurochem. Int. 60, 782–790.
- Jozefczuk, S., Klie, S., Catchpole, G., Szymanski, J., Cuadros-Inostroza, A., Steinhäuser, D., Selbig, J., Willmitzer, L., 2010. Metabolomic and transcriptomic stress response of *Escherichia coli*. Mol. Syst. Biol. 6, 364.
- Jurkiewicz, M., Averill-Bates, D.A., Marion, M., Denizéau, F., 2004. Involvement of mitochondrial and death receptor pathways in tributyltin-induced apoptosis in rat hepatocytes. Biochimica Biophysica Acta (BBA)-Molecular Cell Res. 1693, 15–27.
- Liang, X., Zhang, L., Natarajan, S.K., Becker, D.F., 2013. Proline mechanisms of stress survival. Antioxidants redox Signal. 19, 998–1011.
- Lu, J., Feng, J., Cai, S., Chen, Z., 2017. Metabolomic responses of *Haliotis diversicolor* to organotin compounds. Chemosphere 168, 860–869.
- Ogawa, T., Mori, H., Tomita, M., Yoshino, M., 2007. Inhibitory effect of phosphoenolpyruvate on glycolytic enzymes in *Escherichia coli*. Res. Microbiol. 158, 159–163.
- Pagliarani, A., Nesci, S., Ventrella, V., 2013. Toxicity of organotin compounds: shared and unshared biochemical targets and mechanisms in animal cells. Toxicol. Vitro 27, 978–990.
- Ringnér, M., 2008. What is principal component analysis? Nat. Biotechnol. 26, 303–304.
- Roessner, U., Bowne, J., 2009. What is metabolomics all about? Biotechniques 46, 363.
- Rosling, A., Lindahl, B.D., Taylor, A.F., Finlay, R.D., 2004. Mycelial growth and substrate acidification of ectomycorrhizal fungi in response to different minerals. FEMS Microbiol. Ecol. 47, 31–37.
- Rosling, A., Suttle, K.B., Johansson, E., van Hees, P.A., Banfield, J.F., 2007. Phosphorous availability influences the dissolution of apatite by soil fungi. Geobiology 5, 265–280.
- Rousk, J., Brookes, P.C., Bååth, E., 2009. Contrasting soil pH effects on fungal and bacterial growth suggest functional redundancy in carbon mineralization. Appl. Environ. Microbiol. 75, 1589–1596.
- Różalska, S., Szewczyk, R., Długoński, J., 2010. Biodegradation of 4-n-nonylphenol by the non-ligninolytic filamentous fungus *Glioclavotrichum simplex*: a proposal of a metabolic pathway. J. Hazard. Mater. 180, 323–331.
- Różalska, S., Glińska, S., Długoński, J., 2014. *Metarhizium robertsii* morphological flexibility during nonylphenol removal. Int. Biodeterior. Biodegrad. 95, 285–293.
- Shelp, B.J., Bown, A.W., McLean, M.D., 1999. Metabolism and functions of gamma-aminobutyric acid. Trends plant Sci. 4, 446–452.
- Soboń, A., Szewczyk, R., Długoński, J., 2016. Tributyltin (TBT) biodegradation induces oxidative stress of *Cunninghamella echinulata*. Int. Biodeterior. Biodegrad. 107, 92–101.
- Szewczyk, R., Kowalski, K., 2016. Metabolomics and crucial enzymes in microbial degradation of contaminants. In: Długoński, J. (Ed.), Microbial Biodegradation: from Omics to Function and Application. Caister Academic Press, Norfolk, UK, pp. 43–65.
- Szewczyk, R., Kuśmierska, A., Bernat, P., 2018. Ametryn removal by *Metarhizium brunneum*: biodegradation pathway proposal and metabolic background revealed. Chemosphere 190, 174–183.
- Szewczyk, R., Soboń, A., Staba, M., Długoński, J., 2015. Mechanism study of alachlor biodegradation by *Paecilomyces marquandii* with proteomic and metabolomic methods. J. Hazard. Mater. 291, 52–64.
- Thomsson, E., Gustafsson, L., Larsson, C., 2005. Starvation response of *Saccharomyces cerevisiae* grown in anaerobic nitrogen-or carbon-limited chemostat cultures. Appl. Environ. Microbiol. 71, 3007–3013.
- Tyanova, S., Temu, T., Sinitcyn, P., Carlson, A., Hein, M., Geiger, T., Mann, M., Cox, J., 2016. The Perseus computational platform for comprehensive analysis of (prote) omics data. Nat. Methods 13, 731–740.
- Yamada, S., Kotake, Y., Sekino, Y., Kanda, Y., 2013. AMP-activated protein kinase-mediated glucose transport as a novel target of tributyltin in human embryonic carcinoma cells. Metallomics 5, 484–491.
- Yamada, S., Kotake, Y., Demizu, Y., Kurihara, M., Sekino, Y., Kanda, Y., 2014. NAD-dependent isocitrate dehydrogenase as a novel target of tributyltin in human embryonic carcinoma cells. Sci. Rep. 4.
- Yamada, S., Kotake, Y., Nakano, M., Sekino, Y., Kanda, Y., 2015. Tributyltin induces mitochondrial fission through NAD-IDH dependent mitofusin degradation in human embryonic carcinoma cells. Metallomics 7, 1240–1246.
- Zhou, J., Zhu, X.S., Cai, Z.H., 2010. Tributyltin toxicity in abalone (*Haliotis diversicolor supertexta*) assessed by antioxidant enzyme activity, metabolic response, and histopathology. J. Hazard. Mater. 183, 428–433.

Supplemental Material

Article Title: **Metabolomics of the recovery of the filamentous fungus *Cunninghamella echinulata* exposed to tributyltin**

List of Authors and Affiliation:

Adrian Soboń, Rafał Szewczyk, Sylwia Różalska, Jerzy Długoński*

*Department of Industrial Microbiology and Biotechnology, Institute of Microbiology,
Biotechnology and Immunology, Faculty of Biology and Environmental Protection, University of Lodz,
Lodz, Poland.*

Table S-1. MS/MS parameters and LC-MS/MS method performance for compound standards.

Metabolite Name	Q1	Q3	DP	EP	CE	CXP	RT (min)	Linearity Range (ng/ml) ¹	R	Column ²
2-aminoadipate_1	162.0	98.1	51	10	21	8	0.42	0.5-100	0.9996	1
2-aminoadipate_2	162.0	144.1	51	10	15	6	0.42			1
5-aminovalerate_1	118.0	83.1	21	10	19	6	0.38	1-100	0.9983	1
5-aminovalerate_2	118.0	59.2	21	10	25	6	0.38			1
Acetyl-CoA_1	404.2	78.8	-5	-10	-108	-5	2.29	100-1000	0.9813	3
Acetyl-CoA_2	404.2	729.1	-5	-10	-16	-7	2.29			3
Adenine_1	136.0	119.0	86	10	31	10	0.43	0.5-50	0.9982	1
Adenine_2	136.0	92.0	86	10	37	8	0.43			1
Adenosine_1	268.0	136.0	66	10	27	10	0.55	0.25-100	0.9960	1
Adenosine_2	268.0	119.1	66	10	67	4	0.55			1
Adipate_1	144.9	83.0	-40	-10	-14	-7	0.5	10-250	0.9942	3
Adipate_2	144.9	126.9	-40	-10	-18	-7	0.5			3
ADP_1	426.0	78.8	-95	-10	-70	-11	0.54	10-1000	0.9916	3
ADP_2	426.0	158.6	-95	-10	-32	-9	0.54			3
Alanine_1	90.1	44.0	31	10	15	6	0.39	25-250	0.9974	1
Alanine_2	90.1	45.0	31	10	39	6	0.39			1
AMP_1	345.9	78.8	-100	-10	-58	-13	0.64	5-1000	0.9946	3
AMP_2	345.9	96.8	-100	-10	-26	-29	0.64			3
Arginine_1	175.1	70.2	46	10	29	8	0.34	1-100	0.9988	1
Arginine_2	175.1	60.1	46	10	19	6	0.34			1
Asparagine_1	133.1	87.0	46	10	13	8	0.39	2.5-100	0.9951	1
Asparagine_2	133.1	74.1	46	10	21	4	0.39			1
Aspartate_1	134.1	88.1	51	10	15	12	0.39	2.5-100	0.9972	1
Aspartate_2	134.1	74.0	51	10	27	6	0.39			1
ATP_1	506.0	158.7	-15	-10	-32	-5	0.51	25-1000	0.9928	3
ATP_2	506.0	78.8	-15	-10	-84	-21	0.51			3
Betaine_1	118.0	58.0	76	10	39	16	0.41	1-50	0.9972	1
Betaine_2	118.0	59.1	76	10	27	4	0.41			1
Biotin_1	245.0	226.9	76	10	21	8	1.21	0.1-100	0.9994	1
Biotin_2	245.0	97.0	76	10	39	8	1.21			1
CDP_1	401.9	78.8	-105	-10	-68	-5	0.5	25-1000	0.9962	3
CDP_2	401.9	158.8	-105	-10	-28	-11	0.5			3
Cis-aconitate_1	172.8	85.0	-20	-10	-16	-5	0.95	2.5-1000	0.9995	2
Cis-aconitate_2	172.8	129.0	-20	-10	-12	-7	0.95			2
Citrate/Isocitrate_1	190.8	84.9	-15	-10	-22	-9	0.48	5-250	0.9889	3
Citrate_2	190.8	86.9	-15	-10	-24	-7	0.48			3
CMP_1	321.9	78.8	-70	-10	-48	-1	0.51	10-1000	0.9965	3
CMP_2	321.9	96.9	-70	-10	-28	-7	0.51			3
CTP_1	481.9	158.8	-85	-10	-46	-13	0.47	25-1000	0.9966	3
CTP_2	481.9	78.9	-85	-10	-106	-7	0.47			3
Cyanocobalamin_1	678.4	147.1	50	10	92	11	1.12	0.05-250	0.9994	1
Cyanocobalamin_2	678.4	912.5	50	10	50	13	1.12			1
Cysteine_1	122.0	59.1	61	10	35	6	0.4	1-100	0.9974	1
Cysteine_2	122.0	76.1	61	10	19	6	0.4			1
Cystine_1	241.1	152.0	66	10	21	8	0.37	1-100	0.9962	1
Cystine_2	241.1	73.9	66	10	47	16	0.37			1
Cytidine_1	244.0	112.1	16	10	21	6	0.39	0.25-100	0.9963	1
Cytidine_2	244.0	94.9	16	10	55	12	0.39			1
Diaminopimelate_1	191.1	128.1	61	10	21	12	0.36	1-100	0.9998	1
Diaminopimelate_2	191.1	82.0	61	10	31	6	0.36			1
F16bP_1	338.9	78.8	-15	-10	-86	-5	0.47	5-1000	0.9916	3
F16bP_2	338.9	96.8	-15	-10	-28	-7	0.47			3
FAD_1	784.0	437.0	-125	-10	-40	-5	2.6	10-500	0.9927	3
FAD_2	784.0	345.9	-125	-10	-42	-11	2.6			3
Fumarate_1	114.9	70.9	-35	-10	-12	-5	0.88	1-100	0.9970	2
Fumarate_2	114.9	59.1	-35	-10	-14	-5	0.88			2
G6P_1	258.9	96.8	-70	-10	-24	-7	0.5	5-1000	0.9986	3
G6P_2	258.9	78.8	-70	-10	-74	-5	0.5			3
GABA_1	104.1	86.0	30	4	14	5	0.37	5-250	0.9977	1
GABA_2	104.1	69.0	30	4	13	6	0.37			1
GDP_1	441.9	78.9	-90	-10	-94	-7	0.54	10-1000	0.9944	3
GDP_2	441.9	158.8	-90	-10	-34	-9	0.54			3
Gluconate_1	194.9	128.9	-65	-10	-18	-9	0.49	2.5-1000	0.9931	2
Gluconate_2	194.9	74.9	-65	-10	-24	-7	0.49			2
Glucuronate_1	192.8	112.9	-50	-10	-16	-7	0.49	2.5-1000	0.9971	2
Glucuronate_2	192.8	73.0	-50	-10	-18	-5	0.49			2
Glutamate_1	148.0	84.0	46	10	21	6	0.4	1-100	0.9964	1
Glutamate_2	148.0	102.0	46	10	15	6	0.4			1
Glutamine_1	147.1	84.1	36	10	23	4	0.4	1-100	0.9924	1
Glutamine_2	147.1	101.1	36	10	17	8	0.4			1
Glutathione oxidized_1	611.1	305.9	-105	-10	-34	-11	0.86	1-250	0.9894	2
Glutathione oxidized_2	611.1	271.8	-105	-10	-38	-9	0.86			2
Glutathione reduced_1	305.9	142.8	-60	-10	-26	-11	0.75	2.5-1000	0.9966	2
Glutathione reduced_2	305.9	271.9	-60	-10	-20	-13	0.75			2
GMP_1	361.9	78.8	-15	-10	-72	-11	0.55	5-1000	0.9947	3
GMP_2	361.9	96.9	-15	-10	-30	-7	0.55			3
GTP_1	521.9	78.9	-80	-10	-108	-13	0.48	25-1000	0.9973	3
GTP_2	521.9	423.9	-80	-10	-32	-13	0.48			3
Guanidineacetate_1	118.0	76.1	46	10	15	8	0.39	2.5-100	0.9966	1
Guanosine_1	283.9	152.1	6	10	17	8	0.66	0.1-100	0.9998	1
Guanosine_2	283.9	135.0	6	10	55	8	0.66			1
Histidine_1	156.0	110.0	61	10	21	14	0.33	2.5-100	0.9956	1
Histidine_2	156.0	83.1	61	10	35	12	0.33			1
Homocysteine thiolactone_1	118.0	90.0	11	10	15	12	0.37	5-250	0.9960	1
Homocysteine thiolactone_2	118.0	47.0	11	10	39	6	0.37			1
Homocysteine_1	136.0	90.0	40	5	16	6	0.43	2.5-250	0.9990	1
Homocysteine_2	136.0	56.0	40	5	26	6	0.43			1

Homocystine_1	269.0	136.1	51	10	13	6	0.41	10-250	0.9921	1
Homocystine_2	269.0	88.0	51	10	47	8	0.41			1
Homoserine_1	120.0	44.0	40	5	26	11	0.4	1-100	0.9967	1
Hydroxyproline_1	132.0	86.0	1	10	19	8	0.4	2.5-100	0.9947	1
Hydroxyproline_2	132.0	68.0	1	10	27	4	0.4			1
Hypoxanthine_1	136.9	110.1	31	10	29	8	0.59	0.5-100	0.9992	1
Hypoxanthine_2	136.9	94.0	31	10	24	6	0.59			1
IMP_1	347.1	347.0	-10	-10	-8	-13	0.58	25-1000	0.9847	3
IMP_2	347.1	78.9	-10	-10	-72	-7	0.58			3
Inosine_1	268.9	137.0	101	10	19	12	0.62	0.25-100	0.9981	1
Inosine_2	268.9	119.1	101	10	57	8	0.62			1
Isoleucine/Leucine_1	132.1	85.9	51	10	15	10	0.52	2.5-100	0.9962	1
Isoleucine/Leucine_2	132.1	69.3	51	10	23	8	0.52			1
Kynurenate_1	190.1	144.0	55	8	27	5	1.3	0.1-100	0.9992	1
Kynurenate_2	190.1	89.0	55	8	50	7	1.3			1
Lysine_1	147.2	84.2	36	10	21	6	0.33	2.5-100	0.9979	1
Lysine_2	147.2	67.0	36	10	35	10	0.33			1
Malate_1	132.9	114.9	-15	-10	-16	-9	0.65	5-1000	0.9972	2
Malate_2	132.9	70.9	-15	-10	-20	-5	0.65			2
Malonate_1	102.8	59.0	-25	-10	-14	-5	0.5	25-maj	0.9887	3
Melatonin_1	233.1	174.1	75	10	23	8	1.5	0.025-100	0.9999	1
Melatonin_2	233.1	130.0	75	10	63	8	1.5			1
Methionine_1	150.1	104.1	51	10	15	8	0.47	1-100	0.9981	1
Methionine_2	150.1	133.1	51	10	13	6	0.47			1
Myoinositol_1	178.8	86.9	-80	-10	-22	-7	0.48	5-1000	0.9971	2
Myoinositol_2	178.8	71.0	-80	-10	-32	-5	0.48			2
NAD_1	662.0	540.0	-75	-10	-20	-7	1.39	2.5-1000	0.9968	3
NAD_2	662.0	78.9	-75	-10	-110	-7	1.39			3
NADP_1	743.1	621.0	-70	-10	-20	-9	0.52	25-1000	0.9952	3
NADP_2	743.1	78.8	-70	-10	-116	-5	0.52			3
Nicotinate_1	124.0	79.9	26	10	27	8	0.49	1-100	0.9990	1
Nicotinate_2	124.0	53.0	26	10	43	14	0.49			1
Ornithine_1	133.1	70.0	46	10	23	10	0.33	2.5-100	0.9972	1
Ornithine_2	133.1	116.1	46	10	13	6	0.33			1
Oxalacetate_1	131.0	86.9	-55	-10	-18	-5	0.5	50-500	0.9966	3
Oxalacetate_2	131.0	112.9	-55	-10	-16	-7	0.5			3
Piridoxal-5-phosphate (PSP)_1	245.9	78.8	-70	-10	-58	-7	0.63	5-1000	0.9905	3
Piridoxal-5-phosphate (PSP)_2	245.9	96.9	-70	-10	-18	-7	0.63			3
PABA_1	138.0	77.0	56	10	29	10	1.16	0.1-100	0.9999	1
PABA_2	138.0	94.0	56	10	19	8	1.16			1
Pantothenate_1	217.9	87.8	-70	-10	-18	-7	1	0.5-100	0.9980	2
Pantothenate_2	217.9	146.0	-70	-10	-22	-7	1			2
PEP_1	166.8	78.8	-40	-10	-44	-7	0.48	2.5-1000	0.9992	3
PEP_2	166.8	62.8	-40	-10	-90	-3	0.48			3
Phenylalanine_1	166.1	120.1	26	10	17	10	0.64	1-100	0.9988	1
Phenylalanine_2	166.1	103.0	26	10	39	10	0.64			1
Pyridoxine_1	170.0	152.1	36	10	19	6	0.43	0.5-25	0.9963	1
Pyridoxine_2	170.0	134.0	36	10	27	4	0.43			1
Proline_1	116.0	70.1	36	10	19	8	0.42	1-100	0.9981	1
Proline_2	116.0	68.0	36	10	39	4	0.42			1
Quinate_1	190.8	93.0	-80	-10	-28	-7	0.52	5-250	0.9945	3
Quinate_2	190.8	127.0	-80	-10	-24	-5	0.52			3
R5P_1	228.9	96.9	-65	-10	-18	-5	0.5	2.5-1000	0.9944	3
R5P_2	228.9	78.9	-65	-10	-52	-11	0.5			3
Riboflavin_1	377.1	243.0	135	10	44	11	1.15	0.25-250	0.9997	1
Riboflavin_2	377.1	172.1	135	10	44	11	1.15			1
Serine_1	106.0	60.1	1	10	15	4	0.39	5-100	0.9968	1
Serine_2	106.0	42.0	1	10	33	10	0.39			1
Succinate_1	116.8	73.0	-35	-10	-16	-5	0.89	5-500	0.9927	2
Succinate_2	116.8	98.9	-35	-10	-14	-9	0.89			2
Succinyl-CoA_1	432.5	382.4	-15	-10	-14	-11	0.8	10-500	0.9956	3
Succinyl-CoA_2	432.5	78.9	-15	-10	-78	-7	0.8			3
Tartrate_1	148.8	86.9	-5	-10	-18	-7	0.48	5-100	0.9937	3
Tartrate_2	148.8	72.9	-5	-10	-22	-7	0.48			3
Thiamine_1	265.0	122.1	36	10	25	4	0.32	0.25-100	0.9979	1
Thiamine_2	265.0	143.9	36	10	21	12	0.32			1
Threonine_1	120.0	57.1	6	10	25	6	0.4	5-100	0.9916	1
Tocopherol_1	431.2	165.0	16	10	27	8	2.76	2.5-100	0.9977	1
Tocopherol_2	431.2	137.0	16	10	59	10	2.76			1
Tryptophan_1	205.1	188.0	41	10	15	8	0.98	1-100	0.9999	1
Tryptophan_2	205.1	146.1	41	10	25	10	0.98			1
Tyrosine_1	182.0	165.0	36	10	15	6	0.57	0.5-100	0.9993	1
Tyrosine_2	182.0	91.0	36	10	39	6	0.57			1
UDP_1	403.0	78.7	-60	-10	-100	-5	0.51	10-1000	0.9981	3
UDP_2	403.0	158.7	-60	-10	-32	-5	0.51			3
UDP-glucose_1	565.0	323.0	-90	-10	-32	-11	0.52	2.5-250	0.9974	3
UDP-glucose_2	565.0	78.9	-90	-10	-112	-7	0.52			3
UMP_1	322.8	78.9	-90	-10	-100	-7	0.51	10-1000	0.9973	3
UMP_2	322.8	96.9	-90	-10	-26	-7	0.51			3
Uracil_1	113.0	96.0	41	10	23	6	0.55	5-100	0.9990	1
Uracil_2	113.0	70.0	41	10	19	16	0.55			1
Uridine_1	244.9	113.0	31	10	30	10	0.56	0.5-100	0.9988	1
Uridine_2	244.9	70.0	31	10	45	6	0.56			1
UTP_1	482.9	158.7	-85	-10	-34	-5	0.5	10-1000	0.9954	3
UTP_2	482.9	78.8	-85	-10	-102	-5	0.5			3
Valine_1	118.1	57.1	66	10	39	14	0.44	5-250	0.9946	1
α -ketoglutarate_1	144.9	100.8	-5	-10	-12	-3	0.49	10-250	0.9973	3
α -ketoglutarate_2	144.9	73.0	-5	-10	-18	-7	0.49			3

¹ First MRM transition was chosen for quantitative analysis, second was confirmatory transition.

* Column 1: Eksigent 3C8-EP-120 (0.5 × 150 mm, 3 μ m, Eksigent); Column 2: Eksigent 3C18-AQ-120 (0.5 × 150 mm, 3 μ m, Eksigent); Column 3: Synergi Hydro-RP column (2 × 150 mm, 4 μ m, Phenomenex)

P3

*A proteomic study of Cunninghamella echinulata recovery
during exposure to tributyltin*

SOBOŃ A, SZEWCZYK R, DŁUGOŃSKI J, RÓŻALSKA S

Environmental Science and Pollution Research

doi: 10.1007/s11356-019-06416-z



A proteomic study of *Cunninghamella echinulata* recovery during exposure to tributyltin

Adrian Soboń^{1,2} · Rafał Szewczyk^{1,3} · Jerzy Długoński¹ · Sylwia Różalska¹

Received: 29 March 2019 / Accepted: 3 September 2019
© Springer-Verlag GmbH Germany, part of Springer Nature 2019

Abstract

A proteomic study of *Cunninghamella echinulata* recovery during exposure to tributyltin was conducted with 2-D SDS-PAGE protein separation and profiling, MALDI-TOF/TOF protein identification, and PCA analysis. The presence of TBT resulted in an upregulation of enzymes related to energy production via cellular respiration. The unique overexpression of NADH dehydrogenase and mitochondrial malate dehydrogenase, together with an increased level of cytochrome c oxidase, ATP synthase subunits, and inorganic pyrophosphatase, indicates a strong energy deficit in the cells, leading to an increase in the ATP production. The overexpression of Prohibitin-1, a multifunctional protein associated with the proper functioning of mitochondria, was observed as well. The data also revealed oxidative stress condition. Among reactive oxygen species (ROS)-scavenging enzymes, only superoxide dismutase (SOD) showed active response against oxidative stress induced by the xenobiotic. The induction of a series of ROS-scavenging enzymes was supported by a microscopic analysis revealing a considerably large concentration of ROS in the hyphae. The overexpression of cytoskeleton-related proteins in the TBT presence was also noticed. The obtained results allow explaining the recovery strategy of the fungus in response to the energy depletion caused by TBT.

Keywords *Cunninghamella echinulata* · Fungi · Proteomics · Tributyltin, Oxidative stress · Respiratory chain

Introduction

As a result of the human industrial activity, a wide range of toxic compounds are released into the environment. Therefore, the understanding of the mechanisms of their influence and action towards living organisms is crucial. A good

example of a toxic xenobiotic is tributyltin (TBT), an organo-metallic compound, which has been extensively used as an active component of herbicides, biocides, and antifouling paints (Cruz et al. 2015). TBT is highly toxic and has a number of negative effects on living organisms, including bacteria (Martins et al. 2005), fungi (Bernat and Długoński 2012), and higher eukaryotic organisms (Liu et al. 2006). It has also been classified as an endocrine disruption compound (EDC) (Długoński 2016). Several studies assessing its toxicity have been reported; however, the mechanism of interaction is still unclear and remains a subject of research. It is especially important in the case of filamentous fungi as TBT effect on this group of organisms is still poorly described. The negative effects of TBT are manifested by the inhibition of cell growth and a decrease in the metabolic activity (Cruz et al. 2012) or changes in the mycelium and the phospholipid profile (Siewiera et al. 2015). Most of the negative effects point to mitochondria as a site of TBT attacks. TBT induces mitochondrial fragmentation, degrades the mitochondrial fusion proteins (Yamada et al. 2015), and changes the profile of tricarboxylic acid (TCA) cycle metabolites (Zhou et al. 2010). TBT can also inhibit the ATP synthase efficiency (Nesci et al. 2011a).

Responsible editor: Robert Duran

Electronic supplementary material The online version of this article (<https://doi.org/10.1007/s11356-019-06416-z>) contains supplementary material, which is available to authorized users.

✉ Rafał Szewczyk
rafal.szewczyk@dimedical.pl

¹ Department of Industrial Microbiology and Biotechnology, Institute of Microbiology, Biotechnology and Immunology, Faculty of Biology and Environmental Protection, University of Łódź, Łódź, Poland

² Department of Microbial Genetics, Institute of Microbiology, Biotechnology and Immunology, Faculty of Biology and Environmental Protection, University of Łódź, Łódź, Poland

³ Centre of Clinical and Aesthetic Medicine DiMedical, Łódź, Poland

Proteomics, together with other omics techniques, such as transcriptomics, metabolomics, or lipidomics, plays an important role in the rapid development of modern system biology (Desai et al. 2010; Bernat 2016; Szewczyk and Kowalski 2016a, b; Joseph 2017). Proteomics is a helpful tool in determining the changes in the composition of proteins induced by exposure to toxic compounds (Szewczyk et al. 2014, 2015). It allows determining the disturbances of the metabolic pathways and the adverse effects on cell elements (Matsuzaki et al. 2008). It also leads to a better understanding of the cellular defense mechanisms and the strategies of compound elimination and detoxification.

In our earlier studies, the filamentous fungus *C. echinulata* was found to be capable of effective TBT biodegradation at the high concentration 5 mg L⁻¹ (Soboń et al. 2016). The effect of the xenobiotic on the microorganism's metabolic activity and the metabolite profile as well as the possible role of the accumulation of glycolytic-related metabolites and ROS-scavenger compounds were reported (Soboń et al. 2018). A microscopic analysis showed negative changes in the fungus morphology, manifested in strong cell vacuolization. As a continuation of the studies on the influence of TBT on the fungal strain, this paper is focused on the TBT effect on the microbial proteome and cell processes induced by TBT on the proteomic level, which together with the previously obtained metabolomics data (Soboń et al. 2018) allow explaining the mechanisms associated with the unique recovery of the fungus.

Materials and methods

Chemicals and reagents

TBT chloride, ammonium persulfate, and ammonium bicarbonate were obtained from Sigma-Aldrich (Germany). Urea, dithiothreitol (DTT), iodoacetamide, sodium dodecylsulphate (SDS), bromophenol blue, 3-((3-cholamidopropyl)dimethylammonio)-1-propanesulfonate (CHAPS), 2-amino-2-hydroxymethyl-propane-1,3-diol (tris), Coomassie Brilliant Blue G 250, N,N,N',N'-tetramethylethylenediamine (TEMED), Bradford reagent, and the acrylamide:bisacrylamide mix were obtained from Serva (Germany). IPG strips (17 cm pH 3–10 NL) and mineral oil were purchased from Bio-Rad (Germany). Glycine and acetone were obtained from Avantor (Poland). Trypsin (sequence grade) and CHCA came from Promega (Germany) and CovaChem (USA), respectively. Stock solution of TBTCl (5 mg mL⁻¹) was prepared in ethanol.

Microorganism

The filamentous fungus *C. echinulata* IM 2611 obtained from the Department of Industrial Microbiology and Biotechnology

(University of Lodz, Poland) was examined. The capability of this microorganism to efficiently remove TBT had been reported in the earlier paper (Soboń et al. 2016). The fungus was cultured in the Sabouraud medium as described previously (Soboń et al. 2018). Briefly, Sabouraud dextrose liquid medium (Difco) supplemented with 2% glucose was inoculated with *C. echinulata* IM 2611 and incubated on a rotary shaker (160 rpm) for 24 h at 28 °C. After 24 h, the preculture was transferred to fresh medium in the ratio 1:4 and shaken for another 24 h in the same conditions as described above. A homogenous preculture (10%) was introduced into the Sabouraud medium without and with 5 mg L⁻¹ TBT, and incubated at 28 °C for 24, 48, 72, and 96 h as above in triplicates.

Proteome analysis

Protein extraction

The mycelium from each culture sample was obtained by filtration using polycarbonate membrane filters (0.4 µm), washed with 100 mL of deionized water, and lyophilized in a freeze dryer (Christ Alpha, USA). Next, approximately 80 mg of the lyophilized mycelia was homogenized thrice for 30 s at the speed of 5 m/s by using Fast-Prep24 (MP Biomedicals), suspended in 1 mL of the resuspension buffer (7 M urea, 2 M thiourea, 4% CHAPS, and 65 mM DTT), and incubated for 10 min in an ultrasonic bath and for 60 min in the vortex. The samples were centrifuged for 10 min at 17000×g; the supernatant was then transferred to a new lobind Eppendorf tube and precipitated using ice-cold acetone followed by incubation for 2 h at -20 °C. The protein pellet was next centrifuged for 10 min at 15000×g, washed thrice using ice-cold acetone, dried, and equilibrated in the resuspension buffer. The Bradford assay with BSA as a protein standard was used to determine the protein concentration.

2-D SDS-PAGE

Passive rehydration (700 µg protein) was conducted overnight and loaded onto 17 cm IPG strips pH 3–10 NL. The isoelectric focusing (IEF) step was carried out in a Protean i12 device (Bio-Rad, Germany) as follows: 4 h at 50 V, 5 h at 6000 V (gradient), and 50000 Vh at 6000 V. Next, the equilibration step was performed according to the manufacturer's protocol. Electrophoresis was performed overnight on 12% SDS-gels with a wide range marker (6.5–200 kDa; Serva, Germany) using a Protean XL cell (Bio-Rad, Germany), and stained using Coomassie Blue. Image Master 2D Platinum 7 software (GE Healthcare, Germany) was applied to identify differentially expressed protein spots according to the manufacturer's instruction and data described in our previous paper (Szewczyk et al. 2015). Detected protein spots were matched by comparing the gels from control and TBT-treated cells for

the appropriate culturing time (24, 48, 72, and 96 h). Due to the lack of information on the *Cunninghamella* proteome as well as different expression of proteins during exposure to TBT, all visible protein spots were manually excised from the gels. Protein intensity was analyzed using Student's *t* test (GraphPad Prism 6, USA). Spots showing a minimum of 1.1 fold change were considered to be significant ($P < 0.05$). The spots intensity was subjected to principal component analysis (PCA) with normalization using total area sums and Pareto scaling (MarkerView software ver. 1.2.1; AB Sciex, USA).

Protein identification

The protein spots (manually excised from the gels) were digested with trypsin according to the modified procedure described by Szewczyk et al. (2014). The obtained peptides were extracted using three buffers: solution A (2% ACN with 0.2% TFA) for 15 min, solution B (50% ACN with 0.2% TFA) for 60 min, and solution C (90% ACN with 0.2% TFA) for 15 min. The extracts were combined, dried, dissolved in 5 μ L of solution A, mixed with an equal volume of α -Cyano-4-hydroxycinnamic acid (CHCA) solution (10 mg mL^{-1} in 50% ACN with 0.2% TFA), and finally 0.6 μ L of this mixture was dropped onto a metal plate. MALDI-TOF-MS analysis was performed using an AB Sciex 5800 TOF/TOF system (AB Sciex, USA). The detailed information of MALDI parameters had been described previously by Szewczyk et al. (2015). Briefly, the mass spectrometer was externally calibrated in reflectron mode using peptides solution (AB Sciex, USA), and fragments of Glu-fibrinopeptide (1570.677 Da) were chosen for TOF/TOF MS/MS mode calibration. The proteins were identified against the NCBI database (restricted to the *Zygomycota* order, total number of sequences = 333338) by using the Protein Pilot v4.5 software connected with the MASCOT v4.2. MASCOT parameters and Blast searches were performed according to Szewczyk et al. (2014). Search criteria included trypsin as the protein-digesting enzyme, one missed cleavage and the following variable modifications were applied: Acetyl (N-term), Carbamidomethyl (C), Deaminated (NQ), Gln to pyro-Glu (N-term Q), Glu to pyro-Glu (N-term E), and Oxidation (M). Mass tolerance mass parameters were set to 100 ppm for MS and 0.5 Da for MS/MS mode. Peptide sequences with a MASCOT ion score ≥ 75 ($P < 0.05$) were considered to be significant. The proteins established by MASCOT searches were further processed using BLAST search against NCBI non-redundant protein sequence database applying DELTA-BLAST algorithm.

ROS detection

The analysis of ROS production was performed with 2,7-dichlorodihydrofluorescein diacetate (H_2DCFDA) (Sigma-

Aldrich, Germany) by the method described previously (Staba et al. 2015). One-milliliter samples of *C. echinulata* were centrifuged $2000\times g$ for 5 min and the pellet was washed with 1 mL of the 10-mM sodium phosphate buffer pH = 7.5 (PBS). Then, 1-mL PBS with 40 mM H_2DCFDA (dissolved in dimethyl sulfoxide) was added to the mycelial pellet and incubated for 15 min followed by PBS washing. A confocal laser scanning microscope (LSM510 Meta, Zeiss) was used for ROS detection in the mycelium. The H_2DCFDA fluorescence was detected using an argon laser (488 nm) and an LP filter set (505–530 nm). Nomarski DIC was conducted using the same laser line. The results were expressed as a percentage of the green fluorescence area as compared to the total hyphal area.

Measurement of SOD and CAT activity

Assays of SOD and CAT activity were carried out according to the method described by Siewiera et al. 2017. Freshly prepared 50 mM phosphate buffer (pH 7.0) with the addition of 1 mM EDTA, 1 mM ascorbic acid, and 1% PVP was added to 250 mg of wet biomass and homogenized in a cooled mortar followed by centrifugation at 4 °C for 10 min at $15,000\times g$. The obtained supernatant was incubated on ice for further analysis. For measuring the SOD activity, 2.9 ml of mixture containing 50 mM PBS (pH 7.8), 13 mM methionine, 1 mM EDTA, and 75 μ M NBT was mixed with 50 μ L of the obtained supernatant and 2 μ M of riboflavin, incubated for 30 min under UV lamps and analyzed spectrophotometrically at 560 nm. To determine the CAT activity, 100 μ L of supernatant was mixed with 1.8 ml of 50 mM PBS (pH 7.0) and 150 μ L of 1% H_2O_2 . Next, absorbances were measured at $\lambda = 240$ nm for 4 min. The Bradford assay with BSA as a protein standard was used to determine the protein concentration. CAT and SOD activity was expressed in U mg protein $^{-1}$.

Statistical analysis

The experiments were conducted in triplicate. The Student's *t* test was performed using GraphPad Prism 6 (USA). Differences at $P < 0.05$ were considered as significant. Principal component analysis (PCA) with normalization using total area sums and Pareto scaling was performed using MarkerView software (AB Sciex, USA). The results of the antioxidant enzymes activity were estimated by one-way analysis of variance (ANOVA) and Tukey's test using software STATISTICA ver. 13.0 (StatSoft).

Results and discussion

Representative 2-DE maps of the control and TBT-treated samples are depicted in Fig. 1. On average, 119 protein spots

per gel were detected using ImageMaster 2-D software (GE Healthcare, Germany). The proteomic analysis resulted in the identification and matching of 92 spots, and allowed for a comparison of the relative expression levels between the samples based on spot volume quantification after total volume normalization within the gels. The summary results of the proteomic analysis are presented in Table 1, whereas detailed information is presented in Table S-1. The PCA analysis of proteomic data was performed and is presented in Fig. 2. The distribution of samples can be divided into three groups. The greatest differences were observed between the TBT-treated samples after 24 h (TBT24), which deviated from the other samples. This indicates that the protein in the samples from the 24 h culture with TBT had a unique profile, incomparable to the protein profiles obtained for the remaining samples. The TBT-treated cells from 48 h of incubation showed similarity to the control sample from 24 h. Proteins responsible for such a differentiation of samples were, e.g., spots #10 or #17 for TBT24, and spots #15 and #48 for c24 and TBT48 group, respectively. The 3rd group consisted of the remaining samples. This indicates that the differences between samples decrease over time.

Energy and TBT—the pathways switch

Energy plays an essential role in the life of organisms because it is used to perform a number of biochemical reactions in the cells. The most important energy-related compound is ATP, which is produced via the respiratory chain by three main energy pathways: glycolysis, the Krebs cycle, and oxidative phosphorylation (OXPHOS). In the tested samples containing TBT, only the overexpression of fructose-bisphosphate aldolase (ALDO), triosephosphate isomerase (TPI), glyceraldehyde-3-phosphate dehydrogenase (GAPDH), phosphoglycerate kinase (PGK), phosphoglycerate mutase (PGM), and particularly enolase (ENO) was observed (Table 1). The enzymes (hexokinase, glucose-6-phosphate isomerase, and phosphofructokinase) involved in the first three steps in the preparation phase of glycolysis and pyruvate kinase were not detected. Together with the accumulation of glycolytic-related metabolites (Soboń et al. 2018), this result may suggest that the fungus focuses on energy production and simultaneously limits its consumption. This effect may also be supported by the inhibitory action of TBT on the glucose transporter (GLUT) manifested by the reduction of the glucose uptake (Yamada et al. 2013), which was also observed in the tested fungus (Soboń et al. 2018).

Another important pathway for the appropriate functioning of the cell is the pentose phosphate pathway (PPP). Its major role is the generation of reducing agents in the form of NADPH, as well as the metabolites necessary for the synthesis of nucleotides, nucleic acids, and amino acids. Through transketolase and transaldolase, the pentose phosphates can

be converted back to fructose-6-phosphate and glucose-6-phosphate. The proteomic analysis showed a strong upregulation of transaldolase (spot 28) in the TBT samples, which could be responsible for the increased level of fructose-6-phosphate in the cell (Soboń et al. 2018) and its incorporation into glycolysis. The second overexpressed PPP-related enzyme was 6-phosphogluconate dehydrogenase (spot 29), which is involved in the conversion of 6-phosphogluconate to ribulose-5-phosphate with the formation of NADPH (Table 1, Fig. 3). Both enzymes were upregulated in the initial stage of culturing, and together with an increased level of ribose-5-phosphate (Soboń et al. 2018) indicate the role of PPP in the fungus recovery during exposure to TBT. More importantly, NADPH is necessary for the functioning of ROS-scavenger enzymes such as thioredoxins, which were overexpressed during exposure to TBT (Table 1, Fig. 3).

Pyruvate, as a final product of glycolysis, was oxidized and decarboxylated by the pyruvate dehydrogenase complex, leading to the formation of acetyl-CoA, carbon dioxide, and NADH. The proteomic analysis indicated the upregulation of dihydrolipoamide dehydrogenase (DLD) (spot 39), a part of this complex, particularly after 24 h of incubation with TBT (Table 1, Fig. 3). Acetyl-CoA is a starting molecule for the TCA cycle and in a series of redox reactions, harvests a considerable amount of its bond energy in the form of NADH, FADH₂, and ATP. The electron carriers—NADH and FADH₂—generated in the TCA cycle pass their electrons into the electron transport chain and, through OXPHOS, generate most of the ATP (Lapuente-Brun et al. 2013).

Two isoforms of malate dehydrogenase (MDH) were upregulated after 24 h of incubation with TBT. In particular, the unique upregulation of MDH (spot 38) was interesting because it was upregulated only in TBT-containing samples. In contrast, two isoforms of citrate synthase (CS) (spots 34 and 35) and isocitrate dehydrogenase (IDH) (spot 36) were downregulated during exposure to TBT (Table 1). A study conducted by Yamada et al. (2014) showed the decreased activity of NAD-dependent IDH together with a reduced ATP production caused by 100 nM of TBT. Moreover, a reduction in the content of most of the TCA-related compounds as a result of the TBT exposure was observed (Yamada et al. 2014; Soboń et al. 2018).

Mitochondria are excellent ATP producers. Their basic function is the oxidation of organic compounds, such as simple sugars, fatty acids, and amino acids, leading to the transfer of energy in ATP molecules using OXPHOS, which consists of five complexes of enzymes, including NADH dehydrogenase (I), succinate dehydrogenase (II), cytochrome b-c1 (III) complex, and cytochrome c oxidase (IV) (Fig. 3). The last enzyme involved in OXPHOS is ATP synthase, also referred to as the V complex. ATP synthase uses a proton gradient to drive the synthesis of ATP from ADP and phosphate (P_i) (Nakamoto et al. 2008). Exposure to TBT clearly indicated

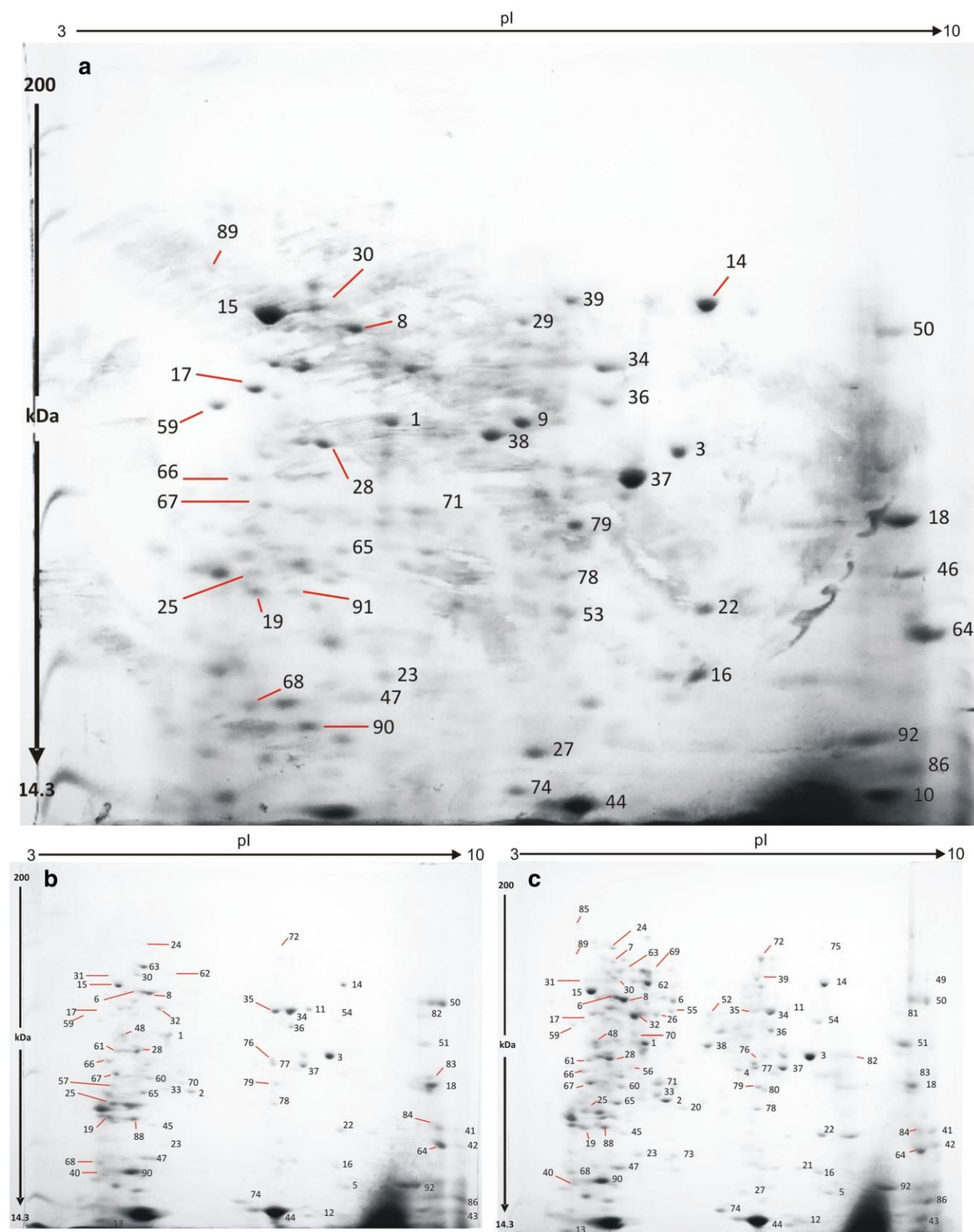
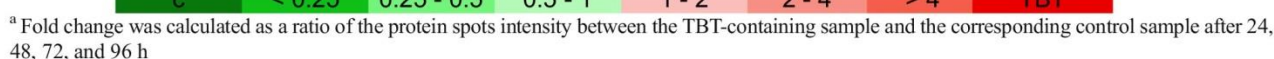


Fig. 1 Representative 2-DE gels of mycelial proteome of *C. echinulata* after exposure to 5 mg L⁻¹ TBT. **a** TBT-treated sample after 24 h, **b** control sample after 96 h, **c** TBT-treated sample after 96 h. The figure shows the numbers of protein spots

Table 1 Summary identification of *C. echinulata* IM 2611 proteins after exposure to 5 mg L⁻¹ of TBT. The protein names in the brackets were identified using a delta-blast algorithm. The proteins which were not detected are presented in white

Spot	Best protein name	Fold change ^a			
		24	48	72	96
Glycolysis					
1	fructose-bisphosphate aldolase, class II				
2	triosephosphate isomerase				
3	glyceraldehyde-3-phosphate dehydrogenase				
4	glyceraldehyde-3-phosphate dehydrogenase				
5	glyceraldehyde-3-phosphate dehydrogenase				
6	hypothetical protein (phosphoglycerate kinase)				
7	2,3-bisphosphoglycerate-independent phosphoglycerate mutase				
8	enolase				
Oxidative Phosphorylation					
9	hypothetical protein (NADH dehydrogenase subcomplex)				
10	hypothetical protein (NADH ubiquinone oxidoreductase)				
11	NADH dehydrogenase [ubiquinone] complex I				
12	cytochrome b-c1 complex subunit 7				
13	cytochrome c oxidase subunit 5A COX5A				
14	ATP synthase subunit alpha				
15	ATP synthase F1 subcomplex beta subunit ATP2				
16	hypothetical protein (ATP synthase D chain)				
64	F1 complex, OSCP/delta subunit of ATPase				
17	inorganic pyrophosphatase				
18	electron transfer flavo protein, beta subunit				
Stress response					
19	thioredoxin-like protein				
20	thioredoxin-like protein				
21	thioredoxin-like protein				
22	manganese and iron superoxide dismutase				
23	Redoxin				
24	heat shock 70 kDa protein 2				
25	hsp71-like protein				
26	hypothetical protein (Hsp70 protein)				
27	superoxide dismutase Cu-Zn				
Pentose phosphate pathway					
28	hypothetical protein (transaldolase B)				
29	hypothetical protein (6-phosphogluconate dehydrogenase)				
Cytoskeleton proteins					
30	Tubulin alpha-1C chain				
31	beta-tubulin, partial				
32	actin-2				
33	Putative Actin (Fragment)				
TCA cycle					
34	citrate synthase				
35	Citrate synthase, mitochondrial				
36	isocitrate dehydrogenase, NAD-dependent				
37	malate dehydrogenase, NAD-dependent				
38	hypothetical protein (malate dehydrogenase)				
Pyruvate oxidation					
39	hypothetical protein (dihydrolipoamide dehydrogenase)				
Protein metabolism					
40	hypothetical protein (Ribosomal protein L7Ae/L30e/S12e/Gadd45)				
41	40S ribosomal protein S7				
42	40S ribosomal protein S5, partial				
43	40S ribosomal protein S8				

Fold change color scalling:



C unique in control samples, *TBT* unique in TBT-containing samples

that the xenobiotic affects the processes involved in energy production, particularly within the mitochondria, which is presented in Fig. 3. First of all, the overexpression of enzymes associated with OXPHOS process strongly indicates disorders in its functioning. A particularly outstanding observation was the high upregulation of the subunits of NADH dehydrogenase (spots 9 and 10), which occurred only after 24 h of exposure to TBT (Table 1). NADH dehydrogenase is the first enzyme complex of OXPHOS; it collects electrons from NADH and releases protons into the intermembrane space. The second enzyme involved in OXPHOS at the electron entry point is succinate dehydrogenase, which was not detected during the entire duration of the experiment. The enzymatic activity of NADH dehydrogenase is the main source of protons for ATP synthase, generating about 40% of the total proton pool (Berrisford et al. 2016). The proton gradient is necessary for the ATP production by ATP synthase. The strong expression of cytochrome c oxidase (spot 13) was observed after the 48-h treatment with TBT (Table 1). The final element involved in the ATP production is ATP synthase. It consists of two main subunits, F_0 and F_1 , which have a rotational motor mechanism allowing for ATP production. Subunits α , β , γ , and δ comprise the F_1 domain. The α and β subunits are involved in the formation of the catalytic site in which ATP synthesis takes place, while the δ and ϵ subunits are responsible for the binding of F_1 to F_0 . During exposure to TBT, α (spot 14), β (spot 15), δ (spot 64), and ϵ (spot 16) subunits were overexpressed (Table 1). Simultaneously, an increased expression of the inorganic pyrophosphatase (spot 17) was observed (Table 1). It catalyzes the conversion of pyrophosphate to phosphate ions, which together with ADP are substrates for the synthesis of ATP by ATP synthase. An overexpression of these enzymes indicates the energy demand of the cell, which cannot be met because of the dysfunction of the OXPHOS pathway. The respiratory chain disorders caused by

TBT have been previously documented; however, the molecular mechanisms of this process are still being investigated. The obtained results strongly indicate that TBT disrupts the energy production in cells and causes a shortage of ATP. The studies performed by Dudimah et al. (2007) on human natural killer (NK) cells showed a decrease in the ATP level during exposure to TBT in a dose-dependent manner. Cell incubation with a high ATP concentration (300 nM and 500 nM) showed a significant decrease in ATP just after 1 h of incubation, together with a significant decrease in cell viability. The lower the concentration, the longer was the waiting time for the effect on the reduction of the ATP content. The inhibition of ATPase–ATP synthase by TBT has been described previously (Pagliarini et al. 2008). It is related to the direct interaction of the compound with the F_1F_0 complex, where the xenobiotic covalently binds to the thiol groups of the F_0 domain, which may promote changes in the enzyme structure (Nesci et al. 2011a). Studies conducted on the sea snail *Haliotis diversicolor* showed that exposure to organotin compounds disturbs the energy production and osmotic balance, and induces oxidative stress (Lu et al. 2017). Another study using the snail as a research model showed a significantly inhibited oxygen consumption and respiratory activity at the first two phosphorylation sites caused by TBT, whereas complex IV was not affected (Nesci et al. 2011b). The study conducted on bacteria showed that TBT was able to inhibit NADH respiration (Martins et al. 2005) and complex III in the photosynthetic purple bacterium *Rhodobacter spheroides* (Hunziker et al. 2002). Our proteomic analysis revealed the overexpression of two forms of malate dehydrogenase (spots 37 and 38), both of which were identified using a delta-blast algorithm as mitochondrial/glyoxysomal malate dehydrogenase (Table S-1). One of the isoforms (spot 38) showed unique overexpression after 24 h in the TBT-containing samples (Table 1). However, the second one identified as malate dehydrogenase,

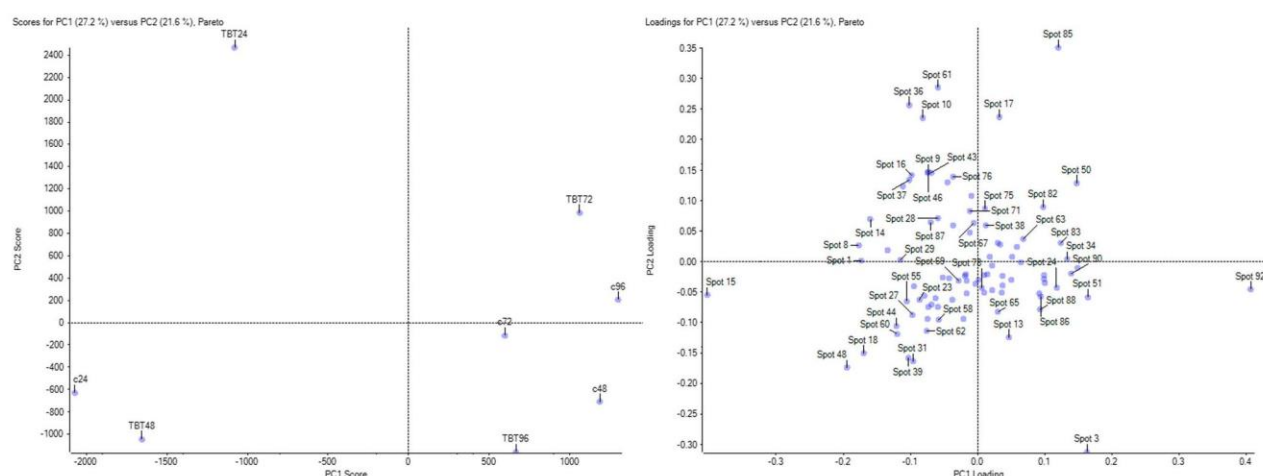


Fig. 2 PCA analysis of protein composition in control (c) and TBT-exposed cultures (TBT) of *C. echinulata* on Sabouraud medium. The numbers on the PC score represent the time of culturing, and protein spots responsible for data clustering were presented in the PC loading section

except in the TBT sample obtained after the 24-h and 96 h exposure, was downregulated during exposure to TBT (Table 1). Because of the fact that fungi have three isoforms of MDH, cytoplasmic, mitochondrial, and peroxisomal, the appropriate identification and determination of their role in the process remain unclear. However, a high level of oxaloacetate and a low level of malate observed previously in the examined fungus (Soboń et al. 2018), together with the strong cellular demand for NADH necessary in the OXPHOS process, suggest that the isoenzyme, which was uniquely overexpressed after 24 h of incubation, is a mitochondrial form of MDH (Fig. 3). The conversion of malate to oxaloacetate by mitochondrial malate dehydrogenase is a major source of NADH, required for NADH dehydrogenase. NAD^+ and NADP^+ were not detected during the examined process; however, the FAD^+ concentration after 24 h in the TBT samples was very low (Soboń et al. 2018), which confirmed the high cell demand for reducing equivalents necessary for the functioning of the electron transfer chain.

Aspartate aminotransferase (spot 54), a part of the malate–aspartate shuttle was strongly upregulated after 72 h and 96 h in the TBT-induced cells (Table 1). The upregulation of the malate–aspartate shuttle pathway also indicated a strong energy deficit.

TBT and enzymatic cell defense

The dark side of mitochondrial activity is the production of free oxygen radicals. It is estimated that approximately 20% of the free radical pool is generated in the process of cellular respiration. However, under abnormal conditions, this proportion can be disturbed, resulting in the increased ROS formation, which leads to oxidative stress conditions. The microscopic analysis presented in Fig. 4 showed a statistically significant increase in the ROS concentration in the fungus hyphae exposed to TBT (5 mg L^{-1}). Its maximum level was observed after 24 h of culturing ($57.60\% \pm 4.03\%$ in comparison to the control $0.82\% \pm 0.03\%$) ($P < 0.05$), slightly

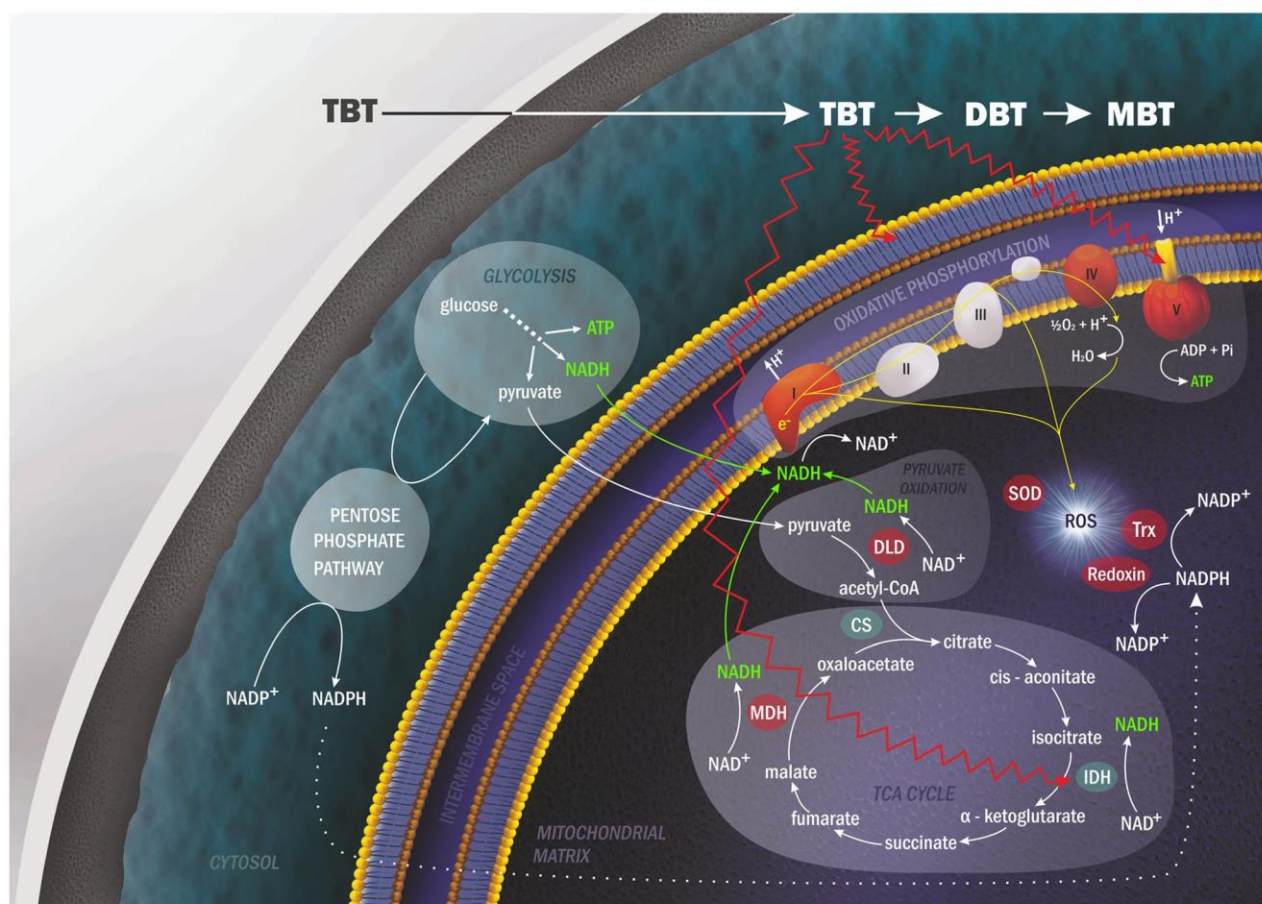


Fig. 3 Fungal response to energy demand and ROS generation during exposure to TBT (5 mg L^{-1}). Enzymes overexpressed during the first 48-h exposure to TBT are marked in red, and downregulated proteins are green. Red arrows indicate known molecular targets of TBT. Yellow arrows in oxidative phosphorylation indicate electron flow through the

ETC. I, complex I; II, complex II; III, complex III; IV, complex IV; V, ATP synthase. (complex V), DLD dihydrolipoamide dehydrogenase, MDH malate dehydrogenase, CS citrate synthase, IDH isocitrate dehydrogenase, SOD superoxide dismutases, Trx thioredoxins

decreased on the second day of incubation ($41.71\% \pm 3.54\%$ in comparison to the control $0.57\% \pm 0.04\%$) ($P < 0.05$). Simultaneously with increased amounts of ROS observed in TBT-exposed cells, the increased activity of SOD and CAT was noticed (Table 2). SOD activity significantly increased over 4-fold in the samples containing TBT after 24 h and decreased over time to a comparable amount between samples to the end of the experiment. CAT showed low activity during the whole time of the experiment in both compared samples indicating no significant role of this enzyme in the tested process. However, in TBT-treated samples, a significantly

enhanced CAT activity was observed after 24 h. After 72 h, a similar enzyme activity was noted between the compared systems. The high ROS concentration might be attributed to an interrupted electron flow of the electron transport chain (ETC) complexes. Complexes I and III of ETC are indicated as the main source of ROS formation (Jastroch et al. 2010). Under normal conditions, complex IV reduces oxygen, which acts as a terminal electron acceptor, forming water. In the TBT-treated cells, an upregulation of NADH dehydrogenase and cytochrome c oxidase belonging to complexes I and IV, respectively, was observed. The inefficient transport of

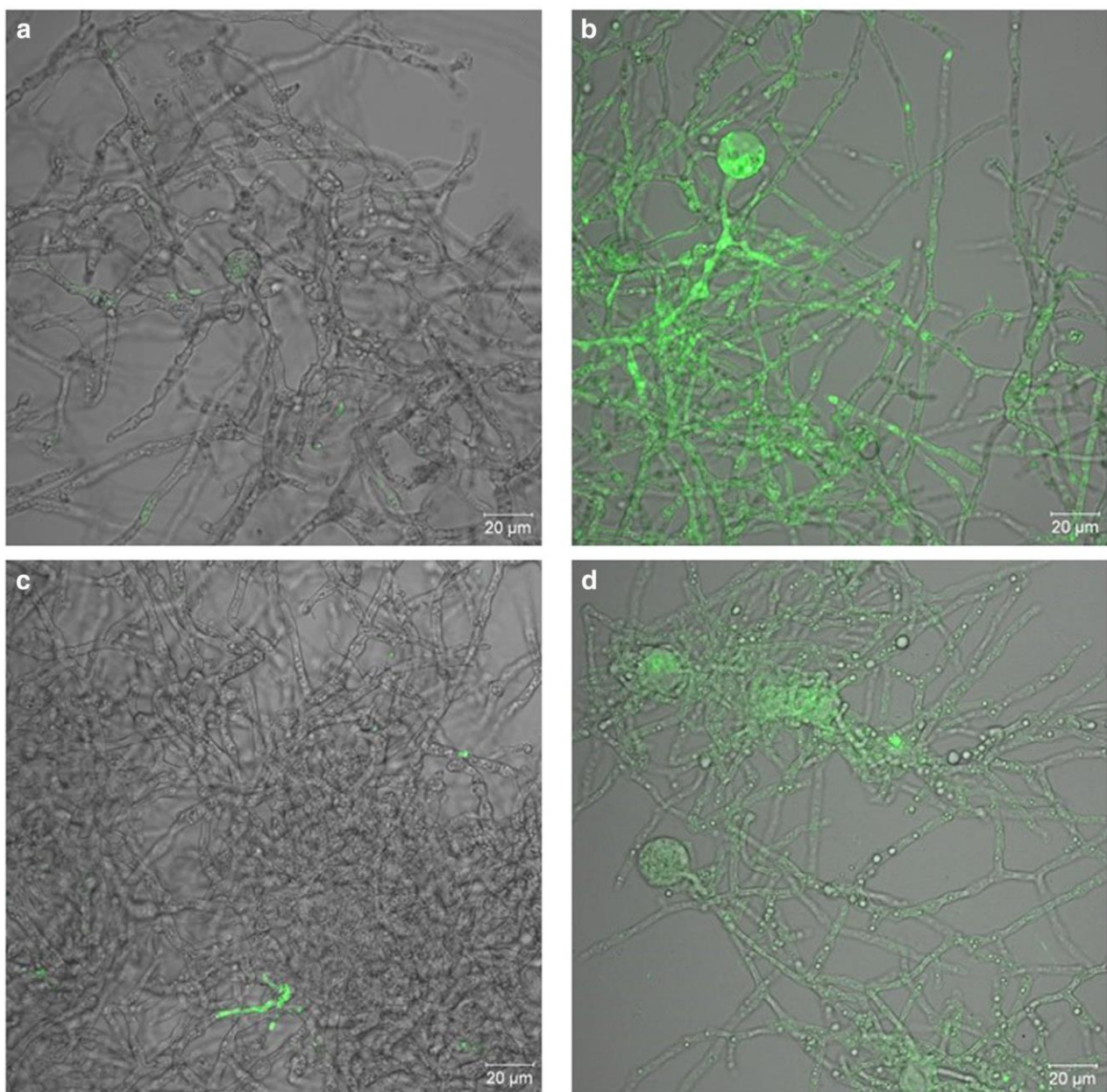


Fig. 4 ROS generation in the *C. echinulata* cultures. Control without TBT after **a** 24 h and **c** 48 h; sample supplemented with TBT after **b** 24 h and **d** 48 h. The hyphal fluorescence indicates ROS generation

Table 2 Activity of superoxide dismutase (SOD) and catalase (CAT) determined in *C. echinulata* biomass incubated in the presence or absence of TBT (initial concentration 5 mg L⁻¹)

Enzyme activity (U mg protein ⁻¹)	24 h		48 h		72 h		96 h	
	Control	TBT	Control	TBT	Control	TBT	Control	TBT
SOD	0.424 ± 0.015	1.920 ± 0.012*	0.085 ± 0.008	0.911 ± 0.015*	1.306 ± 0.014	0.989 ± 0.015*	1.209 ± 0.038	1.089 ± 0.039*
CAT	0.028 ± 0.004	0.067 ± 0.007*	0.038 ± 0.004	0.049 ± 0.005	0.033 ± 0.003	0.035 ± 0.005	0.029 ± 0.003	0.030 ± 0.004

* indicates values that differ significantly from the control at $P < 0.05$

electrons not only reduces the efficiency of ATP production but also contributes to the generation of ROS. Moreover, other mitochondrial enzyme complexes, such as DLD, have been reported to be able to generate superoxides (Starkov 2004). Many studies have demonstrated the interaction of lipophilic TBT with the cell membrane (Martins et al. 2005; Bonarska-Kujawa et al. 2012) against which the cell fights by changes in the lipid composition (Bernat et al. 2014). An increase in membrane permeability caused by TBT could enhance ROS generation and ROS-induced damage because more electrons leak and form more superoxide anions. Several studies have shown that the generation of ROS is a major mechanism of TBT toxicity (Wang et al. 2012; Ferreira et al. 2013). The activation of enzymatic and non-enzymatic defense mechanisms against ROS is required to neutralize the large number of free radicals observed in the examined fungus. In the course of the current and the previous studies, a number of protective factors have been identified. An upregulation of the Heat Shock 70-kDa protein (Hsp70) (spot 24), a marker of oxidative stress, was observed in the TBT-treated samples after 48 h of incubation (Table 1). Cu–Zn superoxide dismutase (SOD) (spot 27) was overexpressed only at 24 h and 96 h, and Mn–Fe SOD (spot 22) was upregulated at 24 h, 72 h, and 96 h during exposure to TBT (Table 1, Fig. 3). In addition, an increased activity of SOD in the mycelia of the fungus incubated with the xenobiotic after 24 and 48 h was observed, while the low CAT activity suggests negligible participation of that enzyme in the examined process. A study conducted by Liu et al. (2006) showed an increased level of SOD in rats after 3 days of exposure and a decreased SOD level after 7 days, which suggested that the antioxidative system was activated by TBT on the first day of incubation. Our results confirmed these findings, indicating the induction of the oxidative stress-related mechanism from the first hour of exposure to TBT. Interestingly, the upregulation of three isoforms of thioredoxin-like protein (Trx) (spots 19–21) as well as redoxin (spot 23) was observed in the TBT-containing samples (Table 1, Fig. 3). Trx together with redoxin was strongly expressed, particularly from 48 h. The expression of Mn SOD is essential for the cellular resistance to ROS owing to the fact that SODs catalyze the dismutation of O₂^{•-} into oxygen and H₂O₂ (Turrens 2003), which is further reduced by catalase, peroxiredoxin (Prx), and glutathione peroxidase

(GPx) as well as by the Trx system (Arner and Holmgren 2000). One of the central antioxidant systems in the cell is the redoxin family, including Prxs, Trxs, and glutaredoxin (Grxs) proteins (Hanschmann et al. 2013). However, the significance of Trxs is not limited to the antioxidant system, because it plays an important role in redox signaling and the regulation of the protein function (Lee et al. 2013; Matsuzawa 2017). Moreover, the occurrence of three isoforms may be attributed to the fact that mitochondria have their own Trx system (Collet and Messens 2010). The metabolomic analysis in the previous work also highlighted a number of non-enzymatic factors involved in the elimination of stress, such as proline, betaine, and GABA (Soboń et al. 2018).

The strong upregulation of prohibitin-1 (PHB1) (Spot 79) after 24 h of exposure to TBT is worth noting. PHB1 together with prohibitin-2 (PHB2) play a crucial role in the proper functioning of mitochondria. They are a universal protein scaffold for key mitochondrial processes involved in cell proliferation, morphogenesis, mitochondrial DNA organization, protein processing, functional integrity of mitochondria, and triggering retrograde signals in response to stress as well as stress tolerance (Merkwirth and Langer 2009). Due to the multifunctional nature of this protein, its role in the examined process is ambiguous. Studies on eukaryotic organisms have shown the cytoprotective role of PHB during oxidative stress, which leads to a decrease in the level of ROS. Studies conducted by Theiss et al. (2007) suggest the protective role of this protein on cells exposed to oxidative stress. In another study by Liu et al. (2006), upregulation of PHB1 in cultured cardiomyocytes was found to protect mitochondria from injury and apoptosis induced by hydrogen peroxide and maintain mitochondrial membrane permeability. A study performed by Li et al. (2015) showed the protective role of PHB1 in the recovery of spinal cord injury in rats by the suppression of ROS formation, reducing apoptosis and restoring the mitochondrial function. Moreover, it has been revealed that PHB interacts with and is required for the optimal activity of complexes I and IV of the ETC and thus preserves mitochondrial respiratory function of cells exposed to oxidative stress (Anderson et al. 2018), which could be correlated with the upregulation and functioning of these complexes in the fungus during exposure to TBT. DNA fragmentation is one of the known mechanisms of TBT action (Zuo et al. 2012;

Morales et al. 2013), and due to the fact that PHB plays a role in mitochondrial DNA organization (Van Aken et al. 2010), its overexpression together with nuclease C1 (spot 71) could be involved in DNA repair processes occurring in fungal cells. Upregulation of nuclease C1 in TBT-treated samples was observed during the whole time of the experiment (except the samples from 48 h where nuclease was not detected in both samples). The role of nuclease C1 in the examined process had been discussed earlier (Soboń et al. 2016) and seems to be another cell-protection element induced in fungus during exposure to TBT. The overexpression of PHB, which plays an anti-apoptotic role in mitochondria (Peng et al. 2015), is also remarkable due to the fact that the induction of apoptosis by TBT has been reported in several studies (Jurkiewicz et al. 2004; Mitra et al. 2013). Because of TBT negative effect on the proper functioning of mitochondria coupled with strong oxidative stress, the upregulation of multifunctional protein PHB1 seems to be another important cell factor involved in fungus recovery during exposure to TBT. In the tested fungus, TBT-induced oxidative stress was noticed, and upregulation of PHB1 could have been involved in mitochondrial functioning and supporting ROS elimination. Taking into account all of the obtained results, we concluded that the enzymatic and non-enzymatic cell defense plays a significant role in ROS-scavenging and leads to a balance of homeostasis in cells exposed to TBT, as well as protective effect of PHB1 on proper mitochondria functioning.

TBT effect on cytoskeleton-related proteins

Filamentous fungi are highly polarized eukaryotic cells, whose characteristic feature is a continuous elongation of their hyphae at the tip. Actin and tubulin, the cytoskeletal elements play essential roles in polar growth and organelle distribution (Horio 2007; Takeshita et al. 2014). TBT leads to morphological damage to the *C. echinulata* hyphae, especially visible after 24 h of culturing (Soboń et al. 2018). The induction of β tubulin (spot 31) and actin (spots 32 and 33) only in the control culture after 24 h, followed by its upregulation in TBT-treated cells in the next measuring points confirmed microscopic observation that TBT disturbs the cell architecture. The adverse influence of TBT on the cytoskeleton system has been reported (Cima et al. 1998; Khondee et al. 2016) and our results confirm the negative effect of TBT on the cell architecture.

Conclusions

The obtained results revealed the multiple negative effects of TBT on fungal hyphae. The fungus focused on energy production via the respiratory chain by the upregulation of the glycolysis enzymes, the NADH delivery system (malate

dehydrogenase), the electron transport chain (NADH dehydrogenase), and ATP synthesis (ATP synthase together with inorganic pyrophosphatase). The upregulation of cellular respiratory pathways including glycolysis and oxidative phosphorylation, together with an increased level of mitochondrial malate dehydrogenase and DLD enzyme, revealed energy depletion and the activation of the systems involved in reducing the equivalents production and the ATP generation by the fungus. The unique overproduction of PHB1 involved in a number of mitochondrial-related processes may indicate the important role of this protein in fungus recovery. Disturbances in the functioning of the electron transport chain resulted in the formation of considerably large amounts of ROS. Exposure to TBT resulted in the generation of oxidative stress, which induced various defense mechanisms in the examined fungus. The fungal response included the upregulation of ROS-scavenging enzymes (SODs, Trx, and redoxin) and the Hsp70 protein with parallel low catalase activity. The morphological damage to hyphae was manifested by the induction of cytoskeletal proteins, which were necessary for cell architecture building, organelle transport and organization of the fungal cell. The characterization of physiological measurements together with proteomic and metabolomic studies provided deeper insights into the approach that the microorganism uses for recovery at various levels of the functionality and cell structure. These techniques showed a wide spectrum of mechanisms involved in the cell recovery and fungus defense strategy towards toxic TBT, which might contribute to increasing the knowledge about the influence of TBT on the cells. However, the transcriptomic analysis in the future studies could increase our knowledge concerning the molecular processes involved in fungus recovery during TBT exposure.

Funding information This study was supported by the National Science Centre, Poland (Project No. 2014/13/N/NZ9/00878), and statutory activity.

Compliance with ethical standards

Conflict of interest The authors declare that they have no conflict of interest.

References

- Anderson CJ, Kahl A, Qian L, Stepanova A, Starkov A, Manfredi G, Iadecola C, Zhou P (2018) Prohibitin is a positive modulator of mitochondrial function in PC12 cells under oxidative stress. *J Neurochem* 146:235–250. <https://doi.org/10.1111/jnc.14472>
- Amér ES, Holmgren A (2000) Physiological functions of thioredoxin and thioredoxin reductase. *FEBS J* 267:6102–6109
- Bernat P (2016) Lipidomics in Studies on Adaptation Mechanisms of Microorganisms to the Toxic Effects of Hazardous Compounds. In: Długoński J (ed) MICROBIAL BIODEGRADATION: FROM OMICS TO FUNCTION AND APPLICATION. Caister Academic Press, Norfolk, UK, pp 85–98

- Bernat P, Długoński J (2012) Comparative study of fatty acids composition during corticosterone hydroxylation and tributyltin chloride (TBT) degradation in the filamentous fungus *Cunninghamella elegans*. *Int Biodeterior Biodegrad* 74:1–6. <https://doi.org/10.1016/j.ibiod.2012.07.001>
- Bernat P, Gajewska E, Szewczyk R, Słaba M, Długoński J (2014) Tributyltin (TBT) induces oxidative stress and modifies lipid profile in the filamentous fungus *Cunninghamella elegans*. *Environ Sci Pollut Res* 21:4228–4235. <https://doi.org/10.1007/s11356-013-2375-5>
- Berrisford JM, Baradaran R, Sazanov LA (2016) Structure of bacterial respiratory complex I. *BBA-Bioenergetics* 1857:892–901. <https://doi.org/10.1016/j.bbabi.2016.01.012>
- Bonarska-Kujawa D, Kleszczyńska H, Przestalski S (2012) The location of organotins within the erythrocyte membrane in relation to their toxicity. *Ecotoxicol Environ Saf* 78:232–238. <https://doi.org/10.1016/j.ecoenv.2011.11.027>
- Cima F, Ballarin L, Bressa G, Burighel P (1998) Cytoskeleton alterations by tributyltin (TBT) in tunicate phagocytes. *Ecotoxicol Environ Saf* 40:160–165. <https://doi.org/10.1006/eesa.1998.1657>
- Collet J-F, Messens J (2010) Structure, function, and mechanism of thioredoxin proteins. *Antioxid Redox Signal* 13:1205–1216. <https://doi.org/10.1089/ars.2010.3114>
- Cruz A, Oliveira V, Baptista I, Almeida A, Cunha Â, Suzuki S, Mendo S (2012) Effect of tributyltin (TBT) in the metabolic activity of TBT-resistant and sensitive estuarine bacteria. *Environ Toxicol* 27:11–17. <https://doi.org/10.1002/tox.20605>
- Cruz A, Anselmo AM, Suzuki S, Mendo S (2015) Tributyltin (TBT): a review on microbial resistance and degradation. *Crit Rev Environ Sci Technol* 45:970–1006. <https://doi.org/10.1080/10643389.2014.924181>
- Desai C, Pathak H, Madamwar D (2010) Advances in molecular and “-omics” technologies to gauge microbial communities and bioremediation at xenobiotic/anthropogen contaminated sites. *Bioresour Technol* 101:1558–1569
- Długoński J (2016) Microbial elimination of Endocrine Disrupting Compounds. In: Długoński J (ed) *MICROBIAL BIODEGRADATION: FROM OMICS TO FUNCTION AND APPLICATION*. Caister Academic Press, Norfolk, UK, pp 99–118
- Dudimah FD, Odman-Ghazi SO, Hatcher F, Whalen MM (2007) Effect of tributyltin (TBT) on ATP levels in human natural killer (NK) cells: relationship to TBT-induced decreases in NK function. *J Appl Toxicol* 27:86–94. <https://doi.org/10.1002/jat.1202>
- Ferreira M, Blanco L, Garrido A, Vieites JM, Cabado AG (2013) In vitro approaches to evaluate toxicity induced by organotin compounds tributyltin (TBT), dibutyltin (DBT), and Monobutyltin (MBT) in Neuroblastoma Cells. *J Agric Food Chem* 61:4195–4203. <https://doi.org/10.1021/jf3050186>
- Hanschmann E-M, Godoy JR, Berndt C, Hudemann C, Lillig CH (2013) Thioredoxins, glutaredoxins, and peroxiredoxins—molecular mechanisms and health significance: from cofactors to antioxidants to redox signaling. *Antioxid Redox Signal* 19:1539–1605. <https://doi.org/10.1089/ars.2012.4599>
- Horio T (2007) Role of microtubules in tip growth of fungi. *J Plant Res* 120:53–60. <https://doi.org/10.1007/s10265-006-0043-2>
- Hunziker RW, Escher BI, Schwarzenbach RP (2002) Acute toxicity of triorganotin compounds: different specific effects on the energy metabolism and role of pH. *Environ Toxicol Chem* 21:1191–1197. <https://doi.org/10.1002/etc.5620210611>
- Jastroch M, Divakaruni AS, Mookerjee S, Treberg JR, Brand MD (2010) Mitochondrial proton and electron leaks. *Essays Biochem* 47:53–67. <https://doi.org/10.1042/bse0470053>
- Joseph P (2017) Transcriptomics in toxicology. *Food Chem Toxicol* 109: 650–662. <https://doi.org/10.1016/j.fct.2017.07.031>
- Jurkiewicz M, Averill-Bates DA, Marion M, Denizeau F (2004) Involvement of mitochondrial and death receptor pathways in tributyltin-induced apoptosis in rat hepatocytes. *BBA-Mol Cell Res* 1693:15–27. <https://doi.org/10.1016/j.bbamcr.2004.04.001>
- Khondee P, Srisomsap C, Chokchaichamnankit D, Svasti J, Simpson RJ, Kingtong S (2016) Histopathological effect and stress response of mantle proteome following TBT exposure in the hooded oyster *Saccostrea cucullata*. *Environ Pollut* 218:855–862. <https://doi.org/10.1016/j.envpol.2016.08.011>
- Lapuente-Brun E, Moreno-Loshuertos R, Acín-Pérez R et al (2013) Supercomplex assembly determines electron flux in the mitochondrial electron transport chain. *Science* (80-) 340:1567–1570. <https://doi.org/10.1126/science.1230381>
- Lee S, Kim SM, Lee RT (2013) Thioredoxin and thioredoxin target proteins: from molecular mechanisms to functional significance. *Antioxid Redox Signal* 18:1165–1207. <https://doi.org/10.1089/ars.2011.4322>
- Li L, Guo J-D, Wang H-D, Shi YM, Yuan YL, Hou SX (2015) Prohibitin 1 gene delivery promotes functional recovery in rats with spinal cord injury. *Neuroscience* 286:27–36. <https://doi.org/10.1016/j.neuroscience.2014.11.037>
- Liu H-G, Wang Y, Lian L, Xu L-H (2006) Tributyltin induces DNA damage as well as oxidative damage in rats. *Environ Toxicol* 21: 166–171. <https://doi.org/10.1002/tox.20170>
- Lu J, Feng J, Cai S, Chen Z (2017) Metabolomic responses of *Haliotis diversicolor* to organotin compounds. *Chemosphere* 168:860–869. <https://doi.org/10.1016/j.chemosphere.2016.10.124>
- Martins JD, Jurado AS, Moreno AJM, Madeira VMC (2005) Comparative study of tributyltin toxicity on two bacteria of the genus *Bacillus*. *Toxicol in Vitro* 19:943–949. <https://doi.org/10.1016/j.tiv.2005.06.019>
- Matsuzaki F, Shimizu M, Wariishi H (2008) Proteomic and metabolomic analyses of the white-rot fungus *Phanerochaete chrysosporium* exposed to exogenous benzoic acid. *J Proteome Res* 7:2342–2350. <https://doi.org/10.1021/pr700617s>
- Matsuzawa A (2017) Thioredoxin and redox signaling: roles of the thioredoxin system in control of cell fate. *Arch Biochem Biophys* 617:101–105. <https://doi.org/10.1016/j.abb.2016.09.011>
- Merkwirth C, Langer T (2009) Prohibitin function within mitochondria: essential roles for cell proliferation and cristae morphogenesis. *Biochim Biophys Acta, Mol Cell Res* 1793:27–32. <https://doi.org/10.1016/j.bbamcr.2008.05.013>
- Mitra S, Gera R, Siddiqui WA, Khandelwal S (2013) Tributyltin induces oxidative damage, inflammation and apoptosis via disturbance in blood-brain barrier and metal homeostasis in cerebral cortex of rat brain: an in vivo and in vitro study. *Toxicology* 310:39–52. <https://doi.org/10.1016/j.tox.2013.05.011>
- Morales M, Martínez-Paz P, Ozáez I, Martínez-Guitarte JL, Morcillo G (2013) DNA damage and transcriptional changes induced by tributyltin (TBT) after short in vivo exposures of *Chironomus riparius* (Diptera) larvae. *Comp Biochem Physiol C Toxicol Pharmacol* 158: 57–63. <https://doi.org/10.1016/j.cbpc.2013.05.005>
- Nakamoto RK, Baylis Scanlon JA, Al-Shawi MK (2008) The rotary mechanism of the ATP synthase. *Arch Biochem Biophys* 476:43–50. <https://doi.org/10.1016/j.abb.2008.05.004>
- Nesci S, Ventrella V, Trombetti F, Pirini M, Pagliarini A (2011a) Tributyltin (TBT) and mitochondrial respiration in mussel digestive gland. *Toxicol in Vitro* 25:951–959. <https://doi.org/10.1016/j.tiv.2011.03.004>
- Nesci S, Ventrella V, Trombetti F, Pirini M, Pagliarini A (2011b) Multi-site TBT binding skews the inhibition of oligomycin on the mitochondrial Mg-ATPase in *Mytilus galloprovincialis*. *Biochimie* 93: 1157–1164. <https://doi.org/10.1016/j.biochi.2011.04.008>
- Pagliarini A, Bandiera P, Ventrella V, Trombetti F, Pirini M, Nesci S, Borgatti AR (2008) Tributyltin (TBT) inhibition of oligomycin-sensitive Mg-ATPase activity in mussel mitochondria. *Toxicol in Vitro* 22:827–836. <https://doi.org/10.1016/j.tiv.2007.12.015>

- Peng YT, Chen P, Ouyang RY, Song L (2015) Multifaceted role of prohibitin in cell survival and apoptosis. *Apoptosis* 20:1135–1149. <https://doi.org/10.1007/s10495-015-1143-z>
- Siewiera P, Bernat P, Różalska S, Długoński J (2015) Estradiol improves tributyltin degradation by the filamentous fungus *Metarhizium robertsii*. *Int Biodeterior Biodegrad* 104:258–263. <https://doi.org/10.1016/j.ibiod.2015.06.014>
- Siewiera P, Różalska S, Bernat P (2017) Estrogen-mediated protection of the organotin-degrading strain *Metarhizium robertsii* against oxidative stress promoted by monobutyltin. *Chemosphere* 185:96–104
- Słaba M, Różalska S, Bernat P et al (2015) Efficient alachlor degradation by the filamentous fungus *Paecilomyces marquandii* with simultaneous oxidative stress reduction. *Bioresour Technol* 197:404–409. <https://doi.org/10.1016/j.biortech.2015.08.045>
- Soboń A, Szewczyk R, Długoński J (2016) Tributyltin (TBT) biodegradation induces oxidative stress of *Cunninghamella echinulata*. *Int Biodeterior Biodegrad* 107:92–101. <https://doi.org/10.1016/j.ibiod.2015.11.013>
- Soboń A, Szewczyk R, Różalska S, Długoński J (2018) Metabolomics of the recovery of the filamentous fungus *Cunninghamella echinulata* exposed to tributyltin. *Int Biodeterior Biodegrad* 127:130–138. <https://doi.org/10.1016/j.ibiod.2017.11.008>
- Starkov AA (2004) Mitochondrial -ketoglutarate dehydrogenase complex generates reactive oxygen species. *J Neurosci* 24:7779–7788. <https://doi.org/10.1523/JNEUROSCI.1899-04.2004>
- Szewczyk R, Kowalski K (2016a) Metabolomics and Crucial Enzymes in Microbial Degradation of Contaminants. In: Długoński J (ed) *MICROBIAL BIODEGRADATION: FROM OMICS TO FUNCTION AND APPLICATION*. Caister Academic Press, Norfolk, pp 43–66
- Szewczyk R, Kowalski K (2016b) Proteomics as a Tool for Metabolic Pathways Inspection in Microbial Cells. In: Długoński J (ed) *MICROBIAL BIODEGRADATION: FROM OMICS TO FUNCTION AND APPLICATION*. Caister Academic Press, Norfolk, pp 67–83
- Szewczyk R, Soboń A, Sylwia R, Dzitko K, Waidelich D, Długoński J (2014) Intracellular proteome expression during 4-n-nonylphenol biodegradation by the filamentous fungus *Metarhizium robertsii*. *Int Biodeterior Biodegrad* 93:44–53. <https://doi.org/10.1016/j.ibiod.2014.04.026>
- Szewczyk R, Soboń A, Słaba M, Długoński J (2015) Mechanism study of alachlor biodegradation by *Paecilomyces marquandii* with proteomic and metabolomic methods. *J Hazard Mater* 291:52–64. <https://doi.org/10.1016/j.jhazmat.2015.02.063>
- Takeshita N, Manck R, Grün N, de Vega SH, Fischer R (2014) Interdependence of the actin and the microtubule cytoskeleton during fungal growth. *Curr Opin Microbiol* 20:34–41. <https://doi.org/10.1016/j.mib.2014.04.005>
- Theiss AL, Idell RD, Srinivasan S, Klapproth JM, Jones DP, Merlin D, Sitarman SV (2007) Prohibitin protects against oxidative stress in intestinal epithelial cells. *FASEB J* 21:197–206. <https://doi.org/10.1096/fj.06-6801com>
- Turrens JF (2003) Mitochondrial formation of reactive oxygen species. *J Physiol* 552:335–344. <https://doi.org/10.1113/jphysiol.2003.049478>
- Van Aken O, Whelan J, Van Breusegem F (2010) Prohibitins: mitochondrial partners in development and stress response. *Trends Plant Sci* 15:275–282. <https://doi.org/10.1016/j.tplants.2010.02.002>
- Wang Y, Jian F, Wu J, Wang S (2012) Stress-response protein expression and DAF-16 translocation were induced in tributyltin-exposed *Caenorhabditis elegans*. *Bull Environ Contam Toxicol* 89:704–711. <https://doi.org/10.1007/s00128-012-0760-2>
- Yamada S, Kotake Y, Sekino Y, Kanda Y (2013) AMP-activated protein kinase-mediated glucose transport as a novel target of tributyltin in human embryonic carcinoma cells. *Metallomics* 5:484–491. <https://doi.org/10.1039/c3mt20268b>
- Yamada S, Kotake Y, Demizu Y, Kurihara M, Sekino Y, Kanda Y (2014) NAD-dependent isocitrate dehydrogenase as a novel target of tributyltin in human embryonic carcinoma cells. *Sci Rep* 4. doi: <https://doi.org/10.1038/srep05952>
- Yamada S, Kotake Y, Nakano M, Sekino Y, Kanda Y (2015) Tributyltin induces mitochondrial fission through NAD-IDH dependent mitofusin degradation in human embryonic carcinoma cells. *Metallomics* 7:1240–1246. <https://doi.org/10.1039/c5mt00033e>
- Zhou J, Zhu X s, Cai Z h (2010) Tributyltin toxicity in abalone (*Haliotis diversicolor supertexta*) assessed by antioxidant enzyme activity, metabolic response, and histopathology. *J Hazard Mater* 183:428–433. <https://doi.org/10.1016/j.jhazmat.2010.07.042>
- Zuo Z, Wang C, Wu M, Wang Y, Chen Y (2012) Exposure to tributyltin and triphenyltin induces DNA damage and alters nucleotide excision repair gene transcription in *Sebastiscus marmoratus* liver. *Aquat Toxicol* 122:106–112. <https://doi.org/10.1016/j.aquatox.2012.05.015>

Publisher's note Springer Nature remains neutral with regard to jurisdictional claims in published maps and institutional affiliations.

Supplementary material for:

A proteomic study of *Cunninghamella echinulata* recovery during exposure to tributyltin

Adrian Soboń^{1#}, Rafał Szewczyk^{1*®}, Jerzy Długoński¹, Sylwia Różalska¹

¹Department of Industrial Microbiology and Biotechnology, Institute of Microbiology, Biotechnology and Immunology, Faculty of Biology and Environmental Protection, University of Łódź, Łódź, Poland.

[#]Present address: Department of Microbial Genetics, Institute of Microbiology, Biotechnology and Immunology, Faculty of Biology and Environmental Protection, University of Łódź, Łódź, Poland.

^{*}Present address: Centre of Clinical and Aesthetical Medicine DiMedical, Łódź, Poland.

[®]Corresponding author. E-mail address: rafal.szewczyk@dimedical.pl

Contents:

Table S-1 – page 1

Table S-1. Detailed results of proteomic identification of *C. echinulata* IM 2611 proteins during exposure to 5 mg L⁻¹ TBT. ^aFold change was calculated as a ratio of the intensity of the protein bands between the TBT-containing sample and the corresponding control sample after 24, 48, 72 and 96 h. The protein spots observed only in the control or TBT-containing sample were marked as 'c' or 'tbt', respectively. If no spots were detected there were marked as '-'.

Spot	MASCOT search results					Delta-BLAST results		Fold change ^a			
	Best protein name	Score	Organism	Accession	MW [Da]			24h	48h	72h	96h
Glycolysis											
1	fructose-bisphosphate aldolase, class II	569	<i>Syncephalastrum racemosum</i>	ORY96155.1	39411	cd00946, Class II Type A, Fructose-1,6-bisphosphate (FBP) aldolases.		0,40	3,64	0,41	2,53
2	triosephosphate isomerase	347	<i>Absidia repens</i>	ORZ22507.1	26942	PTZ00333, triosephosphate isomerase.		c	2,59	1,97	3,55
3	glyceraldehyde-3-phosphate dehydrogenase	348	<i>Absidia repens</i>	ORZ17044.1	35502	TIGR01534, glyceraldehyde-3-phosphate dehydrogenase, type I.		0,44	0,59	0,65	19,03
4	glyceraldehyde-3-phosphate dehydrogenase	209	<i>Absidia repens</i>	ORZ17044.1	35502	TIGR01534, glyceraldehyde-3-phosphate dehydrogenase, type I.		c	-	3,81	tbt
5	glyceraldehyde-3-phosphate dehydrogenase	277	<i>Absidia repens</i>	ORZ17044.1	35502	TIGR01534, glyceraldehyde-3-phosphate dehydrogenase, type I.		-	c	4,03	0,96
6	hypothetical protein	246	<i>Absidia glauca</i>	SAM09852.1	47484	PTZ00005, phosphoglycerate kinase; Provisional.		c	tbt	3,11	tbt

7	2,3-bisphosphoglycerate-independent phosphoglycerate mutase	212	<i>Absidia repens</i>	ORZ08611.1	57856	PRK05434, phosphoglyceromutase; Provisional.	c	tbt	-	tbt
8	enolase	721	<i>Cunninghamella elegans</i>	CAA76735.1	46849	PLN00191, enolase.	0,68	1,77	3,50	0,29
Oxidative Phosphorylation										
9	hypothetical protein BCR42DRAFT_491864	260	<i>Absidia repens</i>	ORZ15863.1	41685	cd05271, NADH dehydrogenase (ubiquinone) 1 alpha subcomplex, subunit 9, 39 kDa, (NDUFA9) -like, atypical (a) SDRs.	5,39	-	-	-
10	hypothetical protein	158	<i>Absidia glauca</i>	SAM04188.1	15166	pfam05071, NADH ubiquinone oxidoreductase subunit NDUFA12.	tbt	-	-	-
11	NADH dehydrogenase [ubiquinone] complex I, assembly factor 7-like protein	74	<i>Smittium culicis</i>	OMJ26490.1	61959	pfam02636, Putative S-adenosyl-L-methionine-dependent methyltransferase.	-	c	tbt	0,39
12	cytochrome b-c1 complex subunit 7	101	<i>Lichtheimia corymbifera</i> JMRC:FSU:9682	CDH56085.1	14616	pfam02271, Ubiquinol-cytochrome C reductase complex 14kD subunit.	-	-	0,81	tbt
13	cytochrome c oxidase subunit 5A COX5A	155	<i>Phycomyces blakesleeanus</i> NRRL 1555(-)	XP_018289694.1	15568	pfam02284, Cytochrome c oxidase subunit Va.	-	1,45	2,08	tbt
14	ATP synthase subunit alpha	967	<i>Hesseltinella vesiculosa</i>	ORX53531.1	59092	PRK09281, F0F1 ATP synthase subunit alpha.	0,99	1,64	1,87	2,76
15	ATP synthase F1 subcomplex beta subunit ATP2	898	<i>Mucor circinelloides f. lusitanicus</i> CBS 277.49	OAD04005.1	52713	PRK09280, F0F1 ATP synthase subunit beta.	1,02	12,17	2,17	3,05
16	hypothetical protein	213	<i>Absidia glauca</i>	SAM02571.1	17762	pfam05873, ATP synthase D chain, mitochondrial (ATP5H).	3,14	tbt	1,17	1,65
64	F1 complex, OSCP/delta subunit of ATPase	225	<i>Hesseltinella vesiculosa</i>	ORX62690.1	23065	COG0712, FoF1-type ATP synthase, delta subunit [Energy production and conversion]	2,52	1,83	0,64	0,73
17	inorganic pyrophosphatase	571	<i>Absidia repens</i>	ORZ15054.1	32653	cd00412, Inorganic pyrophosphatase.	1,23	5,41	3,08	1,43
18	electron transfer flavo protein, beta subunit	271	<i>Hesseltinella vesiculosa</i>	ORX46546.1	28746	cd01714, The electron transfer flavoprotein (ETF).	2,23	2,06	1,25	0,41
Stress response										
19	thioredoxin-like protein	239	<i>Hesseltinella vesiculosa</i>	ORX62243.1	21826	cd03015, Peroxiredoxin (PRX) family, Typical 2-Cys PRX subfamily.	0,22	3,06	2,94	0,57
20	thioredoxin-like protein	207	<i>Rhizopus microsporus</i>	ORE14485.1	24403	cd03016, Peroxiredoxin (PRX) family, 1-cys PRX subfamily.	c	-	2,92	tbt
21	thioredoxin-like protein	164	<i>Absidia repens</i>	ORZ12671.1	18613	cd00340, Glutathione (GSH) peroxidase family.	c	-	1,73	tbt
22	manganese and iron superoxide dismutase	183	<i>Rhizopus microsporus</i>	ORE15744.1	25064	PLN02471, superoxide dismutase [Mn]	3,30	-	2,61	1,83
23	Redoxin	110	<i>Hesseltinella vesiculosa</i>	ORX46097.1	17994	cd03013, Peroxiredoxin (PRX) family, PRX5-like subfamily.	1,56	-	3,14	3,37
24	heat shock 70 kDa protein 2	807	<i>Absidia repens</i>	ORZ12002.1	67482	pfam00012, Hsp70 protein.	c	tbt	tbt	6,20
25	hsp71-like protein	316	<i>Rhizopus microsporus</i>	ORE16196.1	71206	pfam00012, Hsp70 protein.	tbt	0,53	9,47	0,60
26	hypothetical protein	183	<i>Absidia glauca</i>	SAL95812.1	66741	pfam00012, Hsp70 protein.	c	tbt	-	tbt
27	superoxide dismutase Cu-Zn	94	<i>Absidia repens</i>	ORZ18937.1	15863	pfam00080, Copper/zinc superoxide dismutase (SODC).	1,78	-	-	tbt

Pentose phosphate pathway										
28	hypothetical protein	239	<i>Absidia glauca</i>	SAL97358.1	35034	PRK05269, transaldolase B.	0,96	3,70	4,42	1,79
29	hypothetical protein	379	<i>Absidia glauca</i>	SAL98199.1	52769	PRK09287, 6-phosphogluconate dehydrogenase.	1,92	-	-	-
Cytoskeleton proteins										
30	Tubulin alpha-1C chain	578	<i>Choanephora cucurbitarum</i>	OBZ89207.1	49857	PTZ00335, tubulin alpha chain.	0,56	1,04	tbt	1,18
31	beta-tubulin, partial	264	<i>Blakeslea trispora</i>	AAY18773.1	43231	cd02187, The beta-tubulin family.	c	2,34	4,56	2,82
32	actin-2	671	<i>Mucor circinelloides f. circinelloides</i> 1006PhL	EPB91408.1	41710	PTZ00281, actin.	c	2,58	3,27	6,81
33	Putative Actin (Fragment)	356	<i>Lichtheimia ramosa</i>	CDS12119.1	41753	PTZ00281, actin.	c	c	3,14	3,37
TCA cycle										
34	citrate synthase	555	<i>Syncephalastrum racemosum</i>	ORZ00561.1	52635	PRK09569, type I citrate synthase.	1,12	0,38	0,90	0,70
35	Citrate synthase, mitochondrial	79	<i>Choanephora cucurbitarum</i>	OBZ90597.1	52383	PRK09569, type I citrate synthase.	-	c	0,82	0,65
36	isocitrate dehydrogenase, NAD-dependent	799	<i>Absidia repens</i>	ORZ20789.1	40899	PLN00118, isocitrate dehydrogenase	0,90	c	0,73	1,58
37	malate dehydrogenase, NAD-dependent	528	<i>Absidia repens</i>	ORZ25534.1	35197	cd01337, Glyoxysomal and mitochondrial malate dehydrogenases.	2,56	0,30	0,41	1,87
38	hypothetical protein	682	<i>Absidia glauca</i>	SAL95658.1	36703	cd01337, Glyoxysomal and mitochondrial malate dehydrogenases.	3,63	tbt	tbt	tbt
Pyruvate oxidation										
39	hypothetical protein	324	<i>Absidia glauca</i>	SAM04640.1	55520	PRK06327, dihydrolipoamide dehydrogenase	tbt	tbt	0,71	tbt
Protein metabolism										
40	hypothetical protein	246	<i>Absidia glauca</i>	SAL97789.1	15375	pfam01248, Ribosomal protein L7Ae/L30e/S12e/Gadd45 family.	c	1,67	-	1,13
41	40S ribosomal protein S7	92	<i>Hesseltinella vesiculosa</i>	ORX56371.1	21816	pfam01251, Ribosomal protein S7e.	-	-	-	3,80
42	40S ribosomal protein S5, partial	118	<i>Choanephora cucurbitarum</i>	OBZ80663.1	19990	PTZ00091, 40S ribosomal protein S5.	-	-	-	1,80
43	40S ribosomal protein S8	103	<i>Rhizopus delemar</i> RA 99-880	EIE84629.1	22833	COG5256, Translation elongation factor EF-1alpha (GTPase) [Translation, ribosomal structure and biogenesis]	-	-	-	1,09
45	putative transcription factor btf3-like protein	226	<i>Absidia repens</i>	ORZ25666.1	16697	pfam01849, NAC domain.	-	tbt	tbt	1,41
46	translation elongation factor 1 alpha, partial	129	<i>Absidia spinosa</i>	ACI45928.1	39644	COG5256, Translation elongation factor EF-1alpha (GTPase) [Translation, ribosomal structure and biogenesis]	5,31	-	-	-
47	hypothetical protein PHYBLDRAFT_129275	226	<i>Phycomyces blakesleeanus</i> NRRL 1555(-)	XP_018298654.1	17259	PTZ00141, elongation factor 1- alpha.	tbt	2,70	3,91	1,03
48	60S acidic ribosomal protein P0	235	<i>Hesseltinella vesiculosa</i>	ORX46259.1	33272	PTZ00135, 60S acidic ribosomal protein P0.	c	7,02	10,02	1,79
49	elongation factor 1-alpha	198	<i>Absidia repens</i>	ORZ26205.1	49798	PTZ00141, elongation factor 1- alpha.	-	-	c	tbt
50	translation elongation factor 1-alpha, partial	496	<i>Cunninghamella echinulata</i>	AAG28994.1	46461	PTZ00141, elongation factor 1- alpha.	2,62	1,81	0,32	0,80

51	translation elongation factor 1- alpha, partial	407	<i>Cunninghamella echinulata</i>	AAG28994.1	46461	PTZ00141, elongation factor 1- alpha.	-	c	0,82	6,36
79	prohibitin-1	515	<i>Absidia repens</i>	ORZ22100.1	30665	COG0330, Regulator of protease activity HflC, stomatin/prohibitin superfamily [Posttranslational modification, protein turnover, chaperones]	5,54	-	0,53	1,91
81	hypothetical protein PHYBLDRAFT_98645, partial	130	<i>Phycomyces blakesleeana</i> NRRL 1555(-)	XP_018288270 .1	40921	COG1404, Serine protease, subtilisin family [Posttranslational modification, protein turnover, chaperones]	c	-	tbt	tbt
91	nucleophile aminohydrolase	116	<i>Syncephalastrum racemosum</i>	ORY90517.1	22757	cd03759, proteasome beta type-3 subunit.	0,48	1,31	-	-
Amino acids metabolism										
52	hypothetical protein BCR42DRAFT_403787	312	<i>Absidia repens</i>	ORZ23018.1	39265	COG0174, Glutamine synthetase [Amino acid transport and metabolism].	-	tbt	c	tbt
53	Putative Imidazoleglycerol- phosphatedehydratase	126	<i>Lichtheimia ramosa</i>	CDS05525.1	21608	COG0131, Imidazoleglycerol phosphate dehydratase HisB [Amino acid transport and metabolism].	tbt	-	-	-
54	aspartate aminotransferase	212	<i>Absidia repens</i>	ORZ25296.1	47281	PTZ00376, aspartate aminotransferase.	c	c	7,54	5,85
55	S-adenosylmethionine synthase	699	<i>Absidia repens</i>	ORZ05044.1	42262	PTZ00104, S-adenosylmethionine synthase.	c	tbt	2,32	tbt
56	spermidine synthase	180	<i>Absidia repens</i>	ORZ18907.1	33035	PLN02366, spermidine synthase.	-	-	-	tbt
57	glutamate decarboxylase	141	<i>Absidia repens</i>	ORZ25441.1	57584	TIGR01788, glutamate decarboxylase.	c	c	3,10	c
58	hypothetical protein DM01DRAFT_1335954	451	<i>Hesseltinella vesiculosa</i>	ORX54097.1	39869	COG0174, Glutamine synthetase [Amino acid transport and metabolism].	c	tbt	-	-
59	endopeptidase	151	<i>Syncephalastrum racemosum</i>	ORZ01430.1	44046	cd05488, Fungal Proteinase A , aspartic proteinase superfamily.	1,82	c	tbt	1,52
60	peptidase S10, serine carboxypeptidase	145	<i>Hesseltinella vesiculosa</i>	ORX51196.1	56551	pfam00450, Serine carboxypeptidase.	-	c	4,74	0,86
61	adenosylhomocysteinase	138	<i>Absidia repens</i>	ORZ26031.1	46789	PRK05476, S-adenosyl-L-homocysteine hydrolase.	c	1,76	3,25	1,82
70	ketol-acid reductoisomerase	235	<i>Absidia glauca</i>	ORZ12664.1	40254	COG0059, Ketol-acid reductoisomerase [Amino acid transport and metabolism, Coenzyme transport and metabolism].	-	tbt	tbt	tbt
Others										
44	hypothetical protein BCR42DRAFT_399282	86	<i>Absidia repens</i>	ORZ25053.1	11491	pfam12585, Protein of unknown function (DUF3759)	1,21	0,29	1,25	0,90
62	hypothetical protein	932	<i>Absidia glauca</i>	SAM08263.1	57310	COG1156, Archaeal/vacuolar-type H ⁺ -ATPase subunit B/Vma2 [Energy production and conversion].	c	2,06	0,90	19,58
63	V-type proton ATPase catalytic subunit A	113	<i>Absidia repens</i>	ORZ15905.1	67553	COG1155, Archaeal/vacuolar-type H ⁺ -ATPase catalytic subunit A/Vma1 [Energy production and conversion].	c	1,22	tbt	0,74
65	vacuolar atp synthase subunit e	155	<i>Mucor ambiguus</i>	GAN09215.1	26414	COG1390, Archaeal/vacuolar-type H ⁺ -ATPase subunit E/Vma4 [Energy production and conversion].	0,41	0,44	3,67	1,82
66	14-3-3-like protein	372	<i>Hesseltinella vesiculosa</i>	ORX45293.1	28901	COG5040, 14-3-3 family protein [Signal transduction mechanisms].	0,21	3,25	2,32	1,71
67	14-3-3-like protein	174	<i>Hesseltinella vesiculosa</i>	ORX45293.1	28901	COG5040, 14-3-3 family protein [Signal transduction mechanisms].	0,18	1,94	1,96	2,55
68	14-3-3-like protein	196	<i>Hesseltinella vesiculosa</i>	ORX45293.1	28901	COG5040, 14-3-3 family protein [Signal transduction mechanisms].	0,86	c	2,03	1,54
69	hypothetical protein RO3G_12286	137	<i>Rhizopus delemar</i> RA 99-880	EIE87575.1	55679	COG4284, UDP-N-acetylglucosamine pyrophosphorylase [Carbohydrate transport and metabolism]	c	c	2,59	tbt

71	minor nuclease C1B isoform precursor, partial	377	<i>Cunninghamella echinulata</i> var. <i>echinulata</i>	AAF21905.1	28178	cd00091, DNA/RNA non-specific endonuclease	tbt	-	tbt	7,69
72	phosphoesterase family-domain-containing protein	199	<i>Absidia repens</i>	ORZ16986.1	41177	pfam04185, Phosphoesterase family	c	-	2,31	5,90
73	adenine phosphoribosyltransferase	120	<i>Absidia repens</i>	ORZ07684.1	19505	COG0503, Adenine/guanine phosphoribosyltransferase or related PRPP-binding protein [Nucleotide transport and metabolism]	c	-	tbt	tbt
74	nucleoside diphosphate kinase	72	<i>Absidia repens</i>	ORZ21602.1	16548]COG0105, Nucleoside diphosphate kinase [Nucleotide transport and metabolism]	1,11	-	2,75	0,91
75	FAD binding domain-domain-containing protein	268	<i>Absidia repens</i>	ORZ11075.1	68166	COG1053, Succinate dehydrogenase/fumarate reductase, flavoprotein subunit [Energy production and conversion]	c	-	tbt	tbt
76	hypothetical protein PHYBLDRAFT_133989	305	<i>Phycomyces blakesleeianus</i> NRRL 1555(-)	XP_018290866.1	35144	cd00200, WD40 domain, found in a number of eukaryotic proteins that cover a wide variety of functions including adaptor/regulatory modules in signal transduction, pre-mRNA processing and cytoskeleton assembly	c	1,01	0,83	2,07
77	hypothetical protein PHYBLDRAFT_133989	254	<i>Phycomyces blakesleeianus</i> NRRL 1555(-)	XP_018290866.1	35144	cd00200, WD40 domain, found in a number of eukaryotic proteins that cover a wide variety of functions including adaptor/regulatory modules in signal transduction, pre-mRNA processing and cytoskeleton assembly	-	tbt	0,32	1,74
78	Putative GTP-binding nuclear protein GSP1/Ran	332	<i>Lichtheimia ramosa</i>	CDS07831.1	24299	PTZ00132, GTP-binding nuclear protein Ran	tbt	-	1,22	1,84
80	ClpP/crotonase-like domain-containing protein	207	<i>Absidia repens</i>	ORZ19902.1	31957	COG1024, Enoyl-CoA hydratase/carnithine racemase [Lipid transport and metabolism]	-	-	c	tbt
82	FAD/NAD(P)-binding domain-containing protein	254	<i>Hesseltinella vesiculosa</i>	ORX49489.1	47924	COG0446, NADPH-dependent 2,4-dienoyl-CoA reductase, sulfur reductase, or a related oxidoreductase [Lipid transport and metabolism]	-	tbt	c	0,49
83	mitochondrial carrier	526	<i>Hesseltinella vesiculosa</i>	ORX62758.1	33460	pfam00153, Mitochondrial carrier protein	-	tbt	0,09	0,15
84	eukaryotic porin/Tom40	316	<i>Absidia repens</i>	ORZ23420.1	29960	cd07306, Voltage-dependent anion channel of the outer mitochondrial membrane	-	-	1,05	0,74
85	hypothetical protein	107	<i>Absidia glauca</i>	SAL98725.1	47097	cd10952, Catalytic NodB homology domain of Mucor rouxii chitin deacetylase and similar protein	-	c	tbt	tbt
86	hypothetical protein DM01DRAFT_1337961	338	<i>Hesseltinella vesiculosa</i>	ORX49824.1	16470	pfam03501, Plectin/S10 domain	tbt	-	0,62	0,66
87	E3 ubiquitin ligase complex SCF subunit sconC	101	<i>Absidia repens</i>	ORZ08142.1	17958	COG5201, SCF ubiquitin ligase, SKP1 component [Posttranslational modification, protein turnover, chaperones]	-	-	tbt	-
88	immunoglobulin E-set	204	<i>Absidia repens</i>	ORZ24166.1	22105	pfam02115, RHO protein GDP dissociation inhibitor	-	1,31	4,58	0,99
89	hypothetical protein	220	<i>Parasitella parasitica</i>	CEP18291.1	54924	TIGR01130, protein disulfide isomerase, eukaryotic	2,33	tbt	-	tbt
90	cytochrome b5	220	<i>Hesseltinella vesiculosa</i>	ORX50111.1	14166	pfam00173, Cytochrome b5-like Heme/Steroid binding domain	0,62	1,63	3,57	1,03
92	hypothetical protein	334	<i>Absidia glauca</i>	SAL99484.1	24549	COG0105, Nucleoside diphosphate kinase [Nucleotide transport and metabolism]	tbt	1,75	1,38	0,83

X. Podsumowanie i stwierdzenia końcowe

W prezentowanej pracy doktorskiej po raz pierwszy scharakteryzowano proces mikrobiologicznej degradacji TBT u grzyba strzępkowego *Cunninghamella echinulata* IM 2611, jak również oceniono wpływ ksenobiotyku na zmiany w morfologii i w procesach biochemicznych zachodzących w jego strzępkach.

1. Wykazano, że drobnoustrój wydajnie przekształca TBT (5 mg/l), do pochodnych DBT oraz MBT, a proces biodegradacji był skorelowany ze wzrostem grzyba. Jednocześnie zidentyfikowano nową hydroksylowaną pochodną TBT.
2. Obecność ksenobiotyku w środowisku wzrostu wpływała niekorzystnie na badany mikroorganizm. Dodatek TBT do hodowli powodował silne zahamowanie wzrostu i aktywności metabolicznej grzyba, jak również negatywnie oddziaływał na strzępki mikroorganizmu indukując ich wakuolizację i plazmolizę.
3. Związek cynoorganiczny w zróżnicowany sposób wpływał na profil metabolomiczny grzyba, skutkujące nagromadzeniem w grzybni metabolitów glikolizy i szlaku pentozofosforanowego przy jednoczesnym spadku stężenia większości związków cyklu Krebsa.
4. Biocyd indukował stres oksydacyjny, czego objawem jest nadprodukcja RFT w strzępkach grzyba, oraz zwiększona biosynteza białek szoku cieplnego Hsp70 i Hsp71, uważanych za markery stresu oksydacyjnego.
5. W odpowiedzi na stres osmotyczny (plazmoliza komórki) i oksydacyjny, aktywacji uległy nieenzymatyczne i enzymatyczne mechanizmy antyoksydacyjne, poprzez stymulację akumulacji betainy, proliny i GABA, oraz zwiększoną biosyntezę dysmutazy nadtlenkowej cynkowo-miedzianowej (Cu-Zn) i manganowej (Mn), tioredoksyny, redoksyny czy peroksyredoksyny.
6. Zwiększona biosynteza proliny i nukleazy C1 świadczy o indukcji mechanizmów odpowiedzialnych za prawidłowe funkcjonowanie mitochondriów oraz ochronę DNA przed uszkodzeniami.

7. Zwiększonej biosyntezie podlegały białka zaangażowane w produkcję energii w postaci ATP na drodze oddychania komórkowego, co związane jest ze zwiększonym wydatkiem energetycznym komórki.

XI. Literatura uzupełniająca

1. Antizar-Ladislao B. (2008). *Environmental levels, toxicity and human exposure to tributyltin (TBT)-contaminated marine environment. A review*. Environment international, 34(2), 292-308.
2. Bernat P, Długoński J. (2002). *Degradation of tributyltin by the filamentous fungus Cunninghamella elegans, with involvement of cytochrome P-450*. Biotechnology letters, 24(23), 1971-1974.
3. Bernat P, Słaba M, Długoński J. (2009). *Action of tributyltin (TBT) on the lipid content and potassium retention in the organotins degrading fungus Cunninghamella elegans*. Current microbiology, 59(3), 315-320.
4. Bernat P, Gajewska E, Szewczyk R, Słaba M, Długoński J. (2014). *Tributyltin (TBT) induces oxidative stress and modifies lipid profile in the filamentous fungus Cunninghamella elegans*. Environmental Science and Pollution Research, 21(6), 4228-4235.
5. Bernat P, Szewczyk R, Krupiński M, Długoński J. (2013). *Butyltins degradation by Cunninghamella elegans and Cochliobolus lunatus co-culture*. Journal of hazardous materials, 246, 277-282.
6. Bonarska-Kujawa D, Kleszczyńska H, Przestalski S. (2012). *The location of organotins within the erythrocyte membrane in relation to their toxicity*. Ecotoxicology and environmental safety, 78, 232-238.
7. Cima F, Ballarin L, Bressa G, Burighel P. (1998). *Cytoskeleton alterations by tributyltin (TBT) in tunicate phagocytes*. Ecotoxicology and environmental safety, 40(1-2), 160-165.
8. Cruz A, Anselmo AM, Suzuki S, Mendo S. (2015). *Tributyltin (TBT): a review on microbial resistance and degradation*. Critical Reviews in Environmental Science and Technology, 45(9), 970-1006.
9. de Carvalho Oliveira R, Santelli RE (2010). *Occurrence and chemical speciation analysis of organotin compounds in the environment: a review*. Talanta, 82(1), 9-24.
10. Falandysz, J. (2003). *Butyllocyna i produkty jej degradacji w aspekcie toksykologii żywności*. Roczn. Państw. Zakł. Hig., 54, 13-23.
11. Hoch M. (2001). *Organotin compounds in the environment—an overview*. Applied geochemistry, 16(7-8), 719-743.
12. Liu HG, Wang Y, Lian L, Xu LH (2006). *Tributyltin induces DNA damage as well as oxidative damage in rats*. Environmental Toxicology: An International Journal, 21(2), 166-171.
13. Mitra S, Srivastava A, Khandelwal S. (2013). *Tributyltin chloride induced testicular toxicity by JNK and p38 activation, redox imbalance and cell death in sertoli-germ cell co-culture*. Toxicology, 314(1), 39-50.
14. Nakatsu Y, Kotake Y, Ohta S. (2007). *Concentration dependence of the mechanisms of tributyltin-induced apoptosis*. Toxicological sciences, 97(2), 438-447.
15. Nesci S, Ventrella V, Trombetti F, Pirini M, Pagliarani A. (2011). *Tributyltin (TBT) and mitochondrial respiration in mussel digestive gland*. Toxicology in Vitro, 25(4), 951-959.

16. Sillbering J, Drabik A (2010). „Omika” i biologia systemów. W: Kraj A, Drabik A, Silberring J (red) PROTEOMIKA I METABOLOMIKA. Wydawnictwo Uniwersytetu Warszawskiego, 1-4.
17. Sousa AC, Pastorinho MR, Takahashi S, Tanabe S. (2014). *History on organotin compounds, from snails to humans*. Environmental chemistry letters, 12(1), 117-137.
18. Szewczyk R, Kowalski K (2016) *Metabolomics and Crucial Enzymes in Microbial Degradation of Contaminants*. W: Długoński J (red) MICROBIAL BIODEGRADATION: FROM OMICS TO FUNCTION AND APPLICATION. Caister Academic Press, Norfolk, UK, 43–66.
19. Szewczyk R, Kowalski K (2016) *Proteomics as a Tool for Metabolic Pathways Inspection in Microbial Cells*. W: Długoński J (red) MICROBIAL BIODEGRADATION: FROM OMICS TO FUNCTION AND APPLICATION. Caister Academic Press, Norfolk, UK, 67–83.
20. Tiano L, Fedeli D, Santoni G, Davies I, Falcioni G. (2003). *Effect of tributyltin on trout blood cells: changes in mitochondrial morphology and functionality*. Biochimica et Biophysica Acta (BBA)-Molecular Cell Research, 1640(2-3), 105-112.
21. Von Ballmoos C, Brunner J, Dimroth P. (2004). *The ion channel of F-ATP synthase is the target of toxic organotin compounds*. Proceedings of the National Academy of Sciences, 101(31), 11239-11244.

XII. Oświadczenia współautorów o udziale w publikacjach

Oświadczenia współautorów o udziale w publikacjach

Mgr Adrian Soboń

Zakład Genetyki Drobnoustrojów, Wydział Biologii i Ochrony Środowiska,
Uniwersytet Łódzki, ul. Banacha 12/16, 90-237 Łódź,
e-mail: adrian.sobon@biol.uni.lodz.pl

Soboń A, Szewczyk R, Długoński J (2016). *Tributyltin (TBT) biodegradation induces oxidative stress of Cunninghamella echinulata*. International Biodeterioration & Biodegradation, 107, 92-101, doi: 10.1016/j.ibiod.2015.11.013 (IF=2,962; MNiSW=30).

Oświadczam, że mój udział w ww. pracy wynosi 60% i obejmował współudział w koncepcji pracy, wykonaniu doświadczeń, analizie wyników, opracowaniu manuskryptu, a także edycji pracy.

.....Soboń.....

Soboń A, Szewczyk R, Różalska S, Długoński J (2018). *Metabolomics of the recovery of the filamentous fungus Cunninghamella echinulata exposed to tributyltin*. International Biodeterioration & Biodegradation, 127, 130-138, doi: 10.1016/j.ibiod.2017.11.008 (IF=3,828; MNiSW=30).

Oświadczam, że mój udział w ww. pracy wynosi 65% i obejmował współudział w koncepcji pracy, wykonaniu doświadczeń, analizie wyników, opracowaniu manuskryptu, a także edycji pracy.

.....Soboń.....

Soboń A, Szewczyk R, Długoński J, Różalska S (2019). *A proteomic study of Cunninghamella echinulata recovery during exposure to tributyltin*. Environmental Science and Pollution Research 1-14, doi: 10.1007/s11356-019-06416-z (IF=2,914; MNiSW=70).

Oświadczam, że mój udział w ww. pracy wynosi 70% i obejmował współudział w koncepcji pracy, wykonaniu doświadczeń, analizie wyników, opracowaniu manuskryptu, a także edycji pracy.

.....Soboń.....

Wartość IF oraz punktację MNiSW podano zgodnie z rokiem opublikowania.

Oświadczenia współautorów o udziale w publikacjach

Dr Rafał Szewczyk

Centrum Medycyny Klinicznej i Estetycznej DiMedical Sp. z o.o.,
ul. Legionów 40/19, 90-702 Łódź,
e-mail: rafal.szewczyk@dimedical.pl

Soboń A, Szewczyk R, Długoński J (2016). *Tributyltin (TBT) biodegradation induces oxidative stress of Cunninghamella echinulata*. International Biodeterioration & Biodegradation, 107, 92-101, doi: 10.1016/j.ibiod.2015.11.013 (IF=2,962; MNiSW=30).

Oświadczam, że mój udział w ww. pracy wynosi 25% i obejmował współudział w koncepcji pracy, ocenę postępów, konsultacje metodyczne oraz uczestnictwo w przygotowaniu manuskryptu.



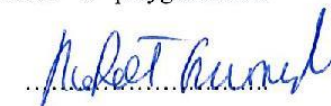
Soboń A, Szewczyk R, Różalska S, Długoński J (2018). *Metabolomics of the recovery of the filamentous fungus Cunninghamella echinulata exposed to tributyltin*. International biodeterioration & biodegradation, 127, 130-138, doi: 10.1016/j.ibiod.2017.11.008 (IF=3,828; MNiSW=30).

Oświadczam, że mój udział w ww. pracy wynosi 15% i obejmował współudział w koncepcji pracy, ocenę postępów, konsultacje metodyczne oraz uczestnictwo w przygotowaniu manuskryptu.



Soboń A, Szewczyk R, Długoński J, Różalska S (2019). *A proteomic study of Cunninghamella echinulata recovery during exposure to tributyltin*. Environmental Science and Pollution Research 1-14, doi: 10.1007/s11356-019-06416-z (IF=2,914; MNiSW=70).

Oświadczam, że mój udział w ww. pracy wynosi 10% i obejmował współudział w koncepcji pracy, ocenę postępów, konsultacje metodyczne oraz uczestnictwo w przygotowaniu manuskryptu.



Wartość IF oraz punktację MNiSW podano zgodnie z rokiem opublikowania.

Oświadczenia współautorów o udziale w publikacjach

Prof. dr hab. Jerzy Długoński

Katedra Mikrobiologii Przemysłowej i Biotechnologii, Wydział Biologii i Ochrony
Środowiska, Uniwersytet Łódzki, ul. Banacha 12/16, 90-237 Łódź,
e-mail: jerzy.dlugonski@biol.uni.lodz.pl

Soboń A, Szewczyk R, **Długoński J** (2016). *Tributyltin (TBT) biodegradation induces oxidative stress of Cunninghamella echinulata*. International Biodeterioration & Biodegradation, 107, 92-101, doi: 10.1016/j.ibiod.2015.11.013 (IF=2,962; MNiSW=30).

Oświadczam, że mój udział w ww. pracy wynosi 15% i obejmował współudział w koncepcji pracy, ocenę postępów pracy oraz uczestnictwo w przygotowaniu manuskryptu.



Soboń A, Szewczyk R, Różalska S, **Długoński J** (2018). *Metabolomics of the recovery of the filamentous fungus Cunninghamella echinulata exposed to tributyltin*. International biodeterioration & biodegradation, 127, 130-138, doi: 10.1016/j.ibiod.2017.11.008 (IF=3,828; MNiSW=30).

Oświadczam, że mój udział w ww. pracy wynosi 15% i obejmował współudział w koncepcji pracy, ocenę postępów pracy oraz uczestnictwo w przygotowaniu manuskryptu.



Soboń A, Szewczyk R, **Długoński J**, Różalska S (2019). *A proteomic study of Cunninghamella echinulata recovery during exposure to tributyltin*. Environmental Science and Pollution Research 1-14, doi: 10.1007/s11356-019-06416-z (IF=2,914; MNiSW=70).

Oświadczam, że mój udział w ww. pracy wynosi 15% i obejmował współudział w koncepcji pracy, ocenę postępów pracy oraz uczestnictwo w przygotowaniu manuskryptu.



Wartość IF oraz punktację MNiSW podano zgodnie z rokiem opublikowania.

Oświadczenia współautorów o udziale w publikacjach

Dr hab. Sylwia Różalska, prof. UŁ

Katedra Mikrobiologii Przemysłowej i Biotechnologii, Wydział Biologii i Ochrony
Środowiska, Uniwersytet Łódzki, ul. Banacha 12/16, 90-237 Łódź,
e-mail: sylwia.rozalska@biol.uni.lodz.pl

Soboń A, Szewczyk R, **Różalska S**, Długoński J (2018). *Metabolomics of the recovery of the filamentous fungus Cunninghamella echinulata exposed to tributyltin*. International Biodeterioration & Biodegradation, 127, 130-138, doi: 10.1016/j.ibiod.2017.11.008 (IF=3,828; MNiSW=30).

Oświadczam, że mój udział w ww. pracy wynosi 5% i obejmował wykonanie eksperymentów obrazowania mikroskopowego *Cunninghamella echinulata* przy pomocy mikroskopu konfokalnego oraz udział w eksperymentach zmierzających do określenia aktywności metabolicznej badanego drobnoustroju.



Soboń A, Szewczyk R, Długoński J, **Różalska S** (2019). *A proteomic study of Cunninghamella echinulata recovery during exposure to tributyltin*. Environmental Science and Pollution Research 1-14, doi: 10.1007/s11356-019-06416-z (IF=2,914; MNiSW=70).

Oświadczam, że mój udział w ww. pracy wynosi 5% i obejmował wykonanie oznaczeń techniką mikroskopii konfokalnej oraz analizę i interpretację uzyskanych wyników.



Wartość IF oraz punktację MNiSW podano zgodnie z rokiem opublikowania.